DESIGN AND EVALUATION OF A CONTINUOUS FIBRE REINFORCED THERMOPLASTIC PREPREG MANUFACTURING LINE

by

Ran Tian

Thesis submitted to the University of Ottawa

in partial fulfillment of the requirements for the

MASTER OF APPLIED SCIENCE

In Mechanical Engineering

Ottawa-Carleton Institute for Mechanical and Aerospace Engineering
University of Ottawa
Ottawa, Canada

August 2022

Acknowledgements

I would like to express my deepest gratitude to Dr. François Robitaille, for his extradentary support for my work, without him any of this would not have been possible. I am grateful for the consistent encouragement, support and inspiration. Dr. François Robitaille is not just a good supervisor, but also a great teacher, great leader, great co-worker and a true friend.

I would like to thank all people at Qingdao Haitie Boat Co., Ltd, for their help and dedication to go through difficult times with the project. Without them, this work would have been hard to finish. Vice President Shengguo Wang provide plentiful experience about thermoset composite material and polymer which gives important guidance led to excellent material selection; Yuanfeng Guan, Xingguo Feng, and Minghai Wu have dedicated working on this project, looking after the production line's set up and cooperate with me while adjusting this production line; Ying Li has provided support while testing the sample product under my supervision.

I would like to thank all my friends in Canada for their encouragement and the good times we have been through.

I would like to thank my father and mother for their steady support, may love and joy always be by their side.

Abstract

Thermoset resin based fibre reinforced polymer-matrix composite materials (PMCs) have provided excellent solutions to many industries based on their great specific strength, high design freedom and other characteristics such as water resistance, corrosion resistance, tailorable electrical conductivity, tailorable thermal performance and many others. But despite of all their benefits, the materials are also limited by uneconomical recycling and management post service life, demanding raw materials storage conditions, less than ideal environmental impact during manufacturing, and relatively low productivity. The purpose of the present work was to investigate economically feasible production of a continuous fibre reinforced thermoplastic composite (CFRTP) alternative solution, for an existing company, that could overcome weak points and limitations of thermosets under increasing environmental needs and pursuit of higher efficiency.

Work aimed at fulfilling the following objectives: 1) document existing thermoplastic composite materials and understand selected manufacturing methods, raw materials, mechanical behaviour and operational feasibility; 2) select, design, and build a fully functional CFRTP manufacturing line; 3) design and run Taguchi methods to analyze the product using multifactorial ANOVA to gently introduce rigorous quality control; and 4) identify the input parameters that most affect output product quality, that could be used to optimize the process, as well as input parameters that have no statistically significant effects on the output and therefore do not warrant investment in funds and time in order to control them.

Throughout the work, it was showed that CFRTP could been produced efficiently with consistent quality. Unidirectional prepreg can be used directly or further processed for usage in many industries

such as pipelines, light construction and automotive components. The design of the CFRTP solution fulfilled necessary conditions and successfully produced CFRTP unidirectional prepreg product. Prepreg produced under 16 different sets of conditions was tested and data was collected. Using Taguchi methods, this study found that the fibre volume fraction, condition of impregnation mould, condition of cooling rollers and extruding temperature all have statistically significant effects on product quality. But limited by restriction from time and cost by production based environments, it is imperative to conduct this work perfectly, in later research a more focused study can be done based on the results of this study.

Still, thesis demonstrates a CFRTP mass production solution, verifies CFRTP impregnation and offers a significant route for upgrading environmental protection and production efficiency. The work also identifies key parameters that affect unidirectional prepregs properties.

List of contents

List of tables

List of figures

Chapter 1:Introduction

1.1 Context

Composite materials are common in the living world, say in plants where many structures consist of a matrix reinforced with flexible filaments. The first applications of composite materials by humans go back to ancient times when early settled populations used mud reinforced with straw for creating durable buildings, some of which still stand today. However, it is not until the late 19th and 20th centuries that the chemical revolution and emergence of synthetic polymers ushered in early developments of modern fibre reinforced composites [1]. Further advances in the latter half of the 20th century brought new synthetic fibres offering high structural performance, from which the development of secondary and then primary structural applications in transport accelerated, primarily for ships and cars but also military aircraft. Since then, fibre-reinforced composites have become the materials of choice for an increasing number of applications, notably in transport [2].

Composites now occupy an ever-increasing market share compared with traditional materials such as metallic alloys, due to their unique properties [3]. Composite materials also offer advantages that single-phase materials cannot match, notably in terms of density and cost of production for small to medium-sized series. In the 21st century, fibre-reinforced composites are widely used for aerospace, automotive, defence, construction, medical and other applications. They have become an important indicator of a country's national capability.

China Railway Rolling Stock Corporation Limited (CRRC) is one of the largest and foremost rolling stock manufacturers in the world, competing with major firms including Alstom, Siemens,

Bombardier and others. Due to China's accelerated development and social background, very strong demand for railway transportation drives accelerated local development of this industry. As of 2020, the overall operational length of Chinese high-speed railways (200 km/h +) exceeds 35 000 km [4]. To further improve railway technology and performance, many components on the high-speed trains are made from composite materials, and their numbers keep increasing.

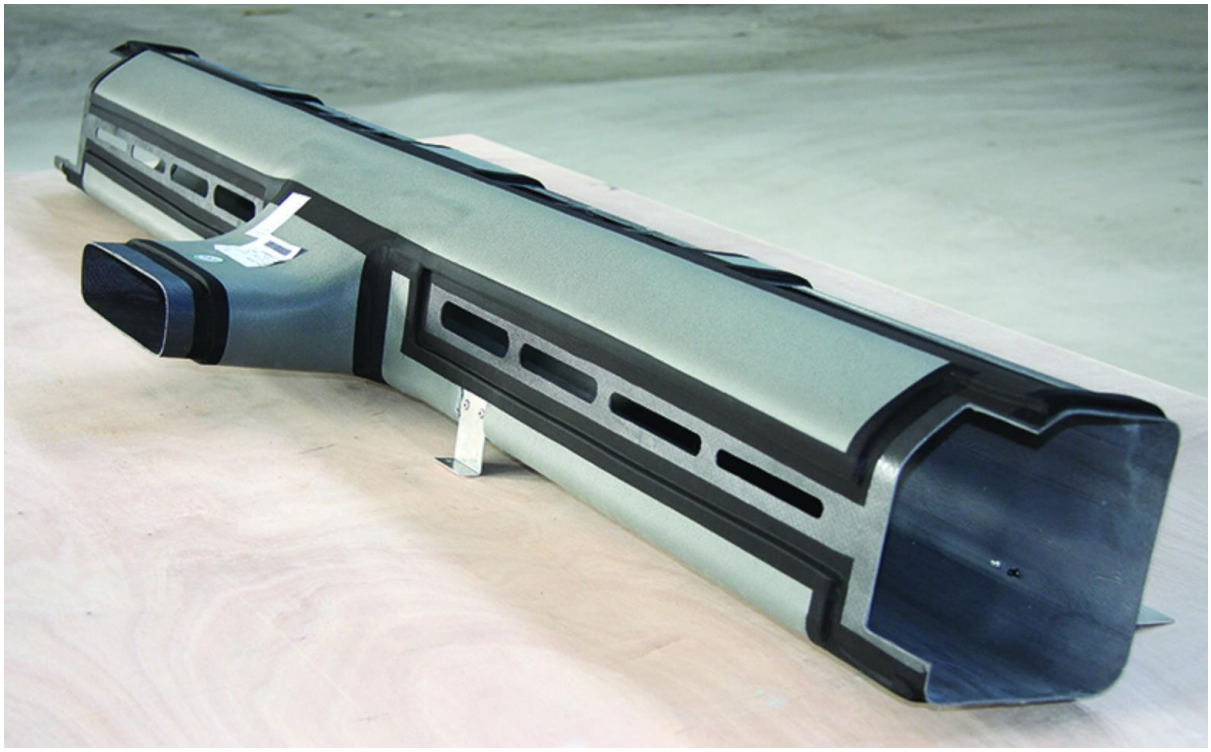

Figure 1.1 Phenolic resin FRP air tunnel system manufactured by Haitie

The performance, productivity, quality and cost of a product are always important for its evaluation, market acceptance and economic success. In the 21st century, environmental sustainability has also become a crucial factor as the environmental awareness of more and more people is heightened. Despite of their numerous other advantages in terms of production and performance, traditional polymer-matrix composite materials (PMCs) featuring thermosetting polymer matrices are not environmentally friendly materials in the current state of industrial technology, especially with regards to the end of the product

life cycle.

With years of experience in producing highest quality fire retardant glass fibre-reinforced PMCs for national and international markets, Qingdao Haitie Boats Co., Ltd, hereinafter referred to as Haitie, has been supplying PMC components to CRRC and HITACHI as their favoured contractor, for years. Figures 1.1 and 1.2 show products manufactured for these customers. Pressing environmental concerns and the complexity of PMC markets and business pushes Haitie to find a new route for its composite business. The goal is to transform, upgrade and optimize its manufacturing processes to become a stronger competitor in the market and to reduce environmental issues that the company and its clients experience.

Figure 1.2 HITACHI FRP train head cover for the UK market, manufactured by Haitie

In order to achieve the goal, Haitie decided upon researching and developing its ability to produce thermoplastic composite pre-impregnated semi-products, known as prepregs, in-house and from scratch. Increasingly popular continuous fibre-reinforced thermoplastic (CFRTP) technology draws most attention. Following a careful business study, the company decided to dive into CFRTP development

from original material selection and modification, thermoplastic prepreg production, product manufacturing all the way to CFRTP end-life handling and recycling. This thesis describes work undertaken towards CFRTP prepreg manufacturing at Haitie, with a focus on unidirectional prepreg.

It is forecast that successful completion of the work will have a major impact on all existing Haitie partners and their competitors in the market. New CFRTP products offering quality and performance as well as environmental sustainability will open broader markets and further improve the reputation of this young company, founded in 2003. Actions resulting from the work presented in this thesis will also enable compliance with governmental regulation and guidance towards increased global environmental awareness; it will help progress the Chinese traditional composite industry to new heights.

1.2 Objective and contents

The objective and finality of this thesis consist in developing a complete production solution for continuous fibre-reinforced thermoplastic prepreg, aiming at replacing Haitie's existing traditional FRP manufacturing processes. The thesis is driven by a key focus on unidirectional thermoplastic prepreg development and process adjustment for improved product quality and performance. The thesis is organized in 5 chapters that focus on different aspects of the work.

Chapter 1 consists in an introduction to the context and objectives of the thesis, and to its contents.

Chapter 2 is a literature review, which provides a summary of the information needed for undertaking development work on the production of unidirectional thermoplastic prepreg. Different types of polymers and composite materials are discussed along with their manufacturing process; primary methods for CFRTP manufacturing are also discussed. This literature review and industrial

context can assist readers at Haitie in understanding which aspects of the development are supported within the scope of this thesis.

Chapter 3 clarifies the physical phenomena involved in CFRTP, including fibre-polymer interfaces and how to optimize them; relationships between manufacturing input factors and impregnation rate; testing methods for PMCs and optimization attempts for unidirectional prepregs.

Chapter 4 discusses the industrial work undertaken. Set up of the impregnation line is introduced along with early trials. All steps of the CFRTP prepreg manufacturing process are detailed, and their functions. The Chapter provides a summary of initial investment, as well as costs of operation and maintenance as best estimates of production capacity, output value, break even volume and contribution margin. Then, the results of a series of 16 trail runs are analyzed using Taguchi plans and multifactorial ANOVAs. Input factors that have a statistically significant effect on output product quality are discussed.

Chapter 5 concludes with essential findings from previous analysis, compares and discusses the relationship between output product properties and the setting of chosen modalities for input parameters. The Chapter also indicates the industrial and commercial road ahead for the production of the materials, and further possible directions for future developments.

Chapter 2: Literature review and industrial context

This chapter provides information relevant to the different aspects of the design and setup of the CFRTP manufacturing process as undertaken in this thesis.

The physical properties of fibres, resins and some additives potentially used for the CFRTP manufacturing are reviewed in Sections 2.1 and 2.2.

Section 2.3 provides a general overview of different manufacturing processes for thermoplastic PMCs. The section also discusses their advantages and limitations and further aspects of CFRTP manufacturing processes that were identified as possible replacement to existing production methods.

Section 2.4 focuses on reviewing different melt impregnation method used in CFRTP production; this information is helpful in better positioning Haitie's direction for its process.

This chapter serves two main purposes. Firstly, it provides broad information on different types of composite materials and production methods in order to help in better positioning Haitie's CFRTP endeavour and products. Secondly, it documents existing CFRTP production methods, to better compare with Haitie's selected production method.

2.1 Properties of reinforcement materials – glass fibres

Glass fibres are one of the most versatile reinforcement materials used in the composites industry. Glass fibres are produced readily and inexpensively as a result of easy supply of their main constituent, silica (silicon dioxide, SiO_2). Glass fibres are made by drawing molten silica and other minerals through bushings that contain numerous small holes, Figure 2.1. Silica glass melting temperature is typically

1250 °C or above; however, it softens from less than 400 °C. After being drawn the fibres are rapidly cooled; final diameters range from 3 to 20 μm. A sizing is applied on the fibres, primarily to protect them from abrasion in further processing operations such as weaving. In some cases, this sizing will also promote better adhesion between fibres and polymer matrix in the composite.

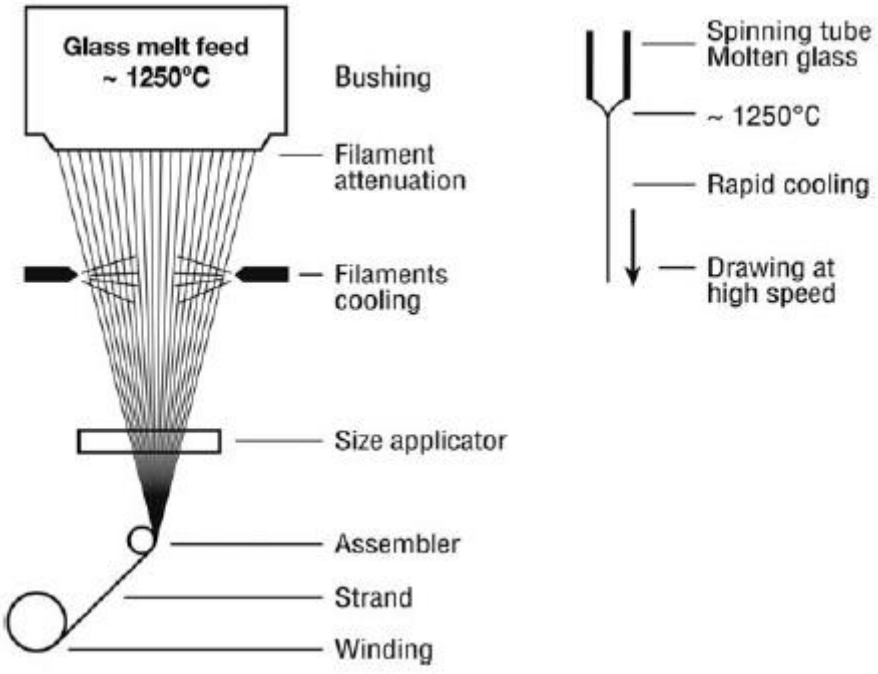

Figure 2.1 Continuous glass fibre filament drawing process [5]

Typical commercial glass fibre strands found on the US market are listed in Table 2.1 with different types of fibres available based on the proportions of constituent materials. The most common type for manufacturing composites is designated as E-glass, which is a low-cost, general-purpose fibre. Other types of glass fibres are listed in Table 2.2 along with their designations and main characteristics. Generally, glass fibres can be sorted in two categories: low-cost general-purpose fibres, and special-purpose fibres sold at premium price. Over 90% of glass fibres produced are general-purpose products as specified in ASTM standards.

Table 2.1 Typical commercial fibre strands [6]

Strand designation			Number of filaments per strand	Average filament diameter (μm)
USA[a]		Metric[b]		
D	1800	EC5 2.75	50	5.33
D	900	EC5 5.5	100	5.33
D	450	EC5 11	200	5.33
D-E	150	EC6 33	400	6.35
E	300	EC6 16.5	200	6.35
E	450	EC7 11	100	7.32
E	225	EC7 22	200	7.32
G	150	EC9 33	200	9.14
G	130	EC9 38	200	9.65
G	75	EC9 66	400	9.14
H	110	EC11 45	200	10.67
H	55	EC11 90	400	10.67
J	90	EC12 55	200	11.75
J	45	EC12 110	400	11.75
J	23	EC12 220	80	11.75
K	31	EC14 160	400	14.19
K	16	EC14 320	800	14.19
K	10	EC14 480	1200	14.19
K	8	EC14 640	1600	14.19
M	6	EC16 800	1600	15.86
M	5	EC16 1000	2000	15.86
N	4	EC17 1200	2000	17.38
N	2	EC17 2400	4000	17.38
T	2	EC24 2200	2000	23.52
T	1	EC24 4400	4000	23.52

[a] Filament designation and count.
[b] E = E glass, C = continuous, then nominal filament diameter and tex.

Tables 2.1 and 2.2 introduce selected physical and mechanical properties for different types of glass fibres available commercially. Tables 2.3 and 2.4 provide specific properties of glass and other fibres in comparison with several common materials. Generally, the density and Young's modulus of glass fibres range around 2.5 to 2.6 g/cm^3 and around 72 to 91 GPa respectively; both ranges are close to those of aluminium for both properties. The strain to failure of dry glass fibres generally ranges from 1.8 to 5.4 %, which compares advantageously with the 0.2% accepted strain for the onset of plastic deformation in aluminium.

Table 2.2 Designations for common types of glass fibres [7]

Letter designation	Property or characteristic
E, electrical	Low electrical conductivity
S, strength	High strength
C, chemical	High chemical durability
M, modulus	High stiffness
A, alkali	High alkali or soda lime glass
D, dielectric	Low dielectric constant

Table 2.3 Physical properties of common types of glass fibres [7]

Fiber	Bulk Density (g/cm^3)	Specific Heat (cal/g/℃)	Tensile Strength at 23 ℃		Young's Modulus 23 ℃	
			Mpa	ksi	Gpa	10^6 psi
Boron-containing E-glass	2.54-2.55	0.192	3100-3800	450-551	76-79	11.0-11.3
Boron-free E-glass	2.62	-	3100-3801	450-552	80-81	11.6-11.7
ECR-glass	2.66-2.68	-	3100-3802	450-553	80-81	11.6-11.7
D-glass	2.16	0.175	2410	349	-	-
S-glass	2.48-2.49	0.176	4380-4590	635-666	88-91	12.8-13.2

Table 2.4 Specific properties of glass and other fibres in comparison to other materials [6]

		E (GPa)	σ_u (GPa)	ρ (g/cm^3)	E/ρ (Mm)	σ_{fu}/ρ (km)	ε_u (%)	d_f/(μm)
E-glass fibre		72	1.5–3.0	2.55	2.8–4.8	58–117	1.8–3.2	10–20
S-glass fibre		87	3.5	2.5	3.5	140	4.0	12
S2-glass fibre		86	4.0	2.49	3.5	161	5.4	10
Carbon fibre		220–350	2.3–3.7	1.8–2.0	12–18	130–190	0.7–1.7	7
High-performance polymer fibres:	Aramid	60–180	2.65–3.45	1.44–1.47	4.0–12.2	180–235	4–1.9	12
	PBT	250	2.4	1.5	17.0	160	1.0	20
	PE	60–120	1–3	1.0	6–12	100–300	—	
Steel		210	0.34–2.1	7.8	2.7	4.3–27	—	—
Aluminium		70	0.14–0.62	2.7	2.6	5–22	—	—
Bulk glass		60	0.05–0.07	2.6	2.3	1.9–2.7	0.08–0.12	—
Resins (epoxy)		2–3.5	0.05–0.09	1.2	0.16–0.29	4–7.5	1.5–6	—
High-density polyethene (PE)		1.3	0.027	0.96	0.135	2.8	—	—

E = Young's modulus, σ_u = tensile strength, ρ = density, E/ρ = specific modulus, σ_u/ρ = specific strength, ε_u = failure strain, d_f = fibre diameter.

E-glass fibres with a composition of 54% SiO_2 , 15% Al_2O_3 and 12% CaO have densities around 2.55 to 2.60 g/cm^3, Young's moduli ranging from 72 to 85 GPa, compressive strengths ranging from 40

to 50 GPa, tensile strengths ranging from 19.5 to 20.5 GPa, shear moduli ranging from 30 to 36 GPa, a maximum service temperature around 350 °C and a glass transition temperature of 820 °C [8]. Fibres that have not undergone further processing and handling are stronger. Fibre surface is progressively scratched through handling, reducing tenacity and strength. Moisture is easily absorbed into the fibre microstructure through surface cracks, and further reduce strength and tenacity [9]–[11].

2.2 Properties of polymer matrix materials

A polymer, either natural or synthetic, is a material that consists of large molecules known as macromolecules. Each macromolecule features many repeated units known as monomers. Individual polymers are generally classified under one of two broad categories, thermosetting and thermoplastic polymers.

Thermosetting polymers are more traditional materials for use as resins in fibre-reinforced composites. In thermosetting polymers, monomers are chemically cross-linked and form a rigid network structure during the curing phase. Once the irreversible curing reaction is complete, industrial thermosetting polymers cannot be molten, reshaped or reused. Industrial thermosetting polymers are typically available as liquid monomers as either one-part or two-parts precursors with relatively low viscosities. This low viscosity is crucially important as it enables longer flow and good wet-out of the fibres during processing. Numerous industrial thermosetting resins are designed for being processed at or near room temperature, without the need for either high-temperature or high-pressure processes, whilst still achieving good fibre-matrix interaction and mechanical performance with a relatively simple manufacturing setup. Thermosetting polymers also offer advantages in terms of thermal stability, chemical resistance, reduced creep fracture and better stress relaxation than thermoplastic polymers

[12]. Limitations associated with thermosetting polymers include limited storage life at ambient temperature for the resins, polymerization reaction (curing) in the mould taking a relatively long time, low strain to failure, and lower impact strength [13].

Contrary to thermosetting polymers, monomers in thermoplastic polymer molecules are assembled in a largely linear way, with limited lateral branching. The different thermoplastic molecules, or chains, are held together by secondary intermolecular forces and physical entanglements. As a result, under applied heat these bonding forces can be weakened and ultimately breached, allowing the macromolecules to flow past one another and the mass of thermoplastic polymer to be reshaped before being cooled again. Consequently, thermoplastic polymers are recyclable hence generally more environmentally friendly than thermoset polymers. Advantages offered by thermoplastic polymers include typically higher impact strength and fracture resistance, imparting higher damage tolerance to thermoplastic composites, higher strain to failure, unlimited shelf life at ambient temperature, post-processing formability, relative ease of joining and repair, potential recyclability, and easier handling. Despite all these advantages, manufacturing processes for thermoplastic polymer composites are generally more difficult to develop than processes for thermosetting polymer composites due to the higher temperatures and much larger viscosities involved. Thermoplastic resins are far more difficult to incorporate into continuous fibre networks.

Table 2.5 features general information pertaining to the basic structural behaviour of a number of neat polymer resins, and for the same resins loaded with a low fraction of glass fibres, for indicative purposes. The following sections and tables discuss the physical properties of specific polymer systems in more detail.

Table 2.5 Typical properties of neat polymer resins and their low volume fraction composites [14]

Polymer	Ultimate Tensile Strength (MPa)		Flexural Modulus (GPa)		Deflection Temperature at 1.8 MPa load (℃)	
	Unfilled	With 30% Glass Fiber	Unfilled	With 30% Glass Fiber	Unfilled	With 30% Glass Fiber
Thermoset Polyester	60	140	3	8	130	220
Phenolic	60	90	3	20	180	250
Epoxy	70	150	2.5	25	175	200
Polyetheretherketone	90	150	4	10	160	285
Polyphenylene Sulfide	70	140	5	11	120	260

2.2.1 Thermoplastic resins: polypropylene (PP)

Polypropylene is a semi-crystalline thermoplastic material used in a wide variety of applications. It offers reasonably good mechanical properties, great chemical resistance with relatively low cost. There are two main types of PP, homopolymer and copolymer. Homopolymer PP is most widely used and is generally stiffer and stronger. Conversely copolymer PP is softer but tougher and more durable. Polypropylene is often used as a structural material in low-cost consumer applications. General property data appear in Table 2.6, along with data for other thermoplastic resins.

2.2.1 Thermoplastic resins: polycarbonate (PC)

Polycarbonate was first commercialized in the 1950s and appeared at the same time in the USA and in Germany. Polycarbonate is an amorphous thermoplastic that offers a great balance of properties. It is stiff, strong, has good ductility and great impact resistance. It is also easy to process and can have good optical clarity, for a moderate price. PC is frequently used for the shell of front lighting cluster units in the automotive industry. Table 2.7 shows general properties for polycarbonate.

Table 2.6 General properties for polycarbonate [15]

Property	Data In Metric Unit
Density	1.20-1.22 g/cc
Shrinkage	0.7-1.0 %
Water Absorption	0.10-0.20 %
Rockwell Hardness, M	70-90
Tensile Strength	55-77 MPa
Tensile Modulus	2.2-2.5 GPa
Flexural Modulus (stiffness)	2.2-2.5 GPa
Izod Impact (Room Temperature	6-8.5 J/m
Glass Transition Temperature	147 ℃

Table 2.7 General properties for some commercially available thermoplastics [16]

	Polypropylene	Polyetherketone	Polyetherimide	Polyamide 6	Polyamide 66	Polyphenylene Sulphide	Polyethersulphone
	PP	**PEEK**	**PEI**	**PA6**	**PA66**	**PPS**	**PES**
Density (g/cm^3)	0.937	1.33	1.35	1.12	1.12	1.43	1.4
Linear Mould Shrinkage (cm/cm)	0.033	0.008	0.005	0.12	0.015	0.01	0.007
Melt Flow (g/ 10 min)	19.1	21.9	8.6	23.1	26	-	85
Tensile Strength (MPa)	36.8	110	100	72.6	73.1	86.7	87.4
Tensile Yield Strength (MPa)	30.7	98.8	100	62.4	63.6	69	99.4
Tensile Modulus (GPa)	1.9	4.5	3.7	1.9	2.1	3.6	3.7
Elongation (%)	120	37	42	94	83	4	30
Flexural Strength (MPa)	36.2	170	130	85.8	88.4	140	130
Flexural Modulus (GPa)	1.4	4.8	4.5	2	2.4	4.9	4.3
Compressive Yield Strength (MPa)	48.5	120	120	28.9	32.5	95	100
Shear Strength (MPa)	-	57.7	-	-	61.7	-	50
CTE @ 20°C (µm/m °C)	120	44.1	40	91.1	100	39.2	49.1
Heat Capacity, Cp (J/g°C)	2	2	-	1.6	2.2	-	1
Thermal Conductivity, λ (W/m K)	0.20	0.25	0.52	0.27	0.26	0.3	0.22
Melt Temp (°C)	160	340	220	220	250	280	-
Maximum Air Service Temp (°C)	85	260	200	100	100	160	200
Vicat Softening Point (°C)	83	-	230	170	190	-	220
Glass Transition Temp (°C)	-	140	220	60	-	88	230
Process Temp (°C)	220	370	360	260	290	330	340
Mould Temp (°C)	43	180	140	73	80	-	120

2.2.2 Thermoplastic resins: polyphenylene sulfide (PPS)

Polyphenylene sulfide (PPS) was first introduced in 1968 by Phillips Petroleum as a semi-crystalline specialty engineering thermoplastic with a unique balance of properties. PPS provides high stiffness and strength at elevated temperatures along with exceptional chemical resistance. It has very high viscosity, fire resistance, dimensional and thermal stability. Its extreme inertness toward organic solvents and inorganic salts and bases leads to outstanding performance as a corrosion resistant material.

2.2.3 Thermosetting resins: phenolics

Phenolic resins are thermosetting resins produced by the reaction of a phenol or substituted phenol with an aldehyde, usually formaldehyde. These resins were amongst the first polymer materials produced commercially from a low molecular weight compound [17]. General applications for phenolic resins include wood adhesives, moulding compounds, foundry binders, laminate mouldings, electrical laminates, ablative coatings, accessories for the automotive, aircraft and construction markets, electrical and lighting fittings, and many others. As a commonly used matrix material for fibre-reinforced composites, phenolic resins have an acceptable ultimate tensile strength of about 50 MPa and a relatively high service temperature normally above 150 °C. Inexpensive, they also offer advantages including limited flame spread, smoke generation and smoke toxicity. But phenolic resins also have limitations including brittleness, short shelf-life, corrosive nature, emission of toxic volatiles, high filler loading, high shrinkage and a hydrophilic behavior that brings about 50% water absorption rate [20, 21]. Table 2.8 provides mechanical property for an injection grade phenolic resin.

Table 2.8 Mechanical properties of general-purpose injection grade phenolic moulding compound Durez® 32962 from Sumitomo Bakelite [19]

Properties	Data In Metric	Testing Method
Bulk Density	0.580 g/cc	ASTM D1895
Specific Gravity	1.45 g/cc	ASTM D792
Water Absorption	50%	ASTM D570
Linear Mold Shrinkage	0.0090 cm/cm	ASTM D6289
Ultimate Tensile Strength	48.0 MPa	ASTM D638
Tensile Modulus	6.9 GPa	ASTM D639
Flexural Strength	76.0 MPa	ASTM D790
Compressive Strength	207 MPa	ASTM D695
Izod Impact, Notched	0.214 J/cm	ASTM D256
Maximum Service Temperature (Air)	150 ℃	-
Deflection Temperature at 1.8 MPa	177 ℃	ASTM D648

2.2.4 Thermosetting resins: polyesters and vinyl esters

Thermosetting polyester was first synthesised in 1940, after phenolic resins. Polyesters form from a condensation reaction between a polyol and an acid. Polyester resins are largely used because of their heat resistance, high tensile, compressive and bending strengths, resistance to chemical corrosion, good dielectric properties, and good fluidity [17]. Table 2.9 lists some mechanical properties for polyester and Table 2.10 compares mechanical properties after reinforcing each resin with different fibre ratios.

Table 2.9 Mechanical properties of unreinforced polyester resins [20]

Resin type	Barcol hardness	Tensile strength (MPa)	Tensile modulus (GPa)	Elongation (%)	Flexural strength (MPa)	Flexural modulus (GPa)	Compressive strength (MPa)	Heat-deflection temperature (℃)
General purpose (Orth)	-	55	3.45	2.1	80	3.45	-	80
Isophthalic	40	75	3.38	3.3	130	3.59	120	90
BPA fumarate	34	40	2.83	1.4	110	3.38	100	130
Chlorendic	40	20	3.38	-	120	3.93	100	140
Vinyl ester	35	80	3.59	4.0	140	3.72	-	100

Thermosetting polyester resins can be further identified as orthophthalic (ortho), isophthalic (iso), BPA fumerated, chlorendic, dicyclopentadiene (DCPD) and other types, Table 2.10. Ortho resins are based upon orthophthalic acid. They are good basic, general-purpose, inexpensive resins. Ortho resins provide better water resistance compared to phenolic resins with a water absorption rate around 0.1% [21]. They are used in applications that do not require elevated service temperature, high corrosion resistance or high mechanical properties.

Isophthalic resins are a step up ortho resins. They exhibit better tensile and flexural properties, higher humidity resistance, and they are also better suited for corrosion and elevated temperatures environments. But at same time, their better properties bring higher cost as compared with ortho resins.

BPA fumarate and chlorendic resins have rigid structures and high heat distortion temperatures from more aromatic backbones in BPA fumarate resins and chlorine in chlorendic resins. This leads to high brittleness and low mechanical performance, but excellent chemical and corrosion resistance.

Dicyclopentadiene resins are used in situations that require high gloss surface finishes. They have similar physical properties to ortho resins but low volumetric shrinkage rate, and they are commonly blended with other resins to minimize their negative aspects.

Table 2.10 Effect of glass content on mechanical properties of fibreglass reinforced polyester composites [20]

		Flexural strength		Flexural modulus		Tensile strength		Tensile modulus		Compressive strength	
Material	Glass content, wt%	MPa	ksi	GPa	10^6 psi	MPa	ksi	GPa	10^6 psi	MPa	ksi
Orthophthalic	30	170	25	5.5	0.80	140	20	4.8	0.70	. . .	. . .
	40	220	32	6.9	1.00	150	22	5.5	0.80	. . .	. . .
Isophthalic	30	190	28	5.5	0.80	150	22	8.27	1.20	. . .	. . .
	40	240	35	7.58	1.10	190	28	11.7	1.70	210	30
BPA fumarate	25	120	17	5.1	0.74	80	12	7.58	1.10	170	24
	35	150	22	8.27	1.20	100	14	10.3	1.50	170	24
	40	160	23	8.96	1.30	120	18	11.0	1.60	180	26
Chlorendic	24	120	17	5.9	0.85	80	11	7.58	1.10	140	21
	34	160	23	6.89	1.00	120	18	9.65	1.40	120	18
	40	190	28	9.65	1.40	140	20	9.65	1.40	120	18
Vinyl ester	25	110	16	5.4	0.79	86.2	12.5	6.96	1.01	180	26.5
	35	260	37.3	9.52	1.38	153.4	22.25	10.8	1.56	230	34
	40	220	32	8.89	1.29	160	23	11.0	1.59	210	30

Vinyl esters (VE) resins are formulations that combine epoxy resin and unsaturated carboxylic acid. They share some desirable properties of polyesters and epoxy. VE resins can be used in all applications that require unsaturated polyester resins, and they offer better corrosion and water resistance compared with general purpose unsaturated polyester resins. At the same time, VE resins have fewer crosslinks in their microstructures, resulting in better flexibility compared with general purpose unsaturated resins. VE resins cost more than unsaturated polyester resins.

2.2.5 Thermosetting resins: epoxies

The first epoxy resin was produced simultaneously in Europe and the United States in the early 1940s. Epoxies have some unique characteristics and useful properties that differentiate them from other

thermoset resins. Epoxy resins require low applied pressure in the liquid state during production, compared to other thermosetting resins. Cured epoxy products show lower cure shrinkage and lower residual stresses than other thermosetting resins, especially unsaturated polyester resins. Using different curing agents, epoxy resins can offer wide operating temperature ranges and different viscosities, from tack-free solid to low-viscosity liquid. Epoxy resins are widely used in several fields including structural adhesives, coating, electrical laminates and engineering composites [17].

Epoxy resins can be divided into two categories: glycidyl and non-glycidyl. Glycidyl resins can be further divided into glycidyl-ether, glycidyl-ester, and glycidyl-amine. Di-glycidyl-ether of bisphenol-A (DGEBA) produced with glycidyl ether is one of the most widely used difunctional epoxies. Multifunctional epoxies, known as novolac epoxies, are also grouped in this category. Multifunctional epoxies result in products with tighter crosslinking, leading to higher performance and functionality. For example, tetraglycidyl-methylenedianiline offers excellent mechanical properties and high glass transition temperatures [22].

Non-glycidyl epoxy resins include aliphatic epoxy which has high reactivity but low glass temperature; cycloaliphatic epoxy which has good electrical resistance, weatherability, and chemical resistance.

Overall, epoxy resins offer strong advantages over polyester and vinyl esters, including better bonding properties, superior mechanical properties, higher resistance to fatigue and cracking, reduced degradation from moisture and increased surface resistance to water [23]. But epoxy resins also suffer from limitations such as shrinkage during cure at an average of 0.0026 cm/cm compared with 0.001 cm/cm from polyesters, long cure times, high cure temperatures, poor stress-strain ratios, water

absorption and high costs [23]. Table 2.11 lists average properties for epoxy moulding compounds.

Table 2.11 Average properties for epoxy moulding compounds [24]

Properties	Data In Metric Unit	Testing Method
Density	1.78 g/cc	-
Water Absorption	0.18%	ASTM D570
Linear Mold Shrinkage	0.00257 cm/cm	ASTM D6289
Rockwell Hardness, M	98.3	-
Ultimate Tensile Strength	85.2 MPa	ASTM D638
Modulus of Elasticity	17.3 GPa	ASTM D639
Flexural Yield Strength	136 MPa	ASTM D790
Compressive Yield Strength	195 MPa	ASTM D695
Izod Impact, Notched	3.06 J/cm	ASTM D256
Process Temperature	172 ℃	-
Glass Transition Temperature	174 ℃	-
Deflection Temperature at 1.8 MPa	248 ℃	ASTM D648
Deflection Temperature at 8.0 MPa	145 ℃	ASTM D648

2.3 Manufacturing methods for thermoplastics

In November 1938 the world-famous glass fibre manufacturer Owens Corning was launched, making the beginning of the glass fibre industry. In 1942, unsaturated polyester reached the market. Then, composites made of glass and polyester were manufactured, leading to the fibre reinforced polymer (FRP) industry. In following years and decades, FRP's good mechanical properties, relatively low density and ease of manufacturing lead to increasing usage in aerospace and military applications. Thermoset composites are polymer-based composite featuring a matrix with excellent structural properties, but limited by unstable chemical properties before cure. However, this enables unique ways for thermoset resins and composites to be handled during manufacturing. Still, limited shelf life remains a weaker point. Furthermore, into the 21st century, difficulties in recycling along with other limitations

gave renewed prominence to the potential of thermoplastic composites.

2.3.1 Short fibre reinforced thermoplastics

Short fibre reinforced polymers (SFRP), or short fibre reinforced thermoplastics (SFT) have become very popular for various applications as adding structural fibres offers numerous important advantages, with very few shortcomings. Structural fibres refer to aramid fibres (AF), basalt fibres (BF), carbon fibres (CF) and glass fibres (GF). Other man-made fibres are less prevalent, and so they are not discussed as a primary concern [25].

Fibre/matrix interaction is an important concept in fibre-polymer composites, and one key factor is the critical fibre length, since if the fibre length is shorter than a critical value, the fibre will be pulled out from the matrix while encountering tension, hence the tensile strength of the composite will be determined by interfacial adhesion. On the other hand, fibres longer that the critical fibre length will be broken by tension applied on the composite, hence the strength of the composite will be determined by the fibres and fibres broken under tension will be used to their full reinforcing potential.

Fibre length in SFTs is greatly reduced to ensure easy manufacturing using traditional injection or extrusion equipment. Therefore, stronger interfacial adhesion will be sought, promoted by silane-based functional groups and maleic anhydride grafted agents.

Injection and extrusion are the preferred techniques for producing SFTs, since SFT composites have relatively low fibre volume fractions hence fibres have good mobility inside moulds. Special care is required such as usage of a twin-screw extruder being preferred to comparable single screw extruders, since the former will give SFT compounds better preparation and mixture [32]. Also, fibres are often

fed into the molten polymer later along the screw in the extrusion process, to protect the fibres from breakage. Compression moulding is also used for manufacturing using SFTs.

2.3.2 Long fibre reinforced thermoplastics

Long fibre reinforced polymer (LFRP) or long fibre reinforced thermoplastic (LFT) composites offer superior specific modulus, strength and impact resistance compared to SFTs due to higher volume fractions of longer reinforcing fibres. This is yet another confirmation for the number one rule of design with composites: fibre volume fraction is one of the most important metrics. Figure 2.2 shows the effect of fibre content on tensile and flexural strength of GF/PP LFT composites, and Figure 2.3 shows the relationship between fibre tensile stress, interfacial shear stress and fibre aspect ratio. However, superior mechanical properties come at the expense of processability.

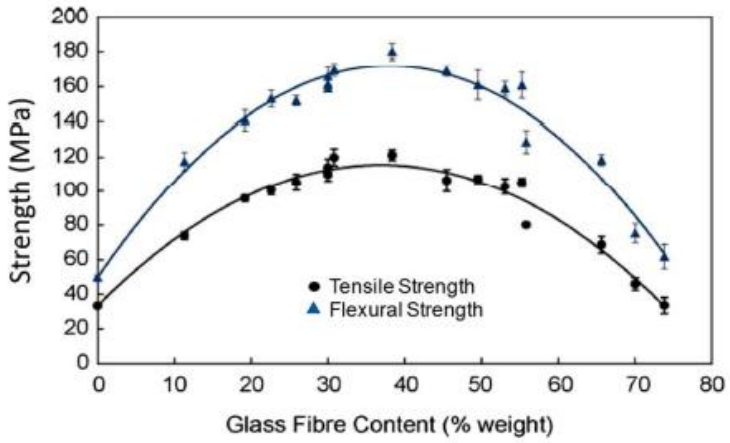

Figure 2.2 Effect of fibre content on tensile and flexural strength of GF/PP LFT composites [26]

Calculating the critical fibre length and critical fibre aspect ratio is important in engineering LFT composites. Equation 2.1 enables this calculation, where l is the fibre length, d is fibre diameter, σ_{fu} is the ultimate tensile strength of the fibre, and τ is the interfacial bonding strength between the fibre and

matrix [27].

$$\left(\frac{l}{d}\right)_c = \frac{\sigma_{fu}}{2\tau} \tag{2.1}$$

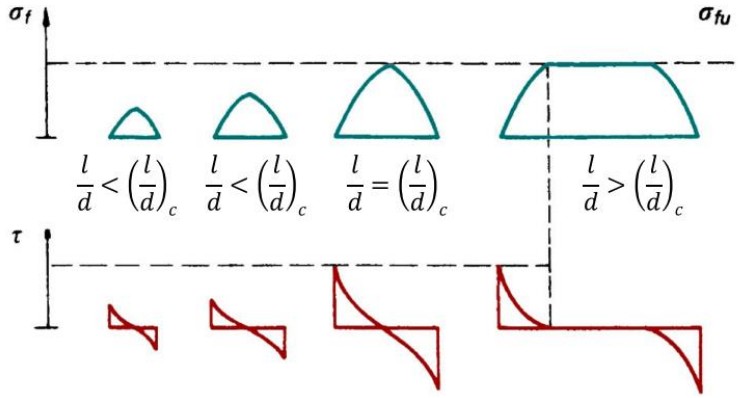

Figure 2.3 Change in fibre tensile stress and interfacial shear stress with fibre aspect ratio [28]

For example, the critical fibre length for kenaf fibres in a PP matrix was calculated to be 2.4 mm for a fibre tensile strength of 374.5 MPa, fibre-matrix interfacial shear strength of 4.9 MPa, and average diameter of the kenaf elementary fibres of 62.2 μm [29]. The critical fibre aspect ratio is approximately 39.

The following figures illustrate two different, general routes for producing LFT parts. The first indirect route consists in extruding LFT pellets, Figure 2.4. The pellets can then be processed into parts using hot melt impregnation, commingling, power impregnation or wire coating [30]–[33].

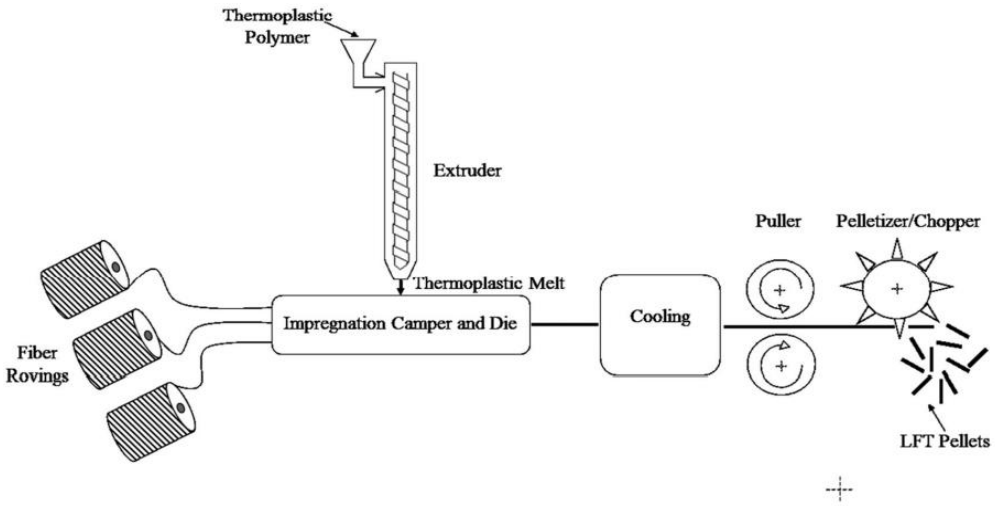

Figure 2.4 Schematic diagram of LFT pellet production [27]

Figure 2.5 shows two direct routes for manufacturing parts from LFT composites called LFT – D (Direct). The direct route eliminates cooling, packing, handling, shipping, and reheating the pellets. These unique advantages can directly reduce costs. Hence, direct processes are becoming increasingly popular for in-site production. [27] But either LFT or LFT-D share one limitation that is the product have to be processed with compression moulding. And the results from that are firstly, greater initiation capital and risk are involved for any project to start due to the cost of making metallic mould. Secondly, the LFT lack of the ability to produce shell or panel structure with ease limits its degree of freedom to expand its usage in many industries such as construction industry which have high interests in light weight and strong sandwich panels.

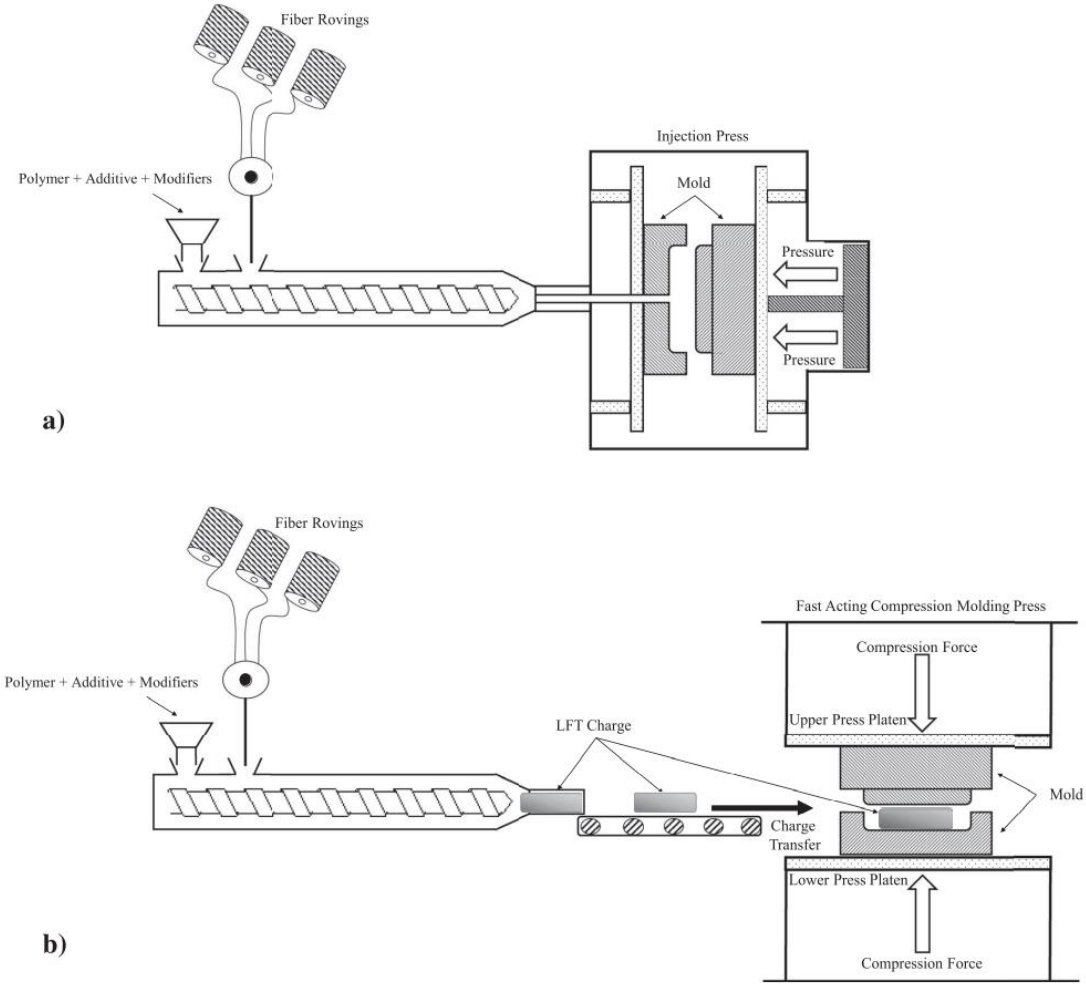

Figure 2.5 Schematic diagram of direct, inline compounding LFT-D processes: a) compression moulding and b) extrusion compression moulding (ECM) processes [27]

2.3.3 Glass mat thermoplastics

Glass mat thermoplastic (GMT) were developed by PPG Industries in the mid 1960s. Figure 2.6 shows an automotive application of GMTs from 1986; the C4 Chevrolet Corvette used up to 18.1 kg of AZDEL's continuous randomly oriented glass mat composite for semi-structural and non-structural, non-exposed elements of the car such as seat structures, trays, etc. [34].

Figure 2.6 GMT parts used in C4 Chevrolet Corvette produced from 1983 to 1996 [34]

The main process for producing commercial grade glass mat reinforced thermoplastic is melt impregnation [35]. The process begins with a specific glass mat used in the GMT manufacturing process, made by laying continuous strands of fibres randomly on a conveyor belt and using needles to push fibres down into the thickness direction of the material. Then the glass mat is combined with molten thermoplastic and forwarded into a double belt conveyor system with heating, pressing and cooling, Figure 2.7.

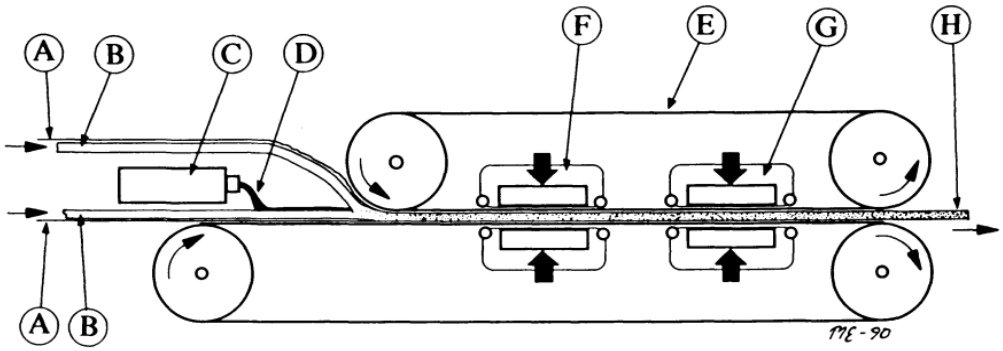

Figure 2.7 Schematic diagram of GMT melt impregnation machine: A) thermoplastic film overlay; B) glass fibre mat; C) extruder; D) thermoplastic extrudate; E) double belt laminator; F) heating zone; G) cooling zone; H) sheet semi-product [35]

The GMT semi-product is then cut to desired size and stored for use as blanks. When processing the semi-product into parts, a rapid procedure is followed as shown in Figures 2.8 and 2.9. The GMT blanks are heated in an infra-red oven, and then dropped into a mould to be pressed. The GMT blanks remain under compaction pressure of 70 to 400 bar until the solidification temperature of the matrix is met; for polypropylene GMT, this is typically below 200℃ [36].

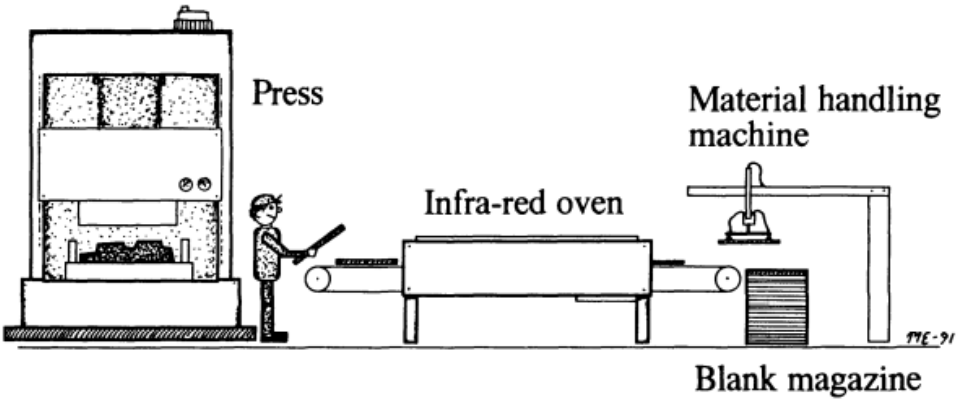

Figure 2.8 GMT thermoforming process [36]

GMT technologies based on PP and GF see widespread use in the automotive industry [34]. However, due to their inhomogeneous microstructure resulting in part from two processing steps, the materials show high variability in their mechanical property, making it difficult for design engineers to use them in more demanding applications [43]. Many solutions were attempted, such as adding minerals into the resin, but overall GMT strength hardly extends beyond 100MPa which is significantly lower than the glass fibre reinforced thermoset composite mentioned in early chapters [43]. Recent work has measurably improved GMT consistency and reduced the variability of mechanical properties, by providing consistent fibre layout [37].

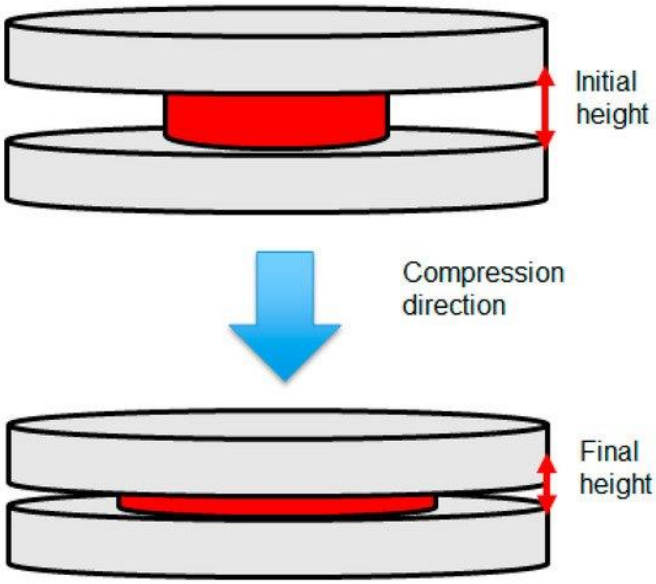

Figure 2.9 Schematic diagram of GMT compression [37]

2.3.4 Continuous fibre reinforcement thermoplastics

Composite materials based on thermoplastic polymers offer are suited to a wide range of applications and many different end usages as described above. However, the main advantage of polymer-matrix composites is their stiffness-to-weight ratio which, in many cases, is larger than common metal alloys such as steels, aluminums and others. SFTs, LFTs and GMTs discuss above do not represent the best available technologies and solutions in that regard, primarily because of limited fibre volume fractions, partial or no control over fibre placement and orientations, and limited impregnation ability. Continuous fibre reinforcement thermoplastics (CFRT/CFT/CFRTP) offer a superior alternative.

CFT prepregs are made by impregnating continuous aligned fibre strands into a thermoplastic resin. This can be accomplished using solution impregnation, melt impregnation, film stacking, powder impregnation, fibre commingling and in-situ polymerization. Two variations of one impregnation

technique relevant to this work, melt impregnation, is illustrated in Figure 2.10. [38]

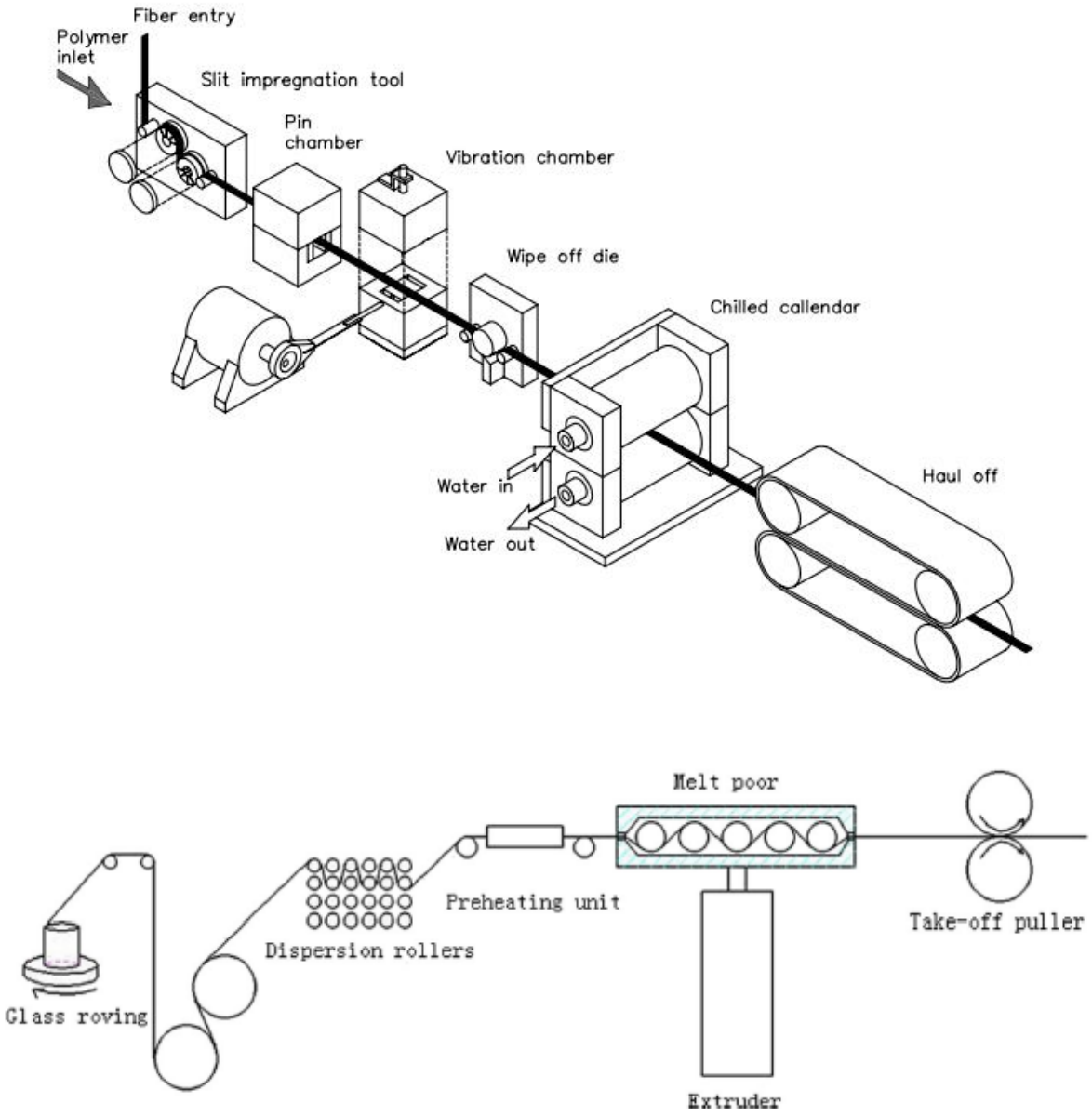

Figure 2.10 Schematic diagram of in-situ melt impregnation production line (top) [38], and a different approach (bottom) [39]

The key point of the process is to lay the fibres evenly and subjecting them to good levels of tension, which facilitates thorough impregnation. PP/GF unidirectional prepregs have shown tensile properties ranging between 400 and 600 MPa [40], even up to and beyond 800MPa from internal tests performed

at Haitie and others, from regular glass fibres, data in later test would substantiate this. Even the minimum strength number provided above largely exceeds similar numbers obtained for any other thermoplastic composite form or semi-product mentioned in previous pages, confirming the value of CFT technology.

Among all CFT production methods, melt impregnation is the most widespread. The reason is as simple as the process: letting fibres go through molten polymer, will result in the fibres being impregnated with said polymer. Whilst the principle is easily understood, many details must be addressed carefully. For instance, higher viscosity molten polymers are more difficult to flow through and penetrate completely into fibre yarns or bundles. Numerous studies were published to optimize CFT production and properties, so that the semi-products and products may be more successful. Kim [41] found that pressure is a major parameter for thermoplastic resin impregnation in CFT composites, working on PEEK/CF systems. Peltonen and Tormala [42] studied the effects of temperature, time, pressure, contact surface length between fibre and mould, tension on fibre and melt flow rate on PP-based CFT composites and found that increases in polymer temperature resulted in an increase in impregnation. The pin assisted impregnation mould is shown below in Figure 2.11. Gaymans [42] analyzed PP/GF CFTs with pins and results showed that during manufacturing, pin diameter, tension in the fibres and melt viscosity are key factors for impregnation. Furthermore, Bates [43], Nygard [38], Ren [39], [44], Ngo [45], Fang [40] and many others worked on optimization of CFT prepregs found similar aspect to control CFT impregnation rate.

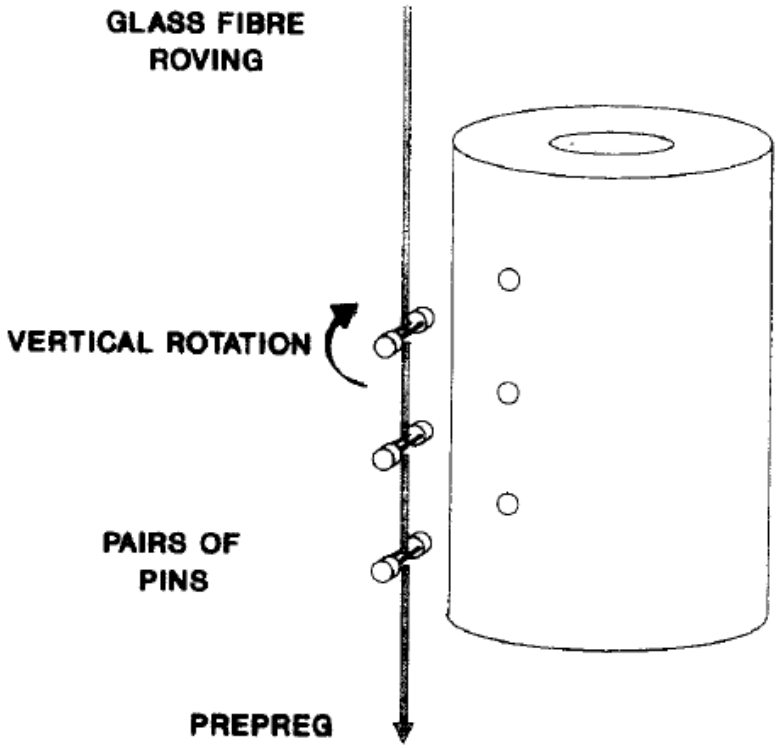

Figure 2.11 The crosshead melt impregnation mould consisting three pairs of pins that could be rotated, fibre roving is pulled around those pins [42]

2.4 CFT melt impregnation process

Melt impregnation was selected as the main research direction for this work due to its clear advantages; furthermore, melt impregnation production lines are simple, flexible and easily controlled. Film stacking requires an additional film extrusion process; despite the ubiquitousness of thin polymer film, manufacturing said film is not easy, and it is even more difficult to do so economically for relatively small volumes because such production line won't start and stop so conveniently. Furthermore, film production deviaties from Haitie's composite material focus. Solution and powder impregnation share similar raw material supply issues; polymer pellets are far easier to source than special solutions and ground polymer powers, and they also make manufacturing lines more complex. Fibre commingling was eliminated due to its relatively low potential mechanical properties, and limited

flexibility and potential for product modification.

Melt impregnation is easy to implement. However, many aspects must be considered. As discussed above, general configurations and designs were proposed for manufacturing lines, which can provide some degree of freedom on adjustments. Discussions with equipment suppliers were conducted by the author.

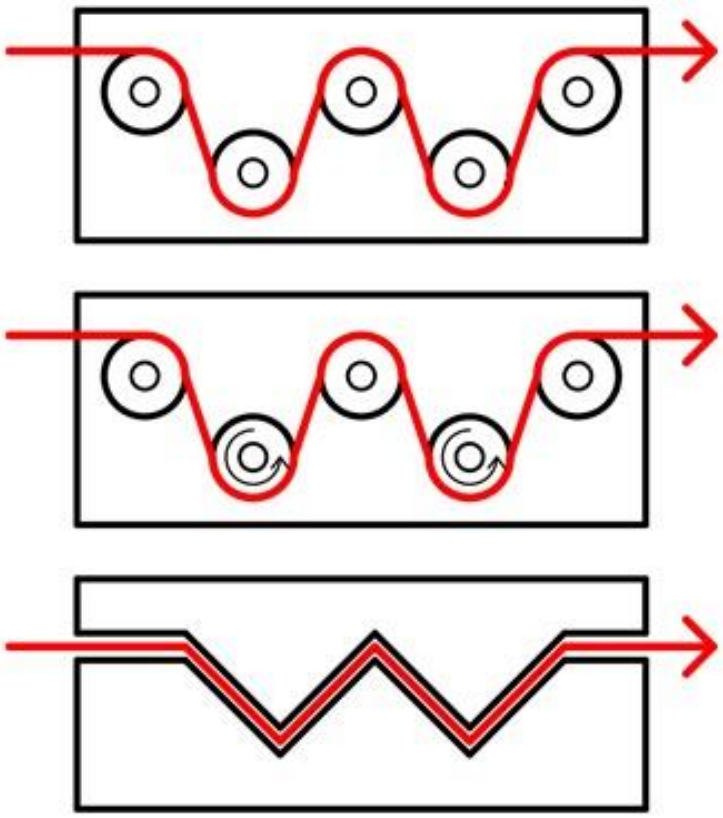

Figure 2.12 From top to bottom, three types of melt impregnation moulds: pin assisted; roller assisted; corrugated plates

Different designs can be chosen for the impregnation mould, Figure 2.12: pin assisted impregnation pool, roller assisted impregnation pool and corrugated plates. Pros and cons were discussed for these

methods and the design of the impregnation was finalized as a corrugated plate configuration. Pin and roller assisted impregnation pools offer advantages whereby the distance and diameter of pins and rollers can be modified easily; however, this does not translate to real benefits in industrial settings. Furthermore, the design of roller assisted mould have higher maximum production rates as they reduce tearing of the fibres from fibre mould contacting surface. But the disadvantage of pin and roller assisted mould are clear to see as well, they require a large amount of polymer to fill up the impregnation chamber which led to wasting polymer and uncontrollable oxidation caused by overstay of the polymer. Other than that, this chamber also puts limitation on polymer selection, polymers with low melt index will have a difficult time flow inside the impregnation chamber. On the other hand, corrugated plates have better stability, are much easier to maintain, and waste less polymer due to their much smaller cavity for polymer to fill up. They still offer flexibility on impregnation angle around the edge of the wave by adjusting upper and lower mould distances.

CFRTP manufacturing theory related with melt impregnation will be discussed in Chapter 3, further chapters will focus on set up and compare the application results with suggestions from related research.

2.5 Conclusion

CRT is not an emerging technology, as it has been studied in the last few decades [41]. The earliest research associated with continues fibre reinforced thermoplastic composites found for this work dates from 1988. However, CRT is not as widespread as other mass-produced PMCs including SMC (Sheet Molding Compound), PCM (Prepreg Compression Molding), SFT, LFT and GMT. These latter materials are either based on thermosetting resins that offer superior mechanical properties to utility

thermoplastics, or their high-volume processing is easier and faster in the case of SFT and LFT, which can be injected. Usage of CFT materials in the global market is only around USD 0.3 billion, which is a small portion comparing to the overall composite material market, sized at USD 86.4 billion [46]. However, sustainability issues have driven customers towards solutions that are cost efficient whilst reducing environmental damage compared to SMC due to the ease of recycle feature of thermoplastic, whilst offering higher fibre volume content than SFT, LFT or GMT. CFT offers a compelling alternative not just on its performance but also another way to produce large surface shell or panel structure; as a result, the market for CFT has shown a 9.3% growth in the market size by 2020 [47].

Chapter 3: Physical phenomena

Chapter 3 reviews aspects of micromechanics, optimization of composite interface and physical phenomena involved in melt impregnation process for CFT, which shall be considered towards material selection and manufacturing line design and optimization. Testing methods used on CFT prepreg are also discussed in this chapter.

3.1 Fibre-polymer interface optimization

A major factor in determining the properties of a polymer-based fibre reinforced composite is its fibre volume fraction. Achieving high mechanical properties for composites requires the presence of many very fine fibres in close alignment, distributed in and saturated with the polymer matrix. Reinforcement wettability is important in letting the matrix impregnate the fibres fully [49].

Beyond good impregnation, the matrix and reinforcing fibres also require good adhesion, especially for the case of transverse loading. Composites reinforced with continuous fibres are loaded in directions deviating from fibre orientations, hence loads must be transferred from the matrix to the fibres through the interface between the two materials. Optimization of adhesion between the materials has been recognised as a very important factor [48]. Various solutions were studied for improving fibre-polymer adhesion but silane-based coupling agents are still the most prevalent and widely used solutions [40].

An interface in composites is not simply the contacting geometric surface between the polymer and reinforcing material. Rather, the interphase is a transition zone including the geometric surfaces on the polymer and reinforcing material sides, along with a thin layer in the polymer which will feature

different morphology [50]. The interface and interphase feature both mechanical and chemical bonds. Generally, stronger bonds lead to greater strength but in some cases, a tailored interfacial strength can improve moduli and toughness [50]. Glass fibre reinforced, phenolic resin composite illustrate the case in point, as the lower mechanical strength of such composites is not mostly due to voids in the resin, but to the fact that coupling agents and sizings applied on the surface of glass fibres are designed for better adhesion to polyester and epoxy [49]. This results in a weak binding interface between the matrix and fibres, even as the resin can impregnate the fibres effectively. Figure 3.1 shows one set of SEM images with Vetrotex® 1200 tex glass yarn and Borealis® PP polymer. The only difference between the two images is that the matrix in image (b) was modified with 5 wt% PP-g-MAH, resulting in a significant and visible change in binding conditions.

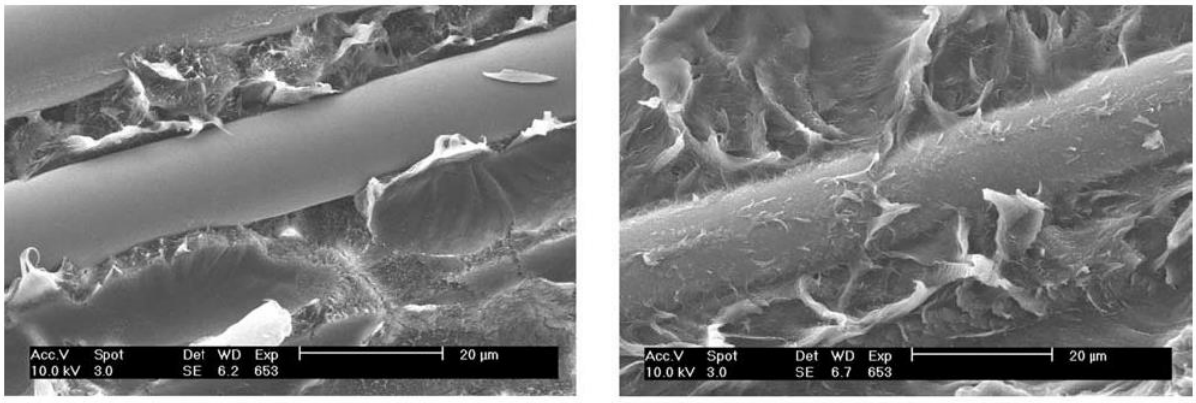

Figure 3.1 SEM images showing: (a) weak coupling between glass fibres and PP matrix, and (b) good coupling between fibres and matrix for the same glass fibre and PP matrix, modified with 5 wt% PP-g-MAH [50]

3.2 Impregnation rate

Difficulty in impregnating reinforcement fibre with a highly viscous resin is a major issue in

thermoplastic composite manufacturing. Nygård's study, based on Darcy's law, Equation 3.1, compared differences between water flowing through sand beds and resin flowing through a fibres bed [38]:

$$u = \frac{dL}{dt} = \frac{K}{\mu} \cdot \frac{dP}{dL} \tag{3.1}$$

where u is the velocity of the fluid, dP/dL is the pressure in the flow direction, K is the permeability which is a function of the porosity of the structure, and μ is the fluid viscosity. Figure 3.2 illustrate the concept of resin flow along different directions through a porous bed of aligned fibres.

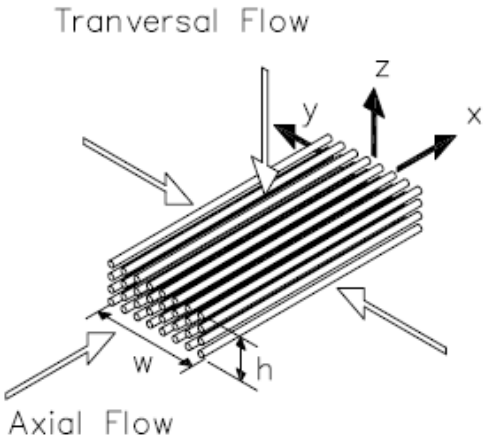

Figure 3.2 Resin flow along different directions through a porous bed of aligned fibres [32]

During this process, the polymer temperature should be increased as high as possible below the decomposition temperature in order to reduce its viscosity. Peltonen and Tormala [51] conducted an experimental study of melt impregnation parameters, comparing the degree of impregnation of prepregs. The degree of impregnation was quantified as the area impregnated divided by the total tow area. Samples were cut into 10 mm pieces and one end was coloured. The number of unimpregnated fibres were counted and the degree of impregnation was calculated. With all parameters kept the same, an increase in polymer temperature form 180 ℃ to 230 ℃ increased the degree of impregnation from

0.711 to 0.895, Figure 3.3.

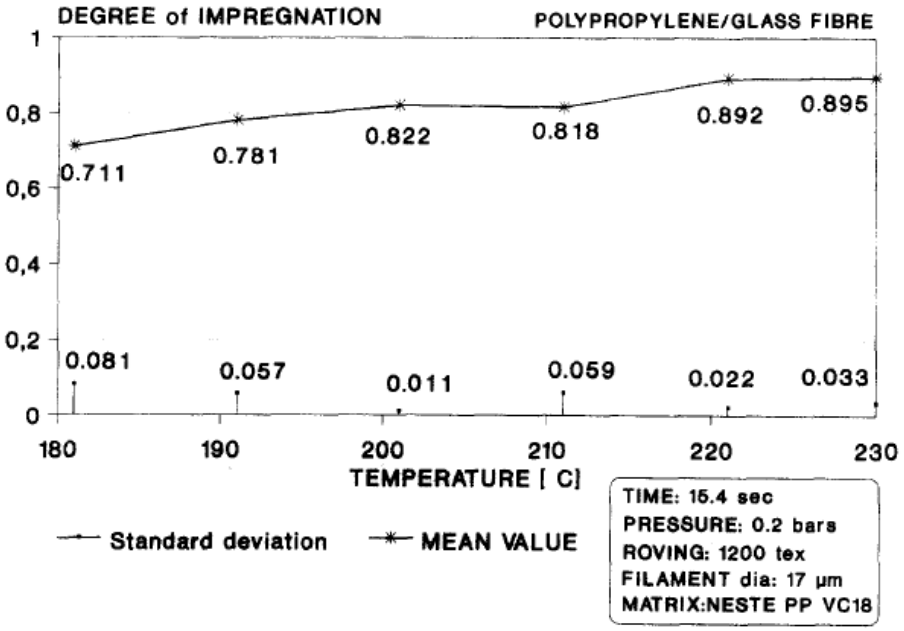

Figure 3.3 Degree of impregnation as a function of polymer temperature [42]

The effect of temperature was also demonstrated by Ren [39], combining Reynold's equation and Darcy's law and using a mathematical model to check the melt impregnation rate of PP in glass fibres. Kim's study of PEEK/CF prepreg [41] and Jia's recent work on PA66/CF [52] also proved the point. In Haitie's laboratory, samples of PP M60T were tested; the melt index showed great increase after polymer temperature exceeded 230 ℃. Conversely, PP samples showed some yellow macula after a short time at a temperature of 280 ℃.

Nygård [38] identified the permeability K as a function of the fibre diameter since viscosity was identified as a scalar entity in his work. Three different productions methods were used in trying to optimize fluid velocity in the transverse direction, they are radial slit impregnation; regular pin assist melt impregnation with 8 pins; crosshead pultrusion with rolls, vibration and ultrasonic assisted.

Impregnation set up will be shown in Figure below. With viscosity set at one value, Nygård found that lower impregnation speeds lead to better impregnation, almost across all three different impregnation methods. Gayman's [42] and Peltonen's [51] early experiments, and Kim's [41] mathematical model also support Nygård's finding.

However, since it was not practically feasible at Haitie to monitor actual impregnation online and in real time as the production line was installed, and the final purpose of this work is not primarily to test the impregnation rate, the speed of the production line will be set to the maximum speed allowable without visual dry fibre area appearing. Tests reported in later Chapters enable evaluation of prepreg impregnation through mechanical behaviour.

According to Darcy's law, increased pressure gradient in the fluid will increase speed of fluid flow inside the fibre bed. In industrial practice, increased pressure levels have two effects. They do increase the flow rate inside fibre bundles, but pressure also applies on the fibre bundle thus, causing them to collapse onto themselves and decreasing the porosity of the fibre bed. Still, Kim and Seo [41] proved that the net effect of an increase in pressure is increased impregnation.

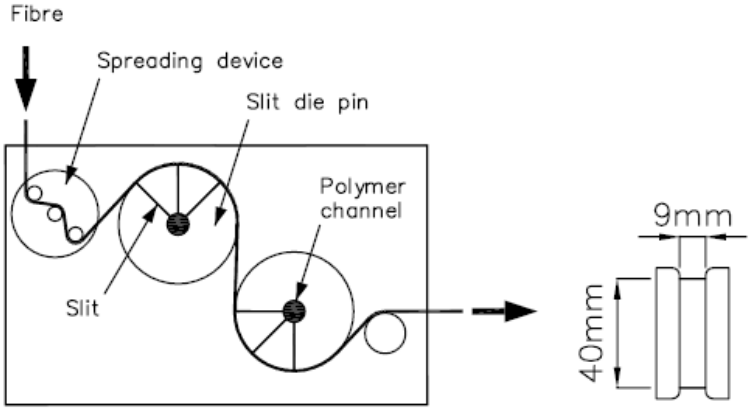

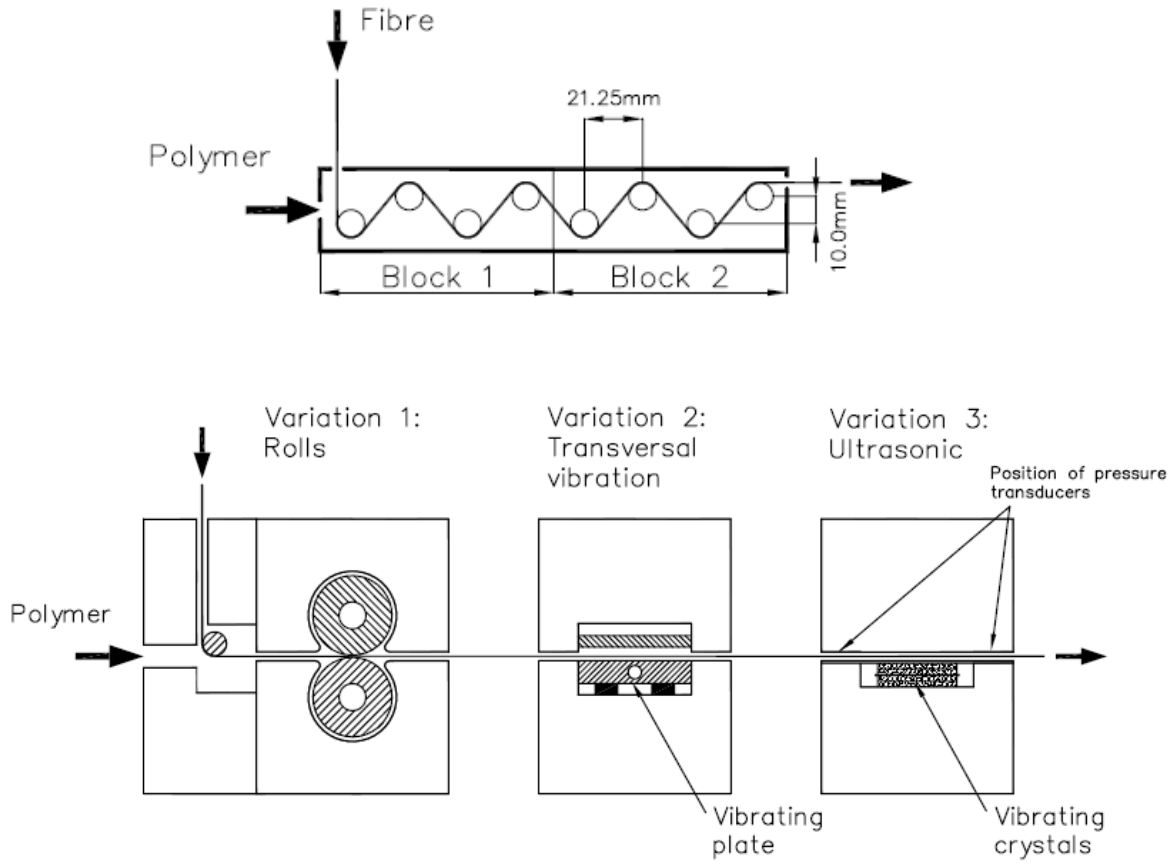

Figure 3.4 Diagram of three different production method Nygård used: radial slit impregnation; regular pin assist melt impregnation with 8 pins; crosshead pultrusion with rolls, vibration and ultrasonic assisted

Pressure on the fluid and fibres can be generated in a few different ways. The first is simply to increase the injection pressure of the molten polymer, in cases where the impregnation mould is a closed environment. Unfortunately, this does not apply in most cases: CFT impregnation moulds are usually semi-closed mould with numerous paths for pressurized fluid to escape, causing waste and other problems.

Furthermore, Peltonen [42] demonstrated that isotropic pressure is not always conducive to better impregnation. The author built an impregnation device to study the relationship between isotropic pressure of the molten polymer and degree of impregnation of the prepreg. However, results showed

that higher levels of isotropic pressure in the molten polymer lowered the impregnation rate, which is contradictory with Kim and Seo's finding, this leaves question to above research credibility thus test must be set up for this specific CFT production line and the result will justify which information provided by literatures is correct and suit for this CFT production solution. The second method for generating pressure on the molten polymer is easier to apply, and it is one of the reasons why melt impregnation is the most widespread CFT production method. With either pin, roller assisted or corrugated fluid tunnel moulds, fibres contact the pins/mould and are pushed against them. With mould filled with molten polymer, the bulges/pins apply pressure on the polymers that flows into fibre bundles at such locations.

At last, the wedge area formed by resin between a pin and a fibre bundle is where pressure builds up and forces the molten polymer into the fibre bundle. Figure 3.5 illustrates the wedge area formed by molten polymer. Ren [39] and his colleagues' mathematical model mentioned above also given the exact way to calculate the melt pressure distribution in the wedge. The authors further found that under same temperature and pulling speed, larger pin radius R and a greater number of pins lead to better prepreg impregnation. This knowledge was used in the design of the impregnation mould with the production line supplier.

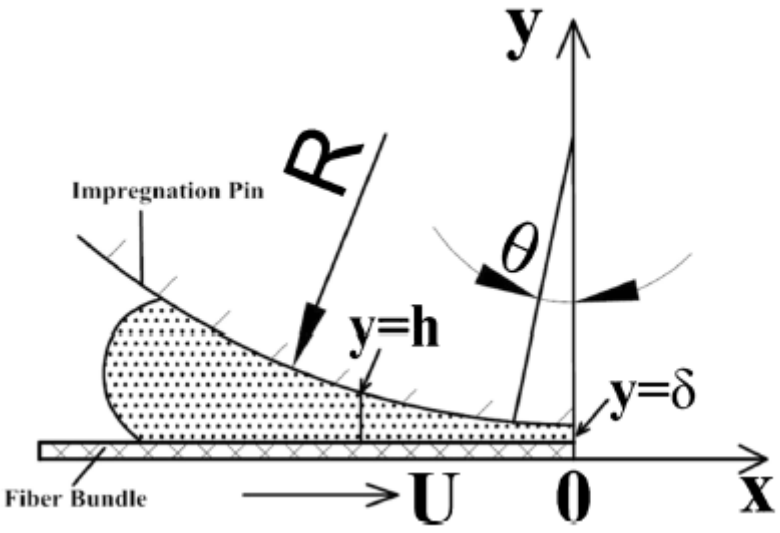

Figure 3.5 Wedge area between impregnation pin and reinforcing fibre [39]

3.3 Testing methods

Standard ASTM D3039 Standard test method for tensile properties of polymer matrix composite materials [52] is the general test method for tensile properties of fibre resin composite, and it has been used widely as a foremost composite material testing standard. ASTM D3518 Standard test method for in-plane shear response of polymer matrix composite materials by tensile test of a ±45° laminate [53] similarly establishes the practice for in-plane shear stress-strain response of unidirectional composites. In this work, both methods were considered carefully but it was decided not to use them for characterization tests, for the following reasons.

The semi-product to be evaluated in this work is a unidirectional prepreg in the form of a thin tape. Standard ASTM D3039 requires samples of a certain thickness to be positioned and held between grips. Making the prepregs into laminates is possible, but the thermoforming or thermal binding processes required to do so will further melt and pressurize the polymer, as well as consolidate the composite,

leading to changes and taking testing results further away from a characterization of the original prepreg. Besides, thermal binding of laminates is time-consuming for the number of samples and tests to be used in this study, and the process of thermal binding itself will require its own probing and optimization trials once the prepreg is optimized as part of this work – optimization of thermal binding is outside of the scope of this thesis.

Tests conducted directly on prepreg still raise issues, for two reasons. Dumbbell samples would effectively solve the issue of stress concentrations caused by clamping forces at the grips, which tend to cause premature failure at the grips and underestimate the failure properties of the prepreg as a result [54]. The problem might be magnified in the present case as it is more difficult to distribute the tensile load evenly in thin prepreg. Alternatively, metal taps joined adhesively to the prepreg on both ends would likely be unreliable as slippage may occur, since adhesive joining to PP is notoriously difficult to achieve.

Testing methods used by Nygård, Figures 3.6 and 3.7 were considered for this work. The single fibre pulls out test was deemed not sufficiently representative of the performance of the prepreg as a whole, which focuses on quantifying how CFT production variables affect product quality for unidirectional prepreg. Furthermore, straightforward measurement of tensile properties was deemed more useful in a first phase of the development of the semi-product, and so the tests were not considered.

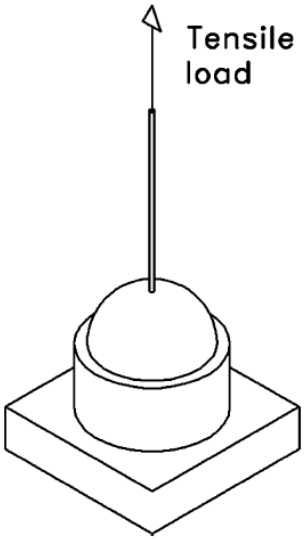

Figure 3.6 Single fibre pull out test [48]

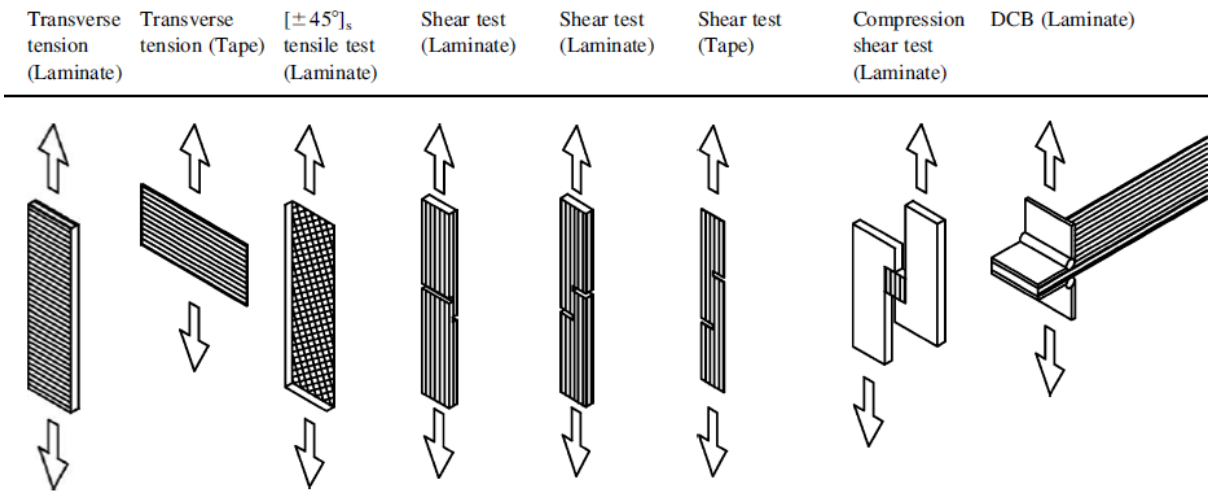

Figure 3.7 Various testing method for continuous fibre reinforced composite [48]

One way to quantify the tensile behaviour of the prepregs was identified. Apparatus dedicated to the testing of cables and belts was selected. Figure 3.8 shows a tensile test being conducted with said apparatus. The benefit of the apparatus is that after the prepreg is wound around pins, it locks in place. When the machine starts extending the sample, the larger radius of the pins help lowering internal stresses applied on the attachment points of the prepreg. As a result, tensile failure is much closer to the

real number. However, it is more difficult to identify a precise value of the gauge length when testing with this apparatus, as the prepreg is not fully locked in place at the beginning of the test.

To remediate the situation and find the true displacement in order to calculate the true moduli of the unidirectional tapes, tensile tests were performed using usual grips on a selected group of single layer of prepreg, and moduli measured with both methods for such group were used in identifying a factor 'X' representing the difference in displacement from two methods. Gauge length to be used with the apparatus shown on the left side of Figure 3.8 were measured from the middle of upper and lower of the largest pin. And this is done for every tensile test after the unidirectional prepreg is secure to hand tight.

This simple conversion came from the use of Young's modulus' Equation 3.2:

$$E_t = \frac{\sigma_t}{\varepsilon_t} = \frac{F_d/A}{\left(\frac{\Delta L_d}{L_d}\right) * X} \tag{3.2}$$

where E_t is the true Young's modulus of elasticity, σ_t is the true stress obtained by tensile test using dedicated apparatus, ε_t is the true strain obtained by apply factor 'X' from Equation 3.3 to strain obtained using dedicated apparatus. L_d is the initial length between the middle of upper and lower of the largest pin for dedicated apparatus after the prepreg is secured to hand tight. ΔL_d is the change in distance after the failure for prepreg for dedicated apparatus. L_t is the initial distance between the upper and lower clamps of typical apparatus after the prepreg is secured. ΔL_t is the change in distance after the failure for prepreg for typical apparatus.

$$X = \frac{\varepsilon_t}{\varepsilon_d} = \frac{\left(\frac{\Delta L_t}{L_t}\right)}{\left(\frac{\Delta L_d}{L_d}\right)} \tag{3.3}$$

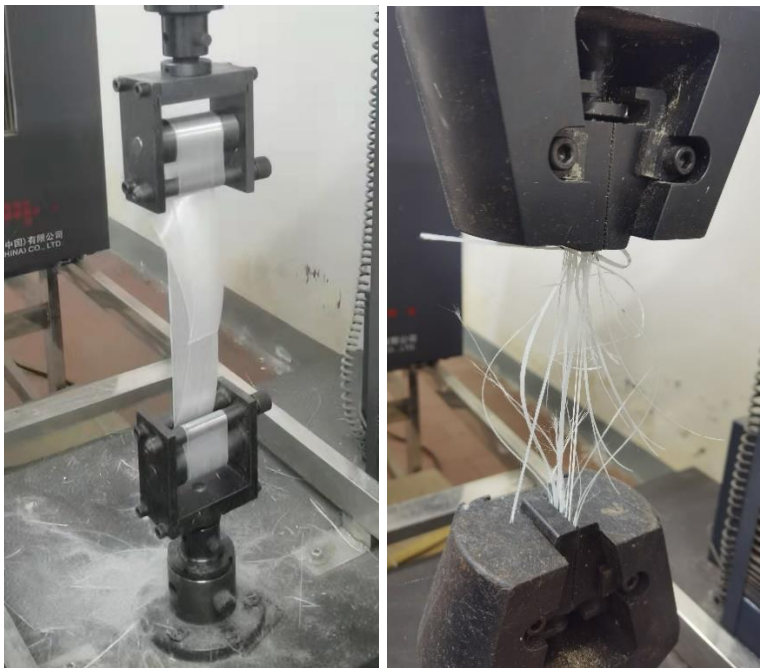

Figure 3.8 Dedicated (left) and typical (right) apparatus for conducting tensile tests on prepreg

Other method could replace this conduct such as using gauges for testing, but Haitie have no such luxury to obtain one in the sense of time and cost, marking the prepreg with two lines and measure the distance difference before and after is difficult because the prepreg will shattered into small strips, using high speed camera is also not feasible. Ten samples were used for each of the 16 subgroups of prepreg semi-product tested for this work. Sampling was not limited to the middle of the prepreg semi-product, but collected in the machine and cross directions, evenly. Thus, considering standard deviations for each subgroup, it is possible to determine whether the semi-product has even performance along the production line.

Chapter 4: Manufacturing set up, trails and analysis

4.1 Materials selection

In this project, a chemical silane-based crosslinked coupling agent was present on the glass fibres, which reacts with hydroxyl groups on the surface of the fibres. Coupling agent application is done during manufacturing of the glass fibres, hence industrial fibres grade was selected in terms of featuring a coating agent specifically developed for thermoplastic melt impregnation process.

Several different industrial fibres suited for melt impregnation were considered, Table 4.1. In part due to availability and supply chain issues, fibres SE4805-1200TEX produced by Owens Corning were selected for producing prepreg in the context of this work.

Table 4.1 Overview of industrial fibres considered for CFT unidirectional prepreg production

FIBRE	SUPPLIER	GRADE
GF	Owens Corning	SE4805-1200TEX
GF	Owens Corning	SE4805-2400TEX
GF	Taishan Fibreglass	T838G-600TEX

Similarly, polypropylene M60T produced by Sinopec Zhenhai was selected as the standard PP for prepreg manufacturing process optimization, Table 4.2. All five polymers listed below were compatibile with the production method, but M60T shows more flexibility and forgiveness in early trials, Figure 4.1; it was also one of the more economical options at the time.

Table 4.2 Overview of industrial polymers considered for CFT unidirectional prepreg production

MATRIX	SUPPLIER	GRADE	POLYMER TYPE	MELT INDEX (ASTM D-1238)
PP	SINOPEC LUOYANG	MN70	Homopolymer	70
PP	SINOPEC ZHENHAI	M60T	Homopolymer	60
PP	SINOPEC YANSHAN	K7100	Copolymer	100
PP	SK	BX3900	Copolymer	60
PP	SK	BX3920	Copolymer	100

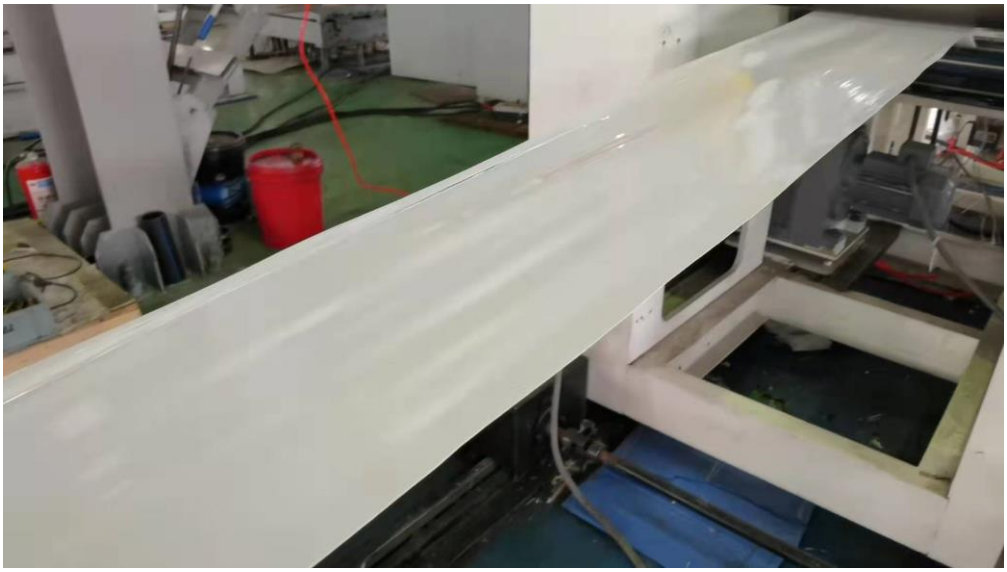

Figure 4.1 Photograph taken during early manufacturing trials

4.2 Cost evaluation

The final goal for the industrial manufacturing line studied in this work is to create business value while

improving the understanding the technology of advanced thermoplastic composite materials. To achieve such goal, commercial information was carefully evaluated and recorded, so that the business value of the industrial activity could be verified. This section provides a brief evaluation of costs, based on present time values at the time of work completion. This may provide following researchers with reference information on how some relevant elements of the composites industry and world economy have changed later in time.

As of year 2021, the cost of PP polymer varies between 1.50 to 2.00 USD/kg, and the specific type of glass fibre used is priced at 1.50 USD/kg. The resulting raw material cost for the unidirectional prepreg product is therefore less than 1.80 USD/kg. To ensure safe and continuous production, a minimum of 3 workers is needed at any time to operate and monitor the production line. Over three 8-hours shifts, the total requirement is for 9 workers. Including the estimated operational costs, management costs and maintenance costs, each kilogram of prepreg will cost close to 3.00 USD.

Maximum production speed tested is at 7.5 m/min. Considering that each glass fibre roll contains 14 to 15 km tested, the production line could operate continuously for about 32 hours cycles without interruption and produce about 4875 kg of unidirectional prepreg. Including holidays and maintaince downtime, one single production line has the ability to produce approximately 731 tons of prepreg for 150 production cycles.

Assuming that the prepreg will have a contribution margin of 20%, a single line will generate USD 438 600 profit per year.

The initial cost of setting up the manufacturing line is around USD 300 000, excluding other related commercial costs and taxes. On this basis, it will need 103 cycles to reach breakeven point, and for the prepreg manufacturing line to be paid in full. The designed maximum production speed is at 9 m/min, if the

production can keep at this speed it will reduce the production cycle to about 24 hours which will resulting a 25% increase on productivity.

4.3 Haitie melt impregnation line set up

A CFT manufacturing line was designed and commissioned. A diagram of the line with the minimum number of required sections appears in Figure 4.2. The function of these 10 sections are briefly introduced below. Furthermore, 11 variable input parameters and their modalities were selected, out of all the adjustable parameters discussed for the 10 sections, as input parameters for the multifactorial ANOVA analysis conducted as part of this work.

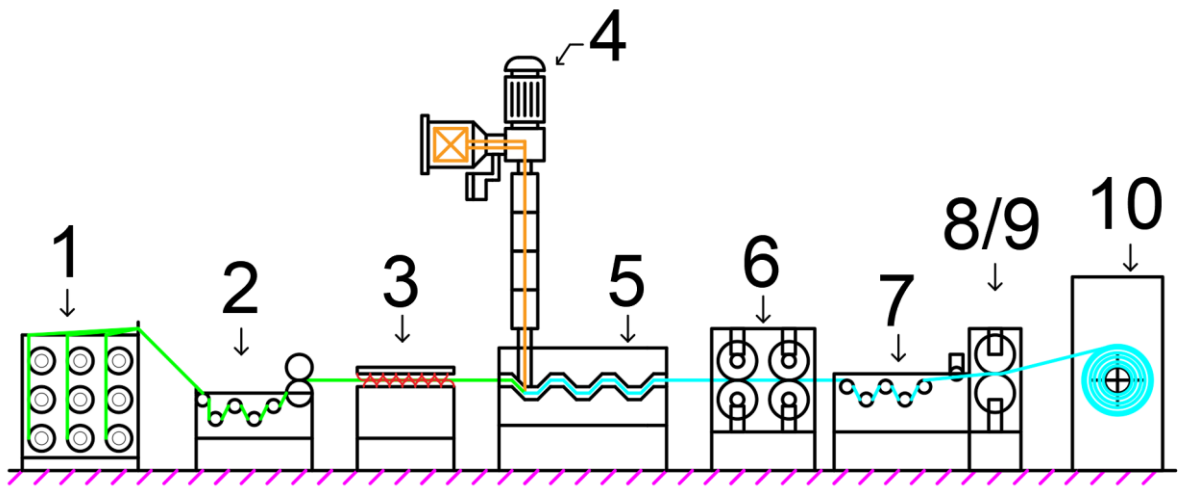

Figure 4.2 Diagram of commissioned Haitie CRT melt impregnation prepreg manufacturing line

4.3.1 Section 1: Fibre shelf

Fibre shelves are used for yarn spool storage. A number of yarn spools are positioned on the shelf, with yarns fed into individual guides. Figures 4.3 and 4.4 show the fibre shelf. The functions of the shelf are to:

- 1. Position yarns in a regular array at the beginning of the line.

- 2. Adjust tension in yarns through control of friction applied on yarn spools, allowing consistent yarn supply.

Variable input factors associated to Section 1 include:

- Factor 1.1: Number of glass fibre yarns used for production. A higher fibre volume fraction, hence fibre to polymer ratio, will improve the specific properties of the composite. The number of glass yarns will also have an effect on prepreg width and thickness.

- Factor 1.2: Friction applied on glass fibre spools. Different levels of tension on glass fibre yarns at initial supply stage might affect fibre spreading, resulting in different product quality.

- Factor 1.3: Type of the glass fibre. This can be changed for different applications. The fibre type was decided for the first round of trials, and so the fibre type will not be a variable parameter in this work.

Figure 4.3 Photograph of Section 1: fibre shelf

Figure 4.4 Photograph of adjustable friction belt behind fibre spool

4.3.2 Section 2: Spreading shelf

The spreading shelf features the first set of driving rollers that pull the yarns, a grille to regulate yarn spacing, and several rollers around which yarns are wrapped. Yarns pass through the grille first, go around a few rollers, and then meet the driving rollers. The rollers apply compressive force on the

yarns and pre-tension them, making them wider and thinner to facilitate impregnation further down the line. Due to friction and the wrapping angle, additional pressure is applied on the yarns. A static electricity removing device is also present. A photograph of the spreading shelf is shown in Figure 4.5.

Variable input factors associated to Section 2 include:

- Factor 2.1: Number of guiding rollers used for spreading the yarns. The number of rollers involved will affect the overall wrapping angle between glass yarns and rollers, and further affect friction between glass fibres and rollers, leading to different levels of tension in the glass rovings.

- Factor 2.2: Width of the grille. The grille regulates overall yarn spreading width before they travel to later sections. The width is expected to have effect on product overall width, which may affect the glass fibre distribution in the prepreg produced.

Figure 4.5 Photograph of section 2, spreading shelf

4.3.3 Section 3: Pre-heating chamber

Beyond Sections 1 and 2, yarns enter the pre-heating chamber. The pre-heating chamber consists of an openable box with heating pipes inside. The chamber is placed immediately before the impregnation mould.

The goal of the pre-heating chamber is to dry the fibres and remove any moisture caught by them. The pre-heating chamber may also be used to assess whether a larger temperature difference between glass fibres and molten PP upon impregnation will make a difference to the final product.

Variable input factors associated to Section 3 include:

- Factor 3.1: Temperature inside of the heating chamber, which can be adjusted from room temperature up to close to 100 ℃.

4.3.4 Section 4: Matrix supply system

This Section includes a few different functional modules, such as the matrix loading module, the polymer extrusion module, and the matrix injection and monitoring module. First, PP polymer and additives are supplied into the storage bucket by the loading system, activated by a vacuum pump. Then the polymer is fed into a common thermoplastic processing single screw extruder for melting, kneading and extruding between the screw and barrel. The extruder has four different temperature control zones. Temperature control is achieved by electric heating cartridges and air-cooling fans mounted outside the barrel. Different independent control zones along the barrel enable gradual melt and plasticizing of the polymer. Once the polymer is molten inside the barrel, it proceeds into the polymer monitoring system,

which consists of a filter and flow regulator; fluid pressure sensors were added between these components to help monitor fluid status and help control extrusion speed. A temperature-controlled barrel is used for connecting this matrix supply section with the impregnation mould.

Variable input factors associated to Section 4 include:

- Factor 4.1: Heated air can be injected into the polymer loading bucket; the aim is to dry the polymer and eliminate moisture absorbed by the polymer, thus affecting product properties.

- Factor 4.2: Based on the calculated theoretical required volume of polymer, the extruder extrusion speed can be adjusted in relation with fibre linear speed. It is expected that by controlling the extrusion speed, the result of the impregnation phase will be different, especially regarding product thickness.

- Factor 4.3: Extruder, flow regulator, and connector temperatures. Modern extruders have several heating zones to heat up and control the temperature of the polymer in multiple steps; it is aimed to determine how temperature differences during the melting stage will affect product quality.

- Factor 4.4: The type of thermoplastic polymer used can be changed for different applications. Here, the polymer was pre-identified for this work hence this factor will not be a variable considered in further steps of this work.

4.3.5 Section 5: Impregnation mould

The impregnation mould is where the polymer and fibre are combined. It is arguably the most important section in the entire manufacturing line, as its design and function directly affect impregnation quality. According to the physical phenomena and industrial context discussed in previous chapters, the impregnation mould was specified as a corrugated mould, and the number of bulges inside the mould was set at 16 with a radius of 10 mm. The impregnation mould contains numerous sensors as well as heating rods on the top, bottom and both sides of the mould, for better temperature control. The mould is made of two parts, machined in such a way that when the two pieces of the mould close on each other, they form a corrugated flow tunnel inside. Figures 4.6 and 4.7 show the impregnation step.

Variable input factors associated to Section 5 include:

- Factor 5.1: The mould closure distance can be adjusted by switching the gap control spacer or adjusting the distance between upper and lower mould plates.

- Factor 5.2: Mould temperature can be controlled precisely; and it is expected to have effect on fibre-polymer impregnation level as different temperatures affect the polymer viscosity, or melt index.

Figure 4.6 Photograph of glass fibres impregnated by PP polymer inside the impregnation mould

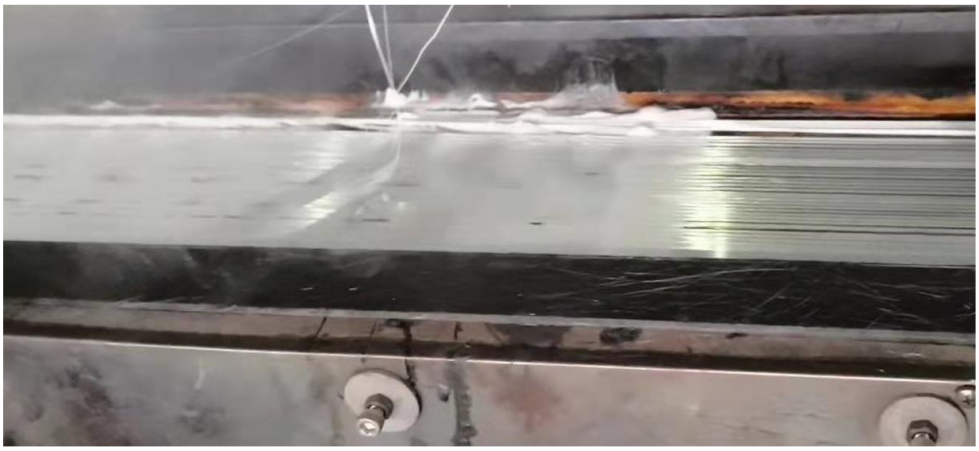

Figure 4.7 Photograph of tests of the impregnation mould and process

4.3.6 Section 6: Cooling rollers

Two sets of cooling rollers are set up immediately after the impregnation mould. The rollers compress the impregnated yarns to further impregnation, and also for cooling and crystallization of the

polymer, giving the product a flat and even surface finish. The horizontal distance between the mould and rollers is adjustable. Pressure and temperature of the two sets of rollers are also adjustable.

Variable input factors associated with Section 6 include:

- Factor 6.1: Distance between cooling rollers and impregnation mould. The cooling rollers and impregnation mould are both set on a pair of rails, so that the distance between the mould and pressing rollers is adjustable. Different distances will result in different exposure time to ambient air for the impregnated yarns and may have an effect on the impregnation level and crystallization degree for the prepreg product.

- Factor 6.2: Temperatures of two sets of cooling rollers can be adjusted from 10℃ to 80℃. This may have an effect on the cooling rate of the impregnated prepreg, thus affect product quality by influencing the crystallization rate.

- Factor 6.3: The compressing pressure of the two sets of cooling rollers can be adjusted from less than 2 MPa up to around 30 MPa. This may either help the resin to impregnate into the yarns; else, high pressure acting on a small contact surface might damage some fibres. This, as other points raised here, will be probed in testing trails. Pressure is also expected to have an effect on prepreg thickness.

4.3.7 Sections 7 and 8: Stretcher and trimmer

Section 7 contains a number of rollers for further cooling the unidirectional prepreg. A higher number of rollers results in higher the tension in the prepreg, to better cool down and release internal

loads in fibres and easier handing at trimming blade and collector Sections. The potential internal loads inside the prepreg came from three sources:

First, the significant pressure applied on it during the melt impregnation process inside the impregnation mould when fibres and polymer are pushed by corrugated hills together. Second, the compression force between each set of cooling rollers that trying to reduce the temperature and make sure the prepreg form in an evenly, thin, flat tape structure. And thirdly from the great temperature difference and associated expansion and shrinkage from the polymer.

An additional static electricity remover is present in this Section, for safety. Trimmers consist of two rolling blades located at both sides of the Section. Prepreg width can be adjusted at this location. Cutaway leftovers are collected by two rolling collectors located lower of the main line. Figure 4.8 shows the prepreg at trimmer.

Variable input factors associated with Sections 7 and 8 include:

- Factor 7.1: Number of stretching rollers. This may have an effect similar to the rollers in Section 2. More rollers will result in higher tension in the prepreg and may affect product quality as at this point, the prepreg still carries heat and potentially internal stress.

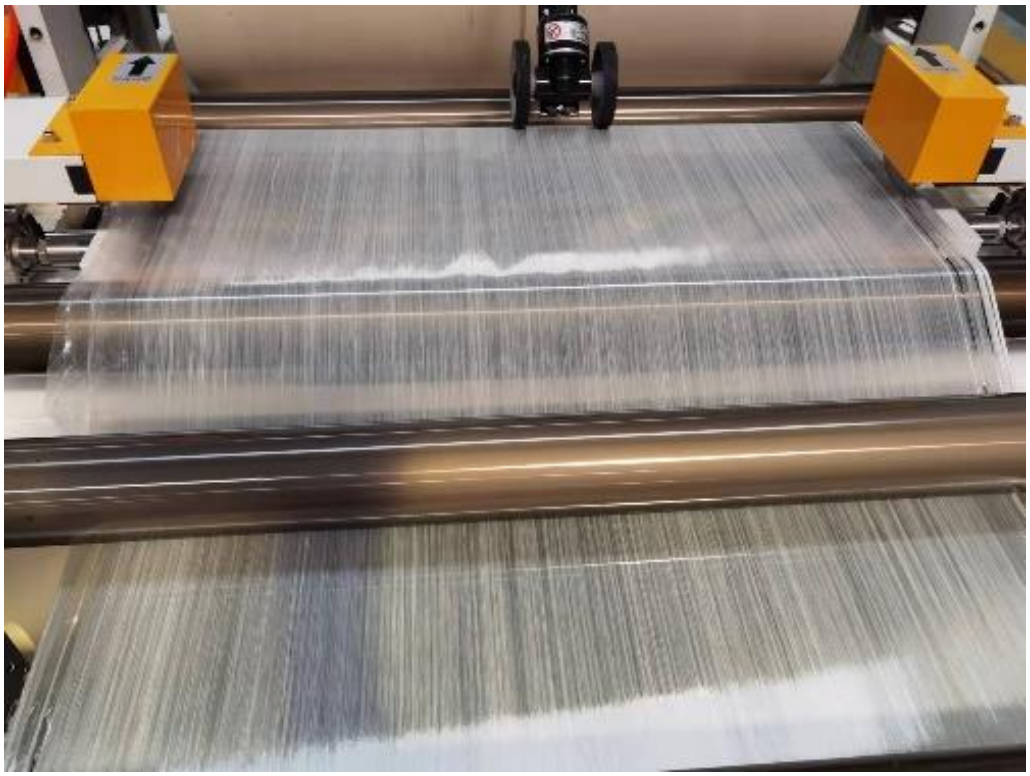

Figure 4.8 Photograph of impregnated prepreg at trimmer

4.3.8 Sections 9 and 10: Driving unit and collector

A pair of nitrile rubber pullers drag the prepreg across the complete line, and a collector unit rolls up the prepreg. All motors across the systems are synchronized, but they also have the degree of freedom for individual adjustment.

Variable input factors associated with Sections 9 and 10 include:

- Factor 9.1: Speed of the driving rollers. In general, the driving unit controls the running speed of the entire manufacturing line, and it is necessary to adjust this driving speed along with extrusion speed. Any difference between these two speeds is expected to affect product quality significantly as it will affect the fibre volume fraction significantly. Therefore, in the work done

here these two parameters will not change. However, speeds of the driving unit, cooling rollers and driving rollers in fibre spreading shelf can show small disparities allowing glass rovings in the line to carry different internal tension levels.

Chapter 5:Manufacturing trials and analysis

5.1 CFT unidirectional prepreg manufacturing trials, results and optimization using Taguchi methods

The performance of engineered components and systems is often affected by a large number of design parameters, and the number parameters and data associated is typically large in the case of mechanization and production lines, as highlighted in Chapter 4. Analytical or computational models might, in some cases, make it possible to predict the performance of components in a system. However, in many cases the required detailed information is simply not available, hence validating the relationship between input factors and output responses experimentally, as well as distinguishing genuine effects from background noise, should be done in a rigorous way. Taguchi or Plackett-Burman experimental plans and methods were designed for separating genuine effects from background noise in multifactorial experiments, whilst reducing the numbers of experimental trials needed [55]. In this section, a fractional factorial design selected for the Haitie CRT prepreg manufacturing line is presented. Tests results are presented, followed by the calculation of contrasts, ANOVA and multifactorial ANOVA for the following output responses: prepreg thickness, maximum stress, maximum strain, and modulus. Results are also analysed graphically using scree plots.

5.1.1 16 runs Taguchi design for Haitie CFRTP

Table 5.1 shows the basic 16-run Plackett-Burman Array that enables the analysis of effects of 9 to 15 input factors and contrasts.

For this work, 11 input factors out of all variable parameters listed in Chapter 4 were retained. The

table of confounding patterns for main factors and factor interactions appears in Table 5.2, for 11 input parameters. The 11 inputs are listed in Table 5.3, along with their two modalities retained for this work; each modality has one maximum value and one minimum value, respectively labelled as + and – in the plan matrix, Table 5.1. All modality values were chosen based on three principles.

First, selected modalities must result a functional and complete unidirectional prepreg product; modalities that lead to failure or obviously required were not selected for trail.

Second, modalities selected for the 11 input factors must be consistent across the manufacturing line, so that the results of optimization and analysis will provide guidelines that are directly applicable to production.

Third, the selected modalities must result in stable manufacturing, and it must be feasible to implement then in regular manufacturing operation.

Below are the plan, confounding pattern and modalities that were selected as clearly modifiable and feasible in production, whilst potentially affecting product quality. Together they form the experimental 16 run Taguchi /Plackett-Burman used for this work.

Table 5.1 Basic 16 runs Placket-Burman array [55]

The Basic 16-Run Plackett-Burman Array shown below is useful for studying from four to fifteen factors having two-levels each. Specific tables of confounding patterns are given for designs using different numbers of factors. Data Collection Worksheets and Calculation Worksheets are included.

	Contrast Labels														
Run	A	B	C	D	E	F	G	H	I	J	K	L	M	N	O
1	-	-	-	-	-	-	-	-	-	-	-	-	-	-	-
2	-	-	-	-	-	-	-	+	+	+	+	+	+	+	+
3	-	-	-	+	+	+	+	+	+	+	+	-	-	-	-
4	-	-	-	+	+	+	+	-	-	-	-	+	+	+	+
5	-	+	+	+	+	-	-	-	-	+	+	+	+	-	-
6	-	+	+	+	+	-	-	+	+	-	-	-	-	+	+
7	-	+	+	-	-	+	+	+	+	-	-	+	+	-	-
8	-	+	+	-	-	+	+	-	-	+	+	-	-	+	+
9	+	+	-	-	+	+	-	-	+	+	-	-	+	+	-
10	+	+	-	-	+	+	-	+	-	-	+	+	-	-	+
11	+	+	-	+	-	-	+	+	-	-	+	-	+	+	-
12	+	+	-	+	-	-	+	-	+	+	-	+	-	-	+
13	+	-	+	+	-	+	-	-	+	-	+	+	-	+	-
14	+	-	+	+	-	+	-	+	-	+	-	-	+	-	+
15	+	-	+	-	+	-	+	+	-	+	-	+	-	+	-
16	+	-	+	-	+	-	+	-	+	-	+	-	+	-	+
	A	B	C	D	E	F	G	H	I	J	K	L	M	N	O

Treatment combinations are defined by rows in this matrix.

Contrast coefficients are defined by columns in this matrix.

Number of changes in level:

A	B	C	D	E	F	G	H	I	J	K	L	M	N	O
1	2	3	4	5	6	7	8	9	10	11	12	13	14	15

Table 5.2 Confounding pattern for 16 runs, 11 factors Plackett-Burman design [55]

ELEVEN FACTORS

Contrast Labels:	A	B	C	D	E	F	G	H	I	J	K	L	M	N	O
Main Effects:	A	B	C	D	E	F	G	H	I	J	K				
Two-Factor Interactions:	BC	AC	AB	AE	AD	AG	AF	AI	AH	AK	AJ	DH	DI	DJ	DK
	DE	DF	DG	BF	BG	BD	BE	BJ	BK	BH	BI	EI	EH	EK	EJ
	FG	EG	EF	CG	CF	CE	CD	CK	CJ	CI	CH	FJ	FK	FH	FI
	HI	HJ	HK		KN							GK	GJ	GI	GH
	JK	IK	IJ												

(Delete Factor Labels L, M, N and O from Data Collection Worksheet.)
(Change Signs of Two Factor Interactions when using Basic 16-Run Design.)

Below are the final modalities that selected for the test trail, modality for the usage of trimmer and product collector's tension will not include due to the fact that they will have less effect on product's mechanical property. Pulling speed was not chosen because a fine speed was selected to cooperate with polymer extruding speed to provide an acceptable CFRTP product when observed by eyes. To give a anchor for finding other uncertain factors.

Table 5.3 Final factor identification and modalities

Label	Factor name	Contrast label	Modality values
A	Mould gap	-	large (2.2 mm)
		+	small (1.5 mm)
B	Spreading of shelf guide	-	loose (680 mm spread)
		+	tight (580 mm spread)
C	Number of Yarns of glass fiber	-	155
		+	130
D	Distance between cooling rollers and mould	-	tight (10 cm)
		+	loose (30 cm)
E	Heating chamber temperature	-	on (80°C)
		+	off (room temperature)
F	Extruder zone temperature 1&2	-	low (165, 175°C)
		+	high (180, 190°C)
G	Extruder zone temperature 3&4	-	low (190, 200°C)
		+	high (200, 210°C)
H	Mould temperature	-	low (235°C overall)
		+	high (265°C overall)
I	Cooling roller temperature 1	-	high (60°C)
		+	low (30°C)
J	Cooling roller temperature 2	-	high (60°C)
		+	low (30°C)
K	Roller pressure	-	10 MPa
		+	0-2 MPa

5.1.2 Visual analysis of CRT unidirectional prepreg

Figure 5.1 shows two common defects occurring in the production of unidirectional prepreg in a stable process: fibre breakage and dry fibres. Both defects are caused by improper impregnation associated with lack of resin. The image on the left shows fibre breakage that occurred because impregnated fibre strands could not bond together with each other as the fibres didn't form into a tight array inside the mould during the impregnation due to poor arrangement in previous sections or fibre breaking and missing in such area. This may also cause by polymer shortage or due to thermoplastic resin's temperature are too low. The image on the right shows localized dry fibre due to inconsistent impregnation, in turn due to polymer shortage or unstable polymer supply. And these might come from low polymer supply from extruder or insufficient processing temperature.

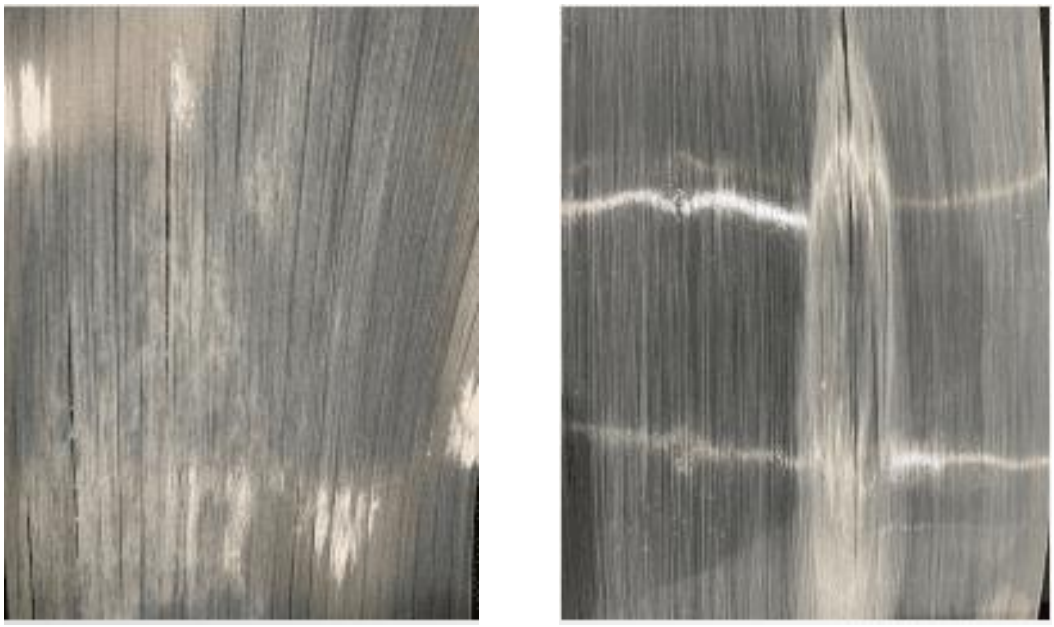

Figure 5.1 Unidirectional prepreg with breakage between fibres (left) and dry fibres (right)

None of the samples produced for the 16-run Taguchi experimental plan showed either defect.

Production speed, polymer feeding speed and other modalities for variable input factors were selected to ensure that that all prepreg produced for the 16 runs was of visually acceptable quality, evaluated as an absence of visual defects as shown in Figure 5.2. It should be noted that for all measured output response and for each run, 10 coupons were extracted from the prepreg and 10 independent tests were conducted, enabling a robust quantification of natural variability present in those results.

Figure 5.2 Unidirectional prepreg with no visual defects

5.1.3 Results and analysis for 16 runs averages and standard deviations

Results for the four output responses appear in Table 5.4. A general review of the results of the 16 run trails already leads some valuable information.

Table 5.4 Average values and standard deviations for 4 output responses,16-run Taguchi experimental plan

	Thickness (mm)		Maximum stress (MPa)		Maximum strain (-)		Initial modulus (GPa)	
Run	**Avg.**	**Std. Dev.**	**Avg.**	**Std. Dev.**	**Avg.**	**Std. Dev.**	**Avg.**	**Std. Dev.**
1	**0.404**	**0.020**	**625.23**	**96.07**	**3.76E-02**	**2.41E-03**	**16.638**	**2.420**
2	**0.328**	**0.019**	**825.56**	**52.63**	**4.60E-02**	**2.75E-03**	**17.949**	**0.965**
3	**0.357**	**0.024**	**750.10**	**63.21**	**4.37E-02**	**2.57E-03**	**17.178**	**1.443**
4	**0.380**	**0.026**	**684.24**	**44.27**	**4.01E-02**	**2.16E-03**	**17.069**	**1.110**
5	**0.335**	**0.025**	**773.74**	**97.62**	**4.01E-02**	**3.61E-03**	**19.296**	**1.760**
6	**0.360**	**0.031**	**673.42**	**94.64**	**3.89E-02**	**2.12E-03**	**17.317**	**2.315**
7	**0.380**	**0.027**	**630.76**	**95.95**	**4.05E-02**	**3.45E-03**	**15.555**	**1.604**
8	**0.376**	**0.021**	**645.92**	**51.20**	**4.03E-02**	**1.48E-03**	**16.063**	**1.522**
9	**0.246**	**0.014**	**811.60**	**89.63**	**4.22E-02**	**2.63E-03**	**19.348**	**2.626**
10	**0.256**	**0.021**	**770.50**	**73.27**	**3.87E-02**	**3.85E-03**	**19.998**	**2.106**
11	**0.249**	**0.015**	**771.53**	**59.40**	**3.66E-02**	**3.10E-03**	**21.138**	**1.769**
12	**0.239**	**0.023**	**699.45**	**38.98**	**3.94E-02**	**3.27E-03**	**17.889**	**2.133**
13	**0.250**	**0.012**	**815.43**	**88.91**	**4.15E-02**	**1.93E-03**	**19.674**	**2.143**
14	**0.265**	**0.018**	**676.26**	**107.10**	**4.13E-02**	**2.88E-03**	**16.500**	**3.167**
15	**0.270**	**0.022**	**650.50**	**99.62**	**4.57E-02**	**6.06E-03**	**14.435**	**2.829**
16	**0.233**	**0.018**	**774.33**	**90.45**	**4.40E-02**	**3.97E-03**	**17.768**	**2.824**

First, target thickness of the unidirectional prepreg product was set at 0.3 mm. However, it is clear that none of the 16 trial runs resulted in measured thickness values that were satisfactorily close to the target value, Figure 5.3. Half of the runs returned averages that were larger than the target value by more than one standard deviation, and the other half returned averages that were smaller than the target value, again by more than one standard deviation in all cases. Data separated so clearly into two groups indicates a very high probability that input factors are associated with product thickness in a statistically significant way, and so that this can be controlled; further analysis will confirm this information. Furthermore, standard deviations for different subgroups show clear differences, which may indicate that different input factors lead to different levels of operational stability on thickness in this Taguchi test. This is also analysed further on in the thesis.

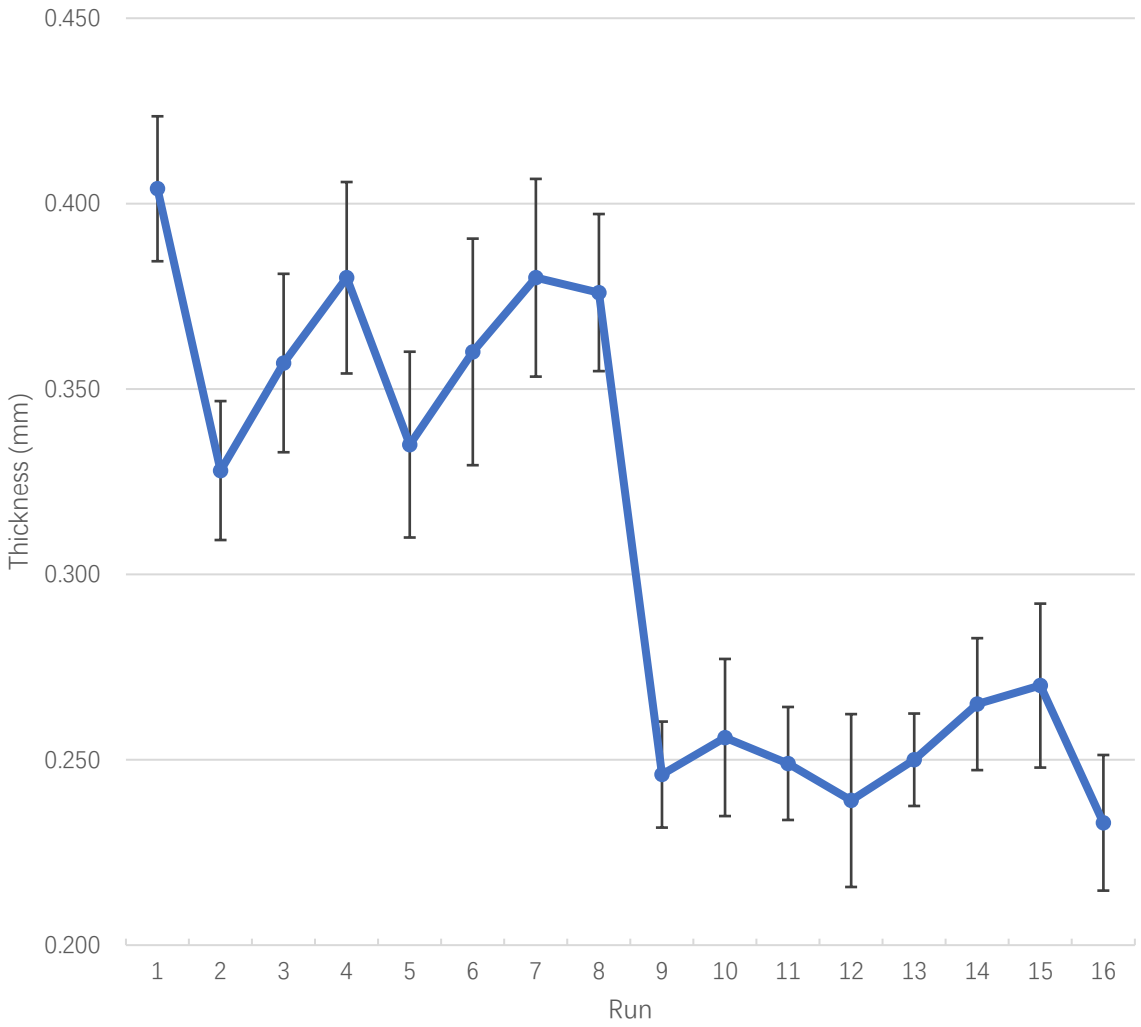

Figure 5.3 Average values and standard deviations for runs 1-16: thickness

Figure 5.4 shows that average maximum tensile stress sustained by the product seems to bear no obvious relationship with average thickness. A higher fibre content in the form of a lower thickness (factor A –) and higher number of yarns (factor C –) would seemingly lead to a higher tensile stress; the graph does not show this prominently but after calculating the average stress divided into two groups, there is a clear signal that the average tensile stresses between thinner and thicker product. The result is thinner products in group 9 to group 16 as one have an average advantage of 45.08 MPa than average tensile from thicker products in group 1 to group 8. This is because overall number of fibres is set to 2

numbers, and the thinner product will have higher fibre-volume ratio in both contrast group than the thicker products. This is a straightforward proof of higher fibre-volume ratio means higher performance for composite material and this can also be seen as a verification of the data acquired in trails are valid. It should also be noted that whilst some runs are differentiated beyond their standard deviations, most standard deviations overlap.

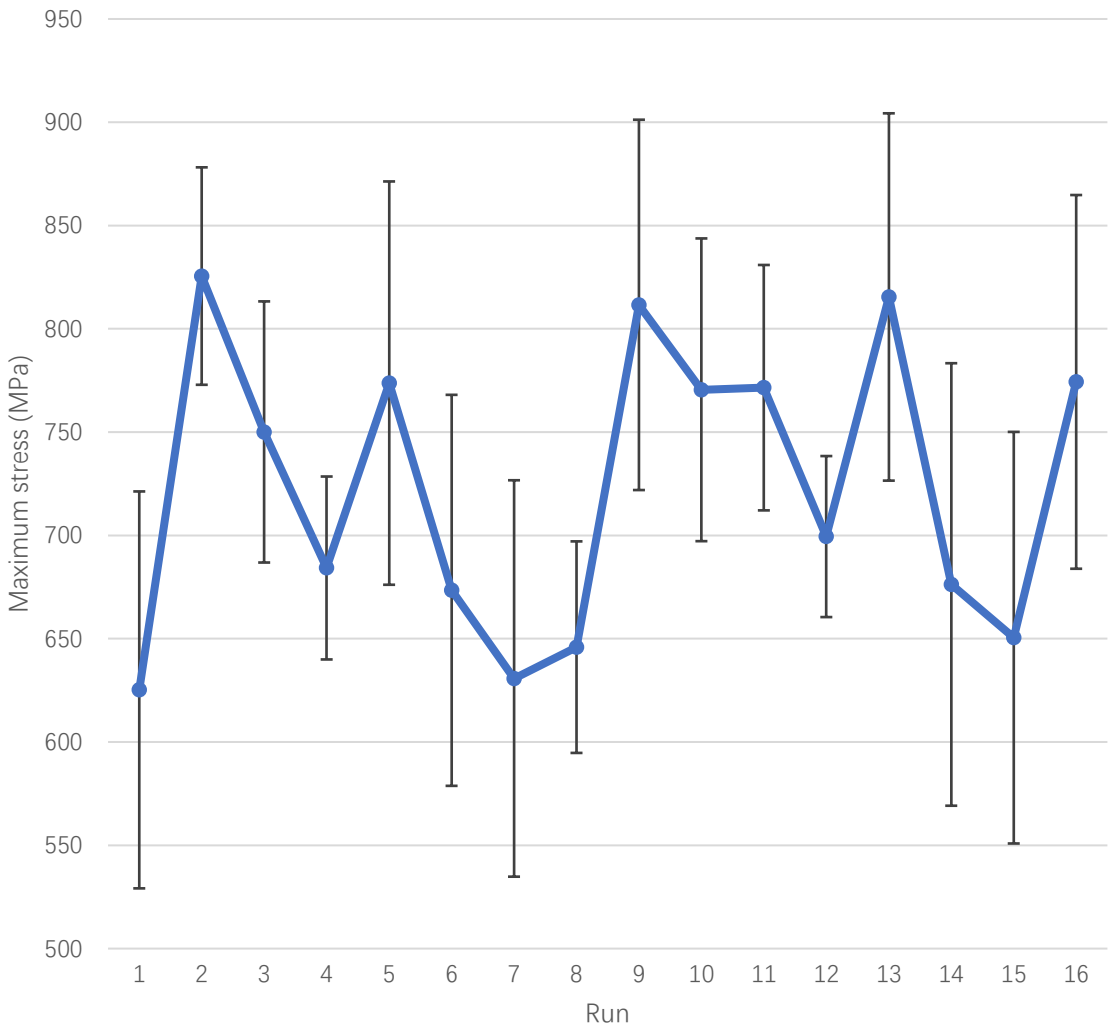

Figure 5.4 Average values and standard deviations for runs 1-16: maximum stress

Comparing maximum stresses and maximum strains, Figure 5.5, for the 16-run trail, stresses fluctuate with more relative amplitude as differences between average values are well over 25 percent, with very large standard deviations observed for some subgroups or runs. The large standard deviations were observed to

result from differences in sampling location over the area of the prepreg. In some subgroups, mechanical properties were observed not to be the same across the unidirectional prepreg, most notably across the width; areas close to the edges were weaker. It was observed that those areas featured lower fibre fractions than the centre of the product. Fluctuations were less pronounced for maximum strains.

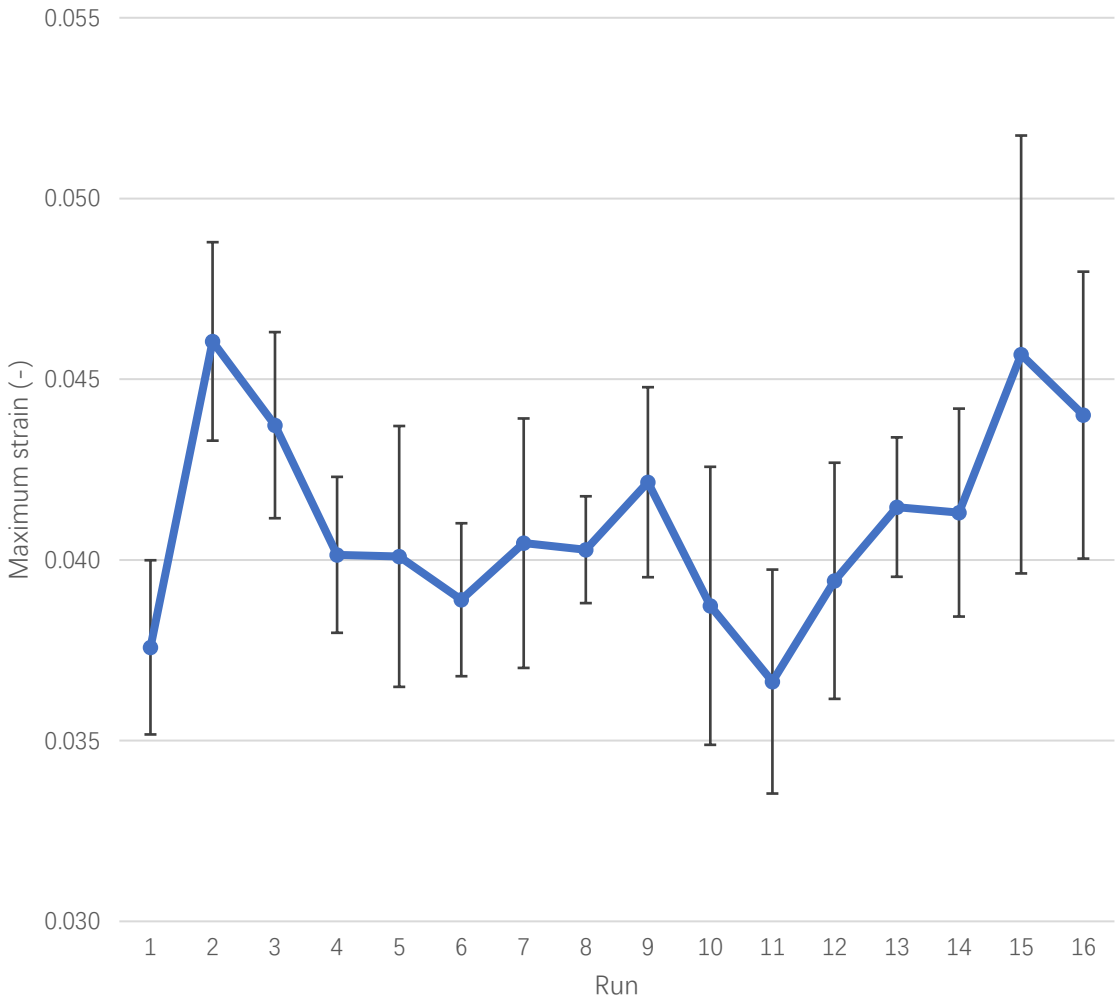

Figure 5.5 Average values and standard deviations for runs 1-16: maximum strain

In some subgroups, say 2, 9, 1, 6 and 7, maximum strain and maximum stress showed the same trend toward above or below average; this could imply that the modalities for these subgroups have a more

prominent effect on product quality. But on the other hand, some groups show divergent and somewhat vague trends that might be undistinguishable from background noise. Again, only a rigorous ANOVA will provide solid answer to such early observations made from raw results.

Moduli for the first 8 subgroups, Figure 5.6, show somewhat more limited variability than the latter subgroups.

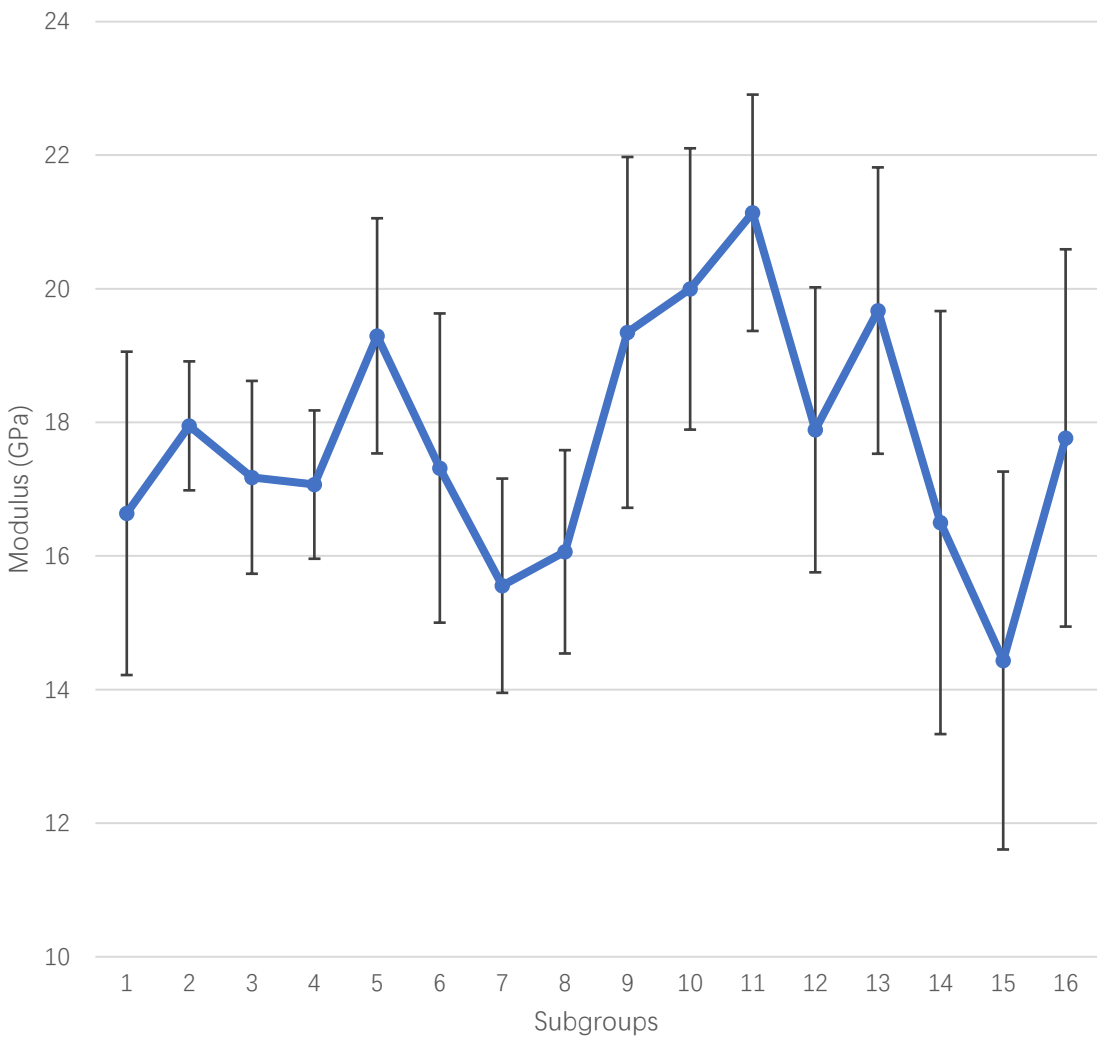

Figure 5.6 Average values and standard deviations for runs 1-16: modulus

5.1.4 Analysis for contrast of key results

A contrast is a weighted comparison of means, with the condition that the sum of all data is centered at zero [55] as shown in Equation 5.1.

$$C = c_1\mu_1 + c_2\mu_2 + \cdots + c_j\mu_j + \cdots + c_k\mu_k = \sum_{j=1}^{k} c_j\mu_j \quad (5.1)$$

Contrast results can be calculated for all main effects as defined in the columns of Table 5.1, and interactions of two factors as defined in Table 5.2. Whilst numerical results appear in Appendix B, the contrasts are presented graphically in the following Figures 5.7 to 5.10. The figures enable a clear understanding of the amplitudes of effects associated with individual contrasts.

For thickness, Figure 5.7 shows that the effect of contrast A, the gap between upper and lower mould pieces, is overwhelming compared to all other contrasts. This is perhaps unsurprising in the specific case of this first output response and demonstrates the effectiveness of contrast calculations. Other contrasts such as those associated with the main effects of factors F, G, I, and K which represent respectively the extruder temperatures, first set cooling roller temperatures and roller pressures, also have a stronger impact on the response than other factors. It is worth noting that when the gap between upper and lower mould was changed from 2.2 mm to 1.5 mm, the products thickness – which is well below those values for all cases – dropped on average by approximately 0.1 mm. Hence while there is a clear effect of gap thickness, neither the prepreg thickness nor its change are proportional to gap heights.

For the extruder, when both temperature zones are higher, in the first 8 runs, thickness tends to increase than the lower temperature runs; however, this analysis of data is not sufficiently clear to make any final conclusions. For the temperature of the first set of rollers, based on last 8 subgroups, a higher roller

temperature, seems to lead to a higher thickness, whilst the effect of roller pressure is more difficult to identify. However, again ANOVA will be needed to reach firm conclusions.

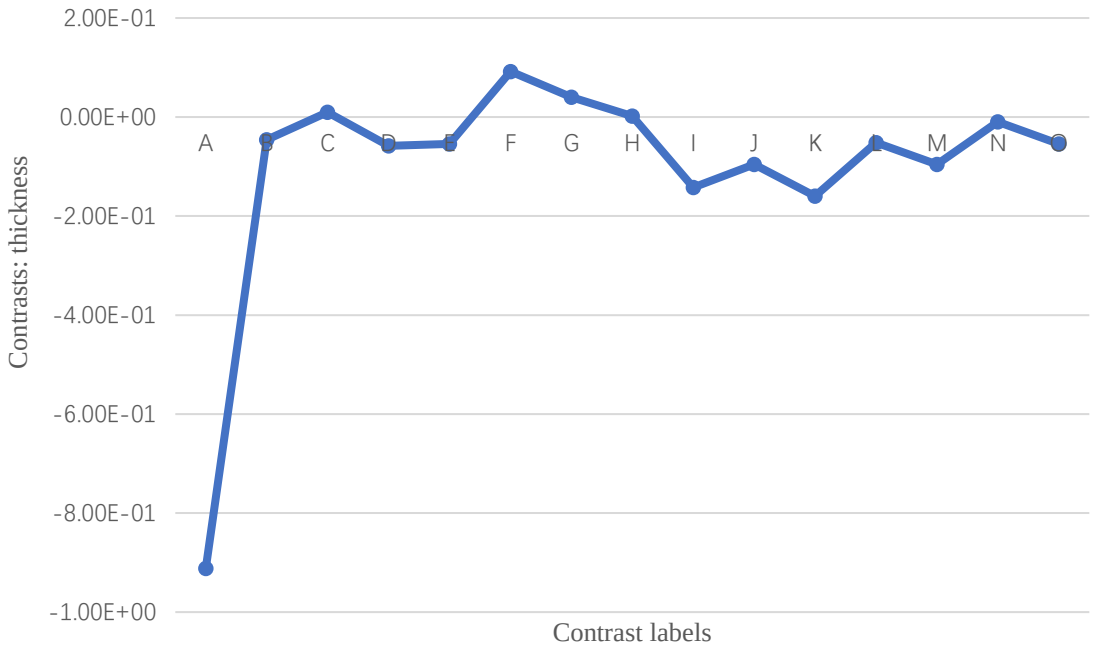

Figure 5.7 Contrasts for thickness

For maximum stress, contrasts A, C, G, I, K, and M deviate more from the general average than other contrasts. Again, it is not possible to readily determine whether those differences in mould gap have a statistically significant on the maximum stress that the product can bear but comparing the first 8 subgroups with the other 8, a minor descending trend is observed. This trend may result from the change in number of yarns used during trails, as less yarns should result in lower maximum tensile strength. The effects of temperatures for the extruder and cooling rollers on maximum stress are difficult to pinpoint, but changes in roller pressure and maximum tensile stress show similar patterns where higher pressure decreases tensile

performance, and vice-versa. Contrast M represent two-factor interactions DI, EH, FK and GJ which include the effect from factors except gap thickness, fibre spreading, and fibre quantity seems trying to provide evidence that stress of the product can be affected not just by fibre volume ratio other factors like processing temperature and roller pressure are important as well.

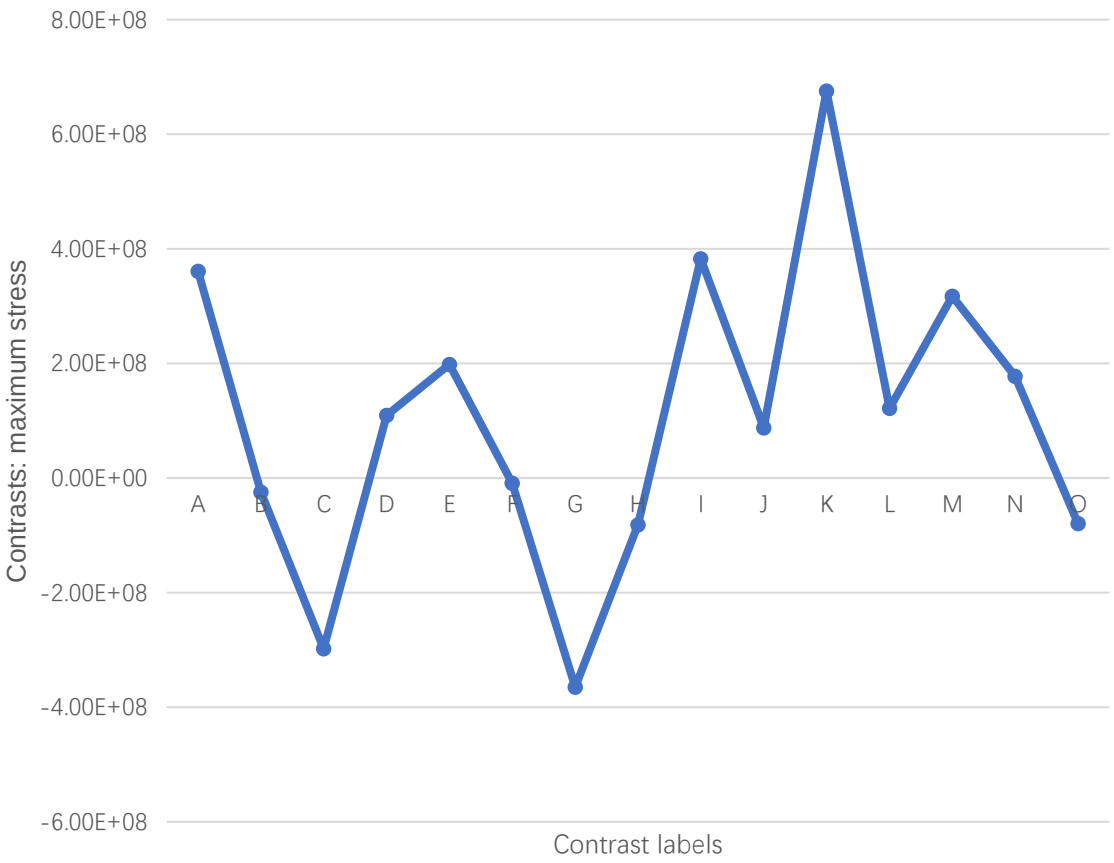

Figure 5.8 Contrasts for maximum stress

For maximum strain, contrasts B, D, and J deviate more from the general average than other contrasts. Wider initial spreading of the fibres appears to correlate with slightly higher maximum strain values. No clear relation can be found by inspection between maximum strain contrasts D and J.

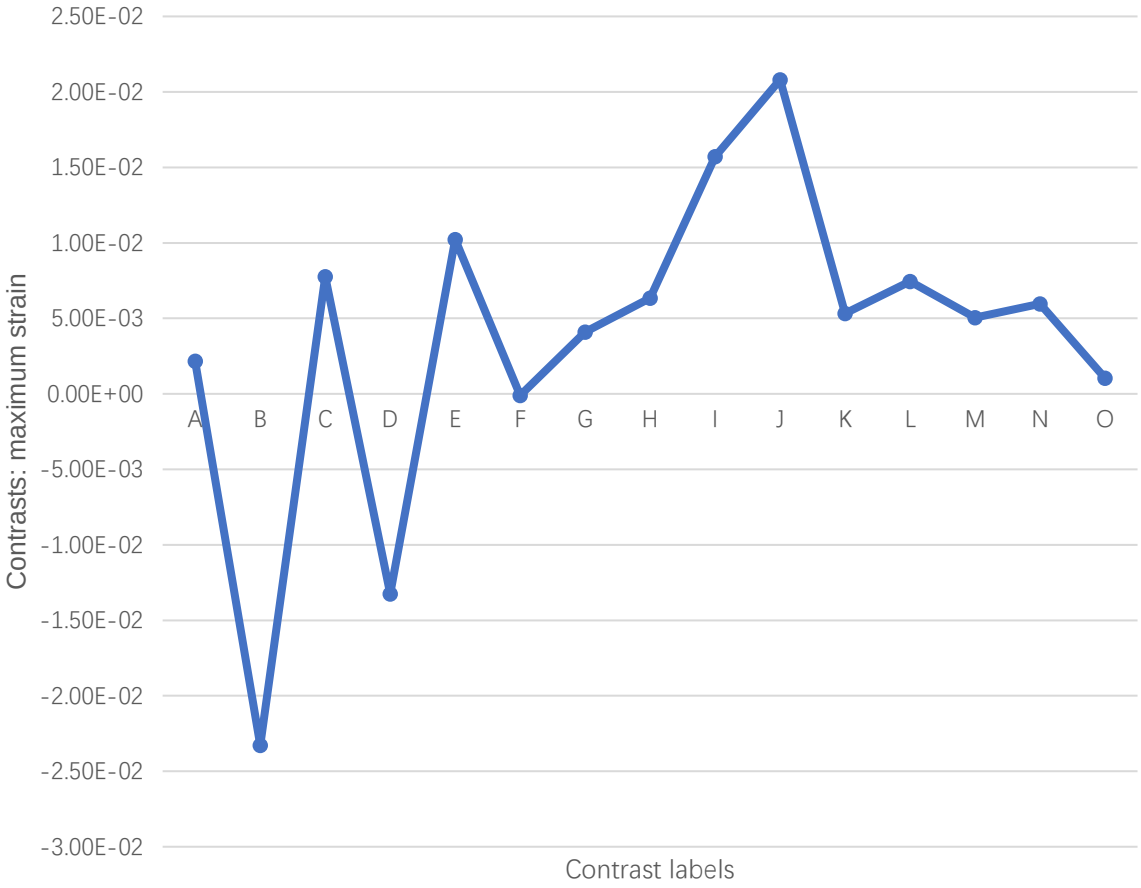

Figure 5.9 Contrasts for maximum strain

For initial modulus, it is not possible to come to any convincing conclusion based on a simple observation of contrast values.

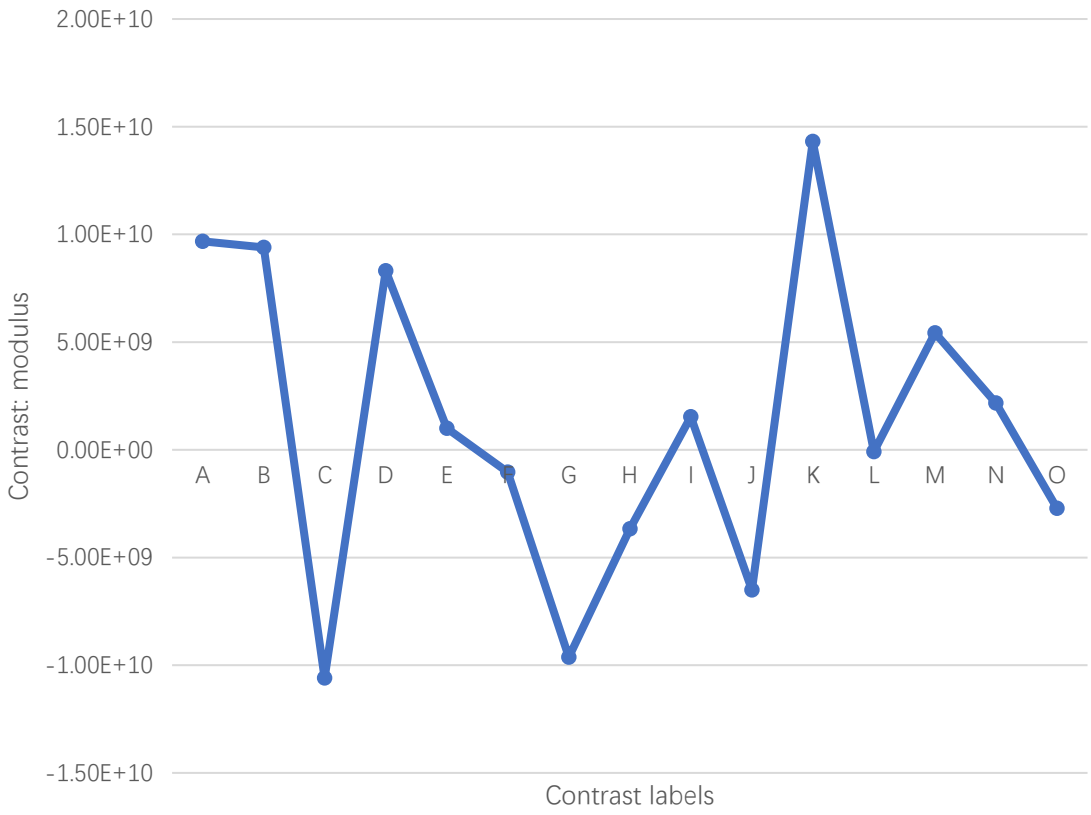

Figure 5.10 Contrasts for modulus

In order to identify statistically significant correlations and effects of factors and interactions, or alternatively to associate contrasts with experimental noise, the information and data reported above was analysed using multifactorial ANOVA. After identification of variability levels associated with noise, the trends identified above may be confirmed, and others identified more formally.

5.1.5 Multifactorial ANOVA analyses

Results of multifactorial ANOVA analyses for the four output responses studied appear in Tables 5.5 to 5.8. In these analyses, values of the Total Variation Estimate, Within Variation Estimate and Between Variation Estimate were calculated separately. The Total Variation Estimate is a one-way sample variance analysis using all collected data, while the Within Variation Estimate is calculated from

the sum of internal variances for each subgroup, and the Between Variation Estimate' quantifies the variance of each subgroup average with respect to the grand average of all data.

Within Variation Estimate and Between Variation Estimate are used for separating signal from noise; values of their sums of square and degrees of freedom should add up to the values obtained for the Total Variation Estimate, enabling direct validation of calculations. The F-ratio is calculated from Within Variation Estimate and Between Variation Estimate. Combined with an F-distribution table provided in Appendix C, each contrast can be deemed to have a statistically significant effect on the process and product, or not.

Figures 5.11 to 5.14 show scree plots that are also used for separating signal from noise visually. For a typical plot, any contrast that lies on the right part of the plot is more likely to represent noise, especially if the values of the sums of square fall off a cliff from the left of the plot, where contrasts that represent signals are positioned.

The F-distribution limiting value of 4.494 was selected from the F-table, using a DOF value for of 1 for Between Variation Estimate, with 16 subgroups.

For thickness results, F-ratio for contrast label A, K, I, M, J and F exceeded the threshold, whilst D was marginal. Therefore, all these contrasts have a statistically significant effect on the product. The analysis indicates that that gap between the upper and lower mould has a very strong effect on product thickness. However, roller pressure, roller temperature for both set of rollers and initial extruder heating temperature also have statistically significant effects on prepreg thickness. These effects are now quantified formally, hence thickness can be controlled more accurately by focusing on significant input

factors. The gap between the mould halves has the largest effect on product final thickness, by a large margin. It is also noted that when the gap is smaller, the standard deviation on thickness is much smaller.

Table 5.5 Multifactorial ANOVA table for thickness

Thickness				
Source	ss	DF	MS	F
Contrast 1A	0.51984	1	0.51984	1120.278
Contrast 2B	0.001323	1	0.001323	2.850045
Contrast 3C	6.25E-05	1	6.25E-05	0.13469
Contrast 4D	0.002102	1	0.002102	4.530979
Contrast 5E	0.001823	1	0.001823	3.927567
Contrast 6F	0.00529	1	0.00529	11.40018
Contrast 7G	0.001	1	0.001	2.155043
Contrast 8H	2.5E-06	1	2.5E-06	0.005388
Contrast 9I	0.012603	1	0.012603	27.15893
Contrast 10J	0.00576	1	0.00576	12.41305
Contrast 11K	0.016	1	0.016	34.48069
Contrast 12L	0.00169	1	0.00169	3.642023
Contrast 13M	0.00576	1	0.00576	12.41305
Contrast 14N	6.25E-05	1	6.25E-05	0.13469
Contrast 15O	0.001823	1	0.001823	3.927567
Within	0.06682	144	0.000464	
Total	0.64196	159		

Temperature for first half of the extruder, roller pressure and the temperature for the first set of rollers have effect on product thickness. Distance between cooling rollers and mould, temperature for the second sets of cooling rollers and two-factor interactions DI, EH, FK and GJ which include all factors except the gap, fibre spreading, and fibre quantity also have an effect on prepreg thickness.

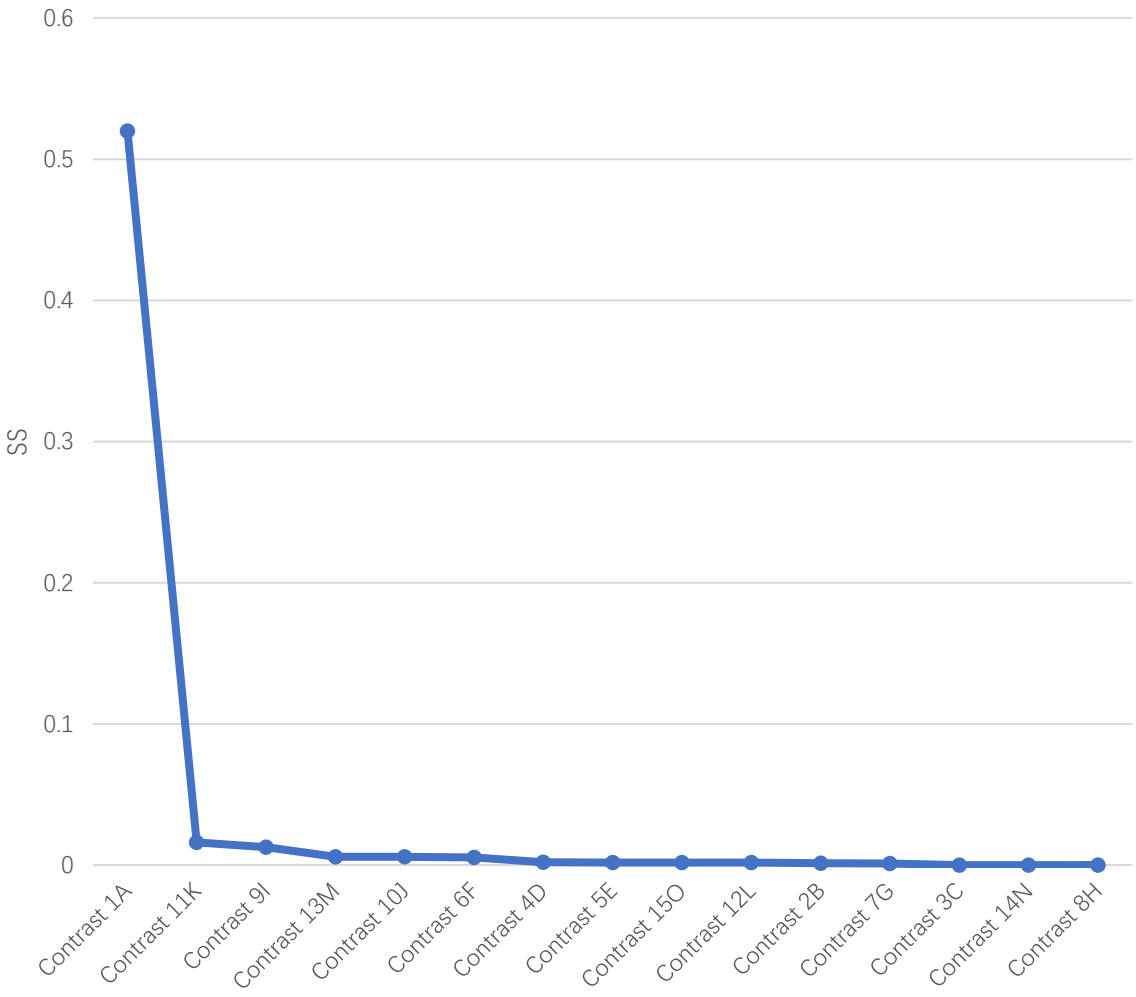

Figure 5.11 Scree plot for thickness

For maximum stress, contrasts K, I, G, A, M and C clearly exceeded the threshold limit. The factors represent the roller pressure, first set of cooling rollers temperature, extruder later section temperature, gap between upper and lower moulds, number of glass yarns and 2-factor interactions DI, EH, FK and GJ. These findings are similar as discussed above, reinforcing previous conclusions.

Table 5.6 Multifactorial ANOVA table for maximum stress

Stress

Source	ss	DF	MS	F
Contrast 1A	8.13E+16	1	8.13E+16	12.48323
Contrast 2B	3.82E+14	1	3.82E+14	0.058697
Contrast 3C	5.54E+16	1	5.54E+16	8.513803
Contrast 4D	7.53E+15	1	7.53E+15	1.156354
Contrast 5E	2.46E+16	1	2.46E+16	3.773286
Contrast 6F	5E+13	1	5E+13	0.007672
Contrast 7G	8.32E+16	1	8.32E+16	12.77983
Contrast 8H	4.13E+15	1	4.13E+15	0.634622
Contrast 9I	9.15E+16	1	9.15E+16	14.05676
Contrast 10J	4.81E+15	1	4.81E+15	0.738038
Contrast 11K	2.85E+17	1	2.85E+17	43.80857
Contrast 12L	9.27E+15	1	9.27E+15	1.423623
Contrast 13M	6.3E+16	1	6.3E+16	9.672772
Contrast 14N	1.98E+16	1	1.98E+16	3.035062
Contrast 15O	3.92E+15	1	3.92E+15	0.602293
Within	9.38E+17	144	6.51E+15	
Total	1.67E+18	159		

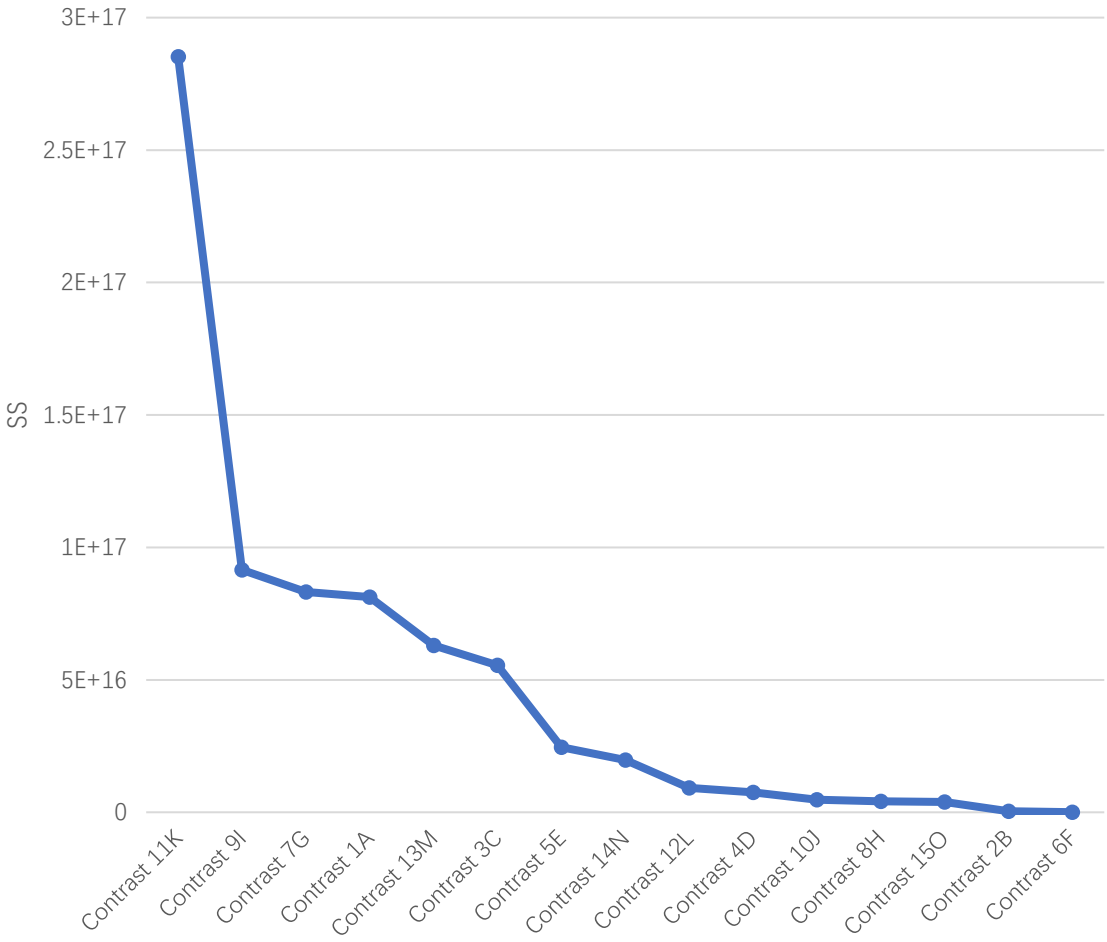

Figure 5.12 Scree plot for maximum stress

For maximum strain, contrasts B, J, I, D and E all exceeded the threshold, corresponding to the width of the spreading grille, both cooling rollers temperature, distance between the cooling roller and mould, and fibre heating chamber temperature. The width of spreading grille, distance between cooling rollers and mould, and temperature of the second set of rollers were identified above. On the other hand, heating chamber temperature and temperature of the first set of rollers further emphasize the importance of temperature.

Finally, contrasts K, C, A, G, B, D and J exceeded the threshold limit for modulus.

Table 5.7 Multifactorial ANOVA table for maximum strain

Strain

Source	ss	DF	MS	F
Contrast 1A	2.93E-06	1	2.93E-06	0.287842
Contrast 2B	0.000339	1	0.000339	33.32146
Contrast 3C	3.77E-05	1	3.77E-05	3.710307
Contrast 4D	0.00011	1	0.00011	10.79473
Contrast 5E	6.54E-05	1	6.54E-05	6.438412
Contrast 6F	6.49E-09	1	6.49E-09	0.000638
Contrast 7G	1.04E-05	1	1.04E-05	1.027613
Contrast 8H	2.52E-05	1	2.52E-05	2.479913
Contrast 9I	0.000154	1	0.000154	15.18583
Contrast 10J	0.000271	1	0.000271	26.60961
Contrast 11K	1.78E-05	1	1.78E-05	1.750182
Contrast 12L	3.47E-05	1	3.47E-05	3.415409
Contrast 13M	1.6E-05	1	1.6E-05	1.570843
Contrast 14N	2.22E-05	1	2.22E-05	2.184527
Contrast 15O	6.71E-07	1	6.71E-07	0.065993
Within	0.001464	144	1.02E-05	
Total	0.00257	159		

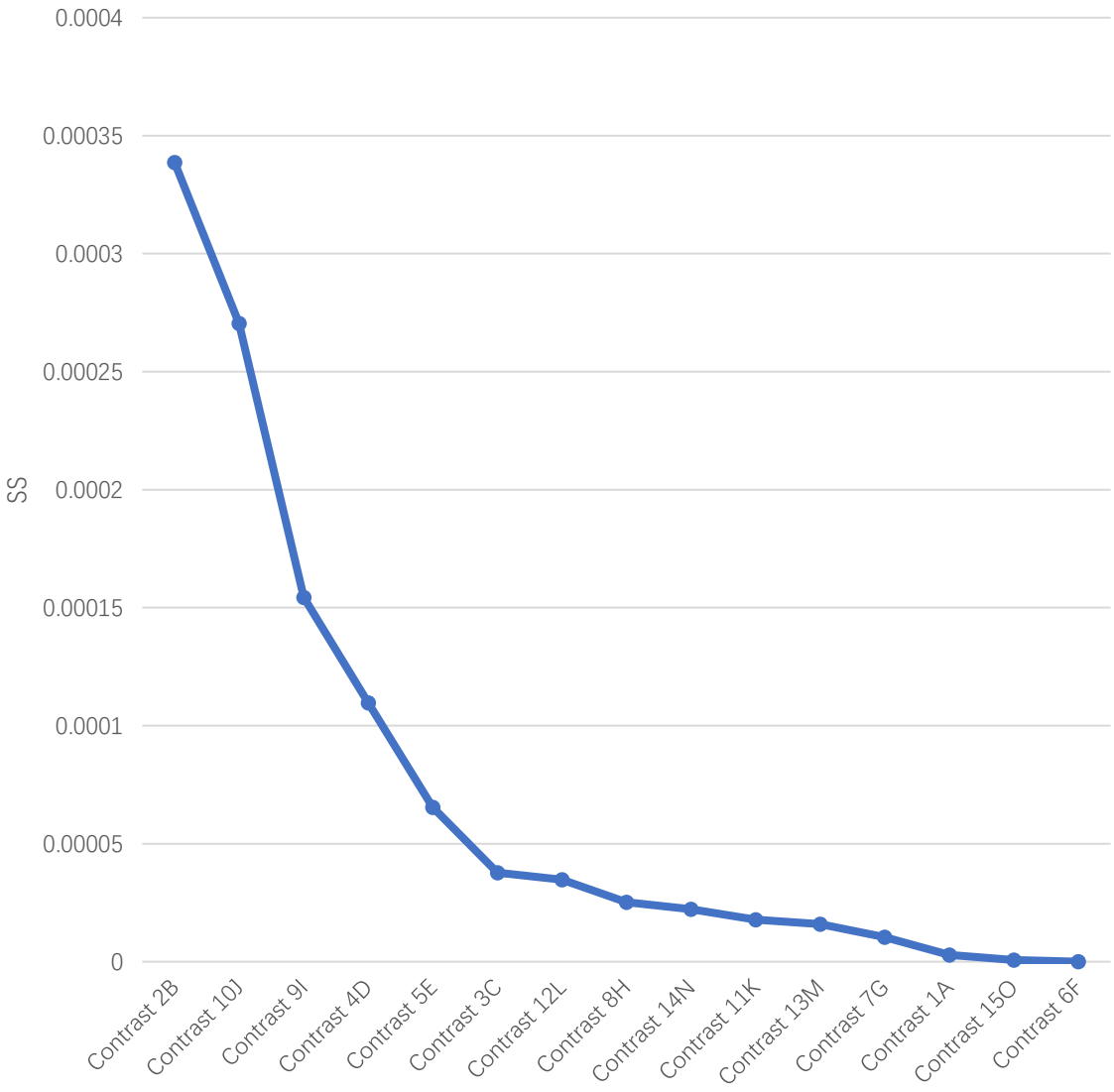

Figure 5.13 Scree plot for maximum strain

Table 5.8 Multifactorial ANOVA table for modulus.

Modulus

Source	ss	DF	MS	F
Contrast 1A	5.86E+19	1	5.86E+19	12.8381
Contrast 2B	5.51E+19	1	5.51E+19	12.07346
Contrast 3C	7.02E+19	1	7.02E+19	15.37348
Contrast 4D	4.31E+19	1	4.31E+19	9.4467
Contrast 5E	6.27E+17	1	6.27E+17	0.137332
Contrast 6F	6.81E+17	1	6.81E+17	0.149173
Contrast 7G	5.79E+19	1	5.79E+19	12.68113
Contrast 8H	8.44E+18	1	8.44E+18	1.848296
Contrast 9I	1.48E+18	1	1.48E+18	0.324457
Contrast 10J	2.64E+19	1	2.64E+19	5.783562
Contrast 11K	1.28E+20	1	1.28E+20	28.03256
Contrast 12L	4.42E+15	1	4.42E+15	0.000968
Contrast 13M	1.84E+19	1	1.84E+19	4.037184
Contrast 14N	2.95E+18	1	2.95E+18	0.645105
Contrast 15O	4.6E+18	1	4.6E+18	1.00664
Within	6.58E+20	144	4.57E+18	
Total	1.13E+21	159		

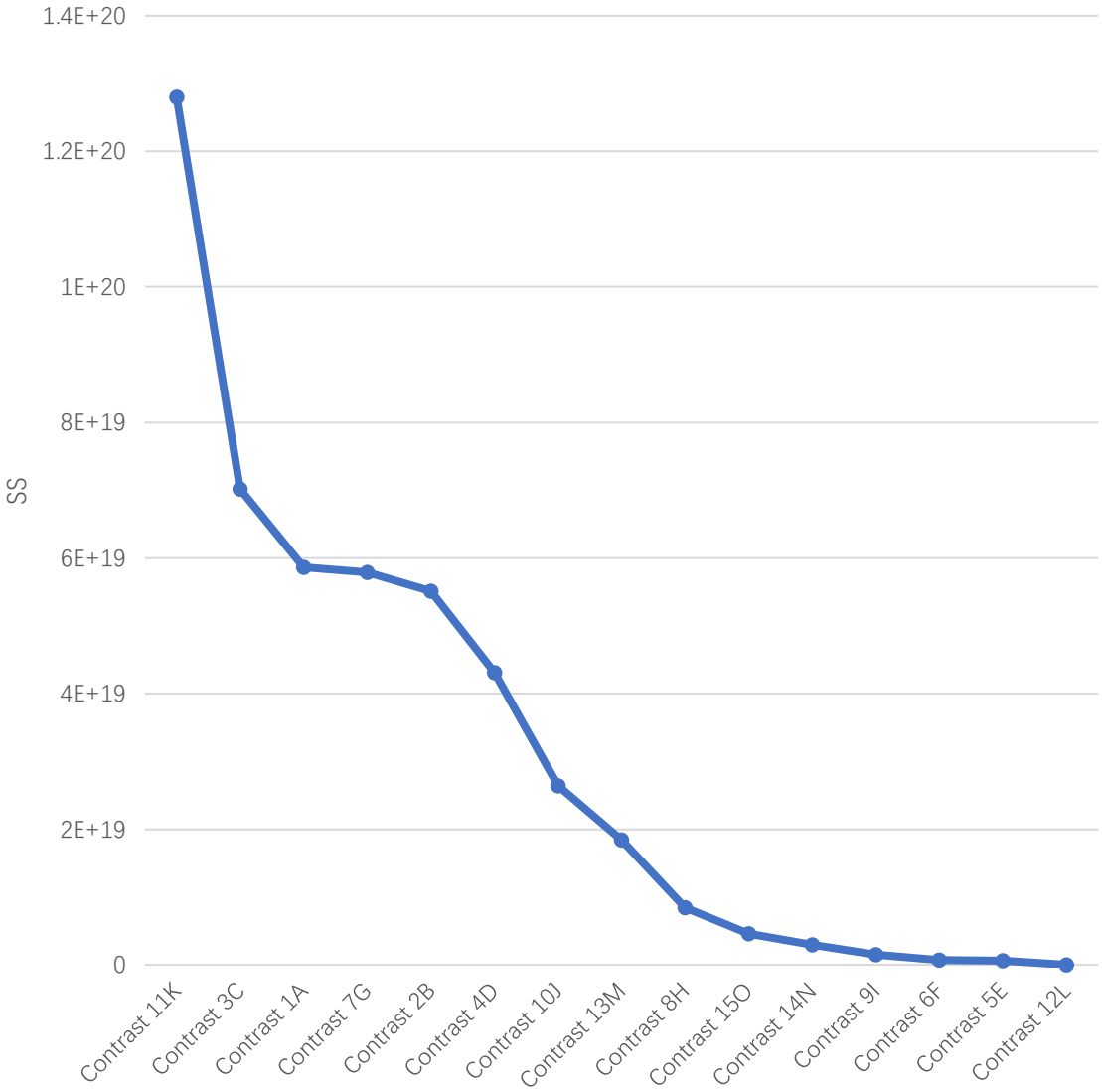

Figure 5.14 Scree plot for modulus

Chapter 6: Conclusion

The goal of this thesis consisted in investigating the operation of a newly installed line for manufacturing continuous fibre reinforced thermoplastic (CFRTP). Deliverables were completed and recorded for this work.

Investigations were conducted on PP/glass CFRTP prepreg. Key factors controlling target output responses in the form of prepreg thickness and mechanical properties were studied. A complete production solution for CFRTP prepreg was built. The manufacturing line has a production capacity of 2.6 kilograms per minute which will allow a production capacity of over 700 tons per year.

Adjustable factors and quality of the prepreg samples were studied. CFRTP prepreg produced in the manufacturing line commissioned at Haitie have reached satisfactory mechanical properties, with 21 GPa modulus on the longitudinal direction. Furthermore, properties of the CFRTP prepreg may be altered based on the work conducted here.

6.1 ANOVA results

Sixteen subgroups can be broadly segregated into two smaller groups, consisting respectively of runs 1-8, and runs 9-16. Subgroups 9-16 showed better performance overall compared with subgroups 1-8. From the testing results generated as part of this work, the CFRTP prepreg with best performance are in subgroups 9, 10, 11 and 12. Because prepreg in these four subgroups had the lowest thickness and highest fibre volume fraction, caused by input factors A and C. The influence of these two factors on the system was confirmed through multifactorial ANOVA. Furthermore, since the gap between upper and lower moulds is dependent on a module that is part of the mould, and the 1.5 mm or 2.2 mm gaps are only setup values for the

module, the precise gap between the mould halves remains to be quantified accurately, as it is impractical to measure the inner space in the mould while it is operating with resin and yarns running inside. By using a multifactorial ANOVA, the module can be adjusted to adequately control the gap and adjust the thickness of the product.

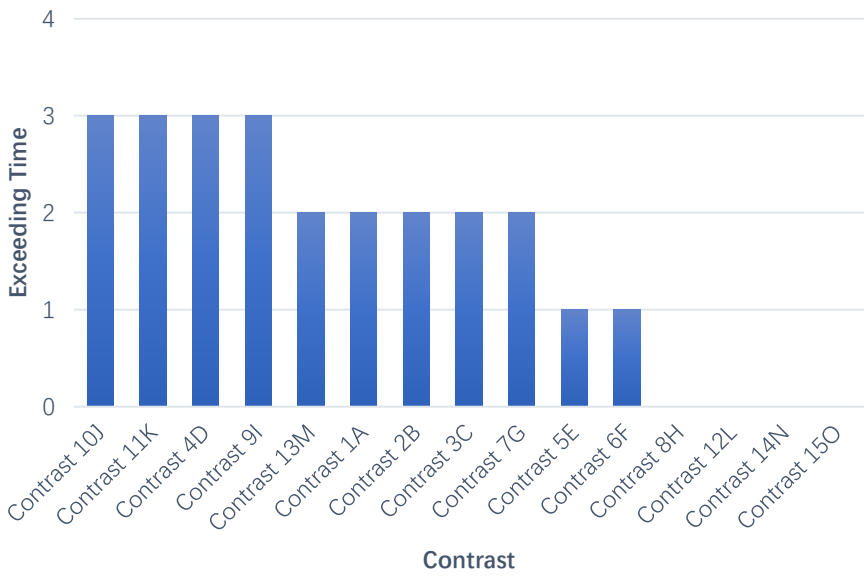

Figure 6.1 Numbers of occurrences when each contrast exceeded the F-ratio threshold limit in multifactorial ANOVA.

Looking at the average actual performance of products, a dropping pattern featuring a cliff can be observed for maximum stress and for modulus, essentially in a group of each 4 subgroups: 1-4; 5-8; 9-12; 13-15. CFRTP prepreg with best performance is observed in subgroups 9, 10, 11 and 12. As a referring template, extruder temperature factor F and G's changing pattern fit on this performance pattern. Whenever the extruding temperature increase from low to high, the performance of the prepreg decrease. And both factors have confirmed effect on the system by multifactorial ANOVA. So, it is safe to guess that even within the operating temperature limit that above melting point and below the decomposition temperature, a higher temperature will be resulting product with less strength. This might cause by the imperceptible

decomposition reaction from some of the polymers that stay or stuck in the extruder or the impregnation mould.

Result For product's strain is different, the middle 8 groups clearly have lower strain values than subgroup 1, 2, 3, 4, 13, 14, 15, and 16. This pattern fit with factor B, which is the spreading grille's width. he pre-spreading of the fibres seems have less effect on product properties because the prepregs were produced nicely and standard deviation result does not show unbalanced properties fit in factor B's pattern. In any conventional judgment, this means the fibre spreading before going into the impregnation mould have no big effect on the final fibre spreading in the prepreg, but multifactorial ANOVA marked this factor and from the data of average strain, narrower spreading will resulting better results.

6.2 Application and future work

What should be mentioned in the end of this work is that there is still unlimited space to explore the science and technology behind the CFRTP uni-directional prepreg. But limited by time and cost of this project, complex modification such as redesign of the mould cannot be done in the middle of the work. Further analysis on existing parameters and factors did not included in this 16 run Taguchi will increase the accuracy of the result.

By the time this thesis is finished, the actual progress of the study on CFRTP material in Haitie is advance more than the production of one type of uni-direction prepreg. CFRTP prepreg with different PP polymers and polyamide were made. Then the prepregs have been made into laminates with different thickness and ply by using double conveyer belt thermal press. Sandwich panel with different core material such as PP honey core, Polyurethane (PU), Polyethylene terephthalate (PET), and Polyvinyl chloride (PVC)

foam were also produced. Variety surface treatment were applied in crease CFRTP laminate and panels practicality in many filed that require high quality lightweight panel. Figure 5.2 shows the pictures of the laminates and sandwich panel made by CFRTP. Products using CFRTP laminate were made, thermal forming process were also successfully applied. Future work will be focusing on how to use thermal forming process combine other technique to produce practical parts with complex geometry which could further advance CFRTP material's application in many industry.

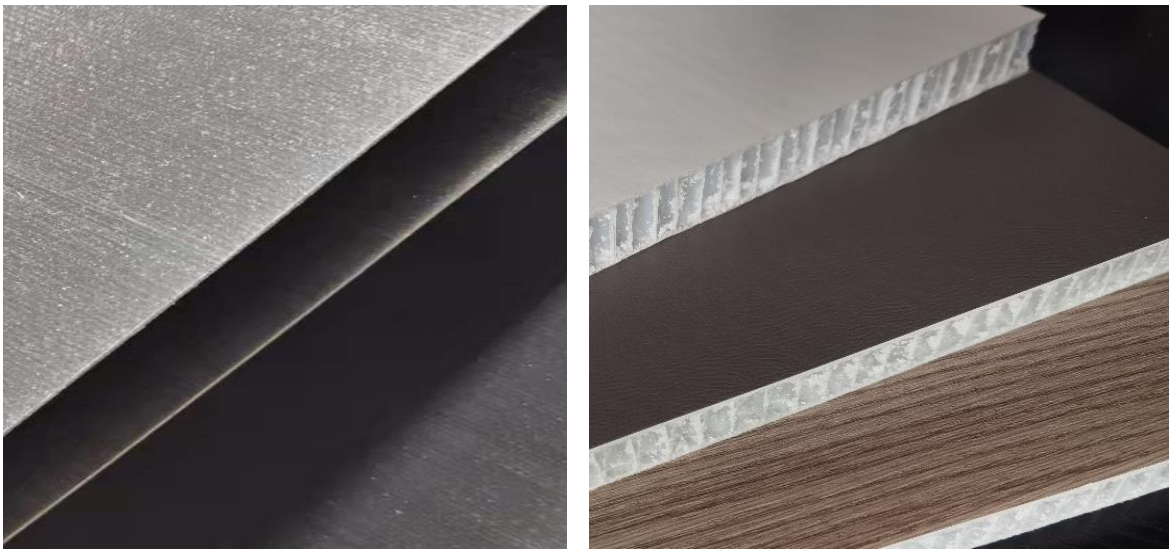

Figure 6.6.2 Photographs of CFRTP laminates and sandwich panel produced by Haitie

References

[1] P. D. Pastuszak and A. Muc, “Application of Composite Materials in Modern Constructions,” *Key Eng. Mater.*, vol. 542, pp. 119–129, Feb. 2013, doi: 10.4028/www.scientific.net/KEM.542.119.

[2] C. T. Herakovich, “Mechanics of composites: A historical review,” *Mech. Res. Commun.*, vol. 41, pp. 1–20, Apr. 2012, doi: 10.1016/j.mechrescom.2012.01.006.

[3] E. Witten, V. Mathes, M. Sauer, and M. Kühnel, “Composites Market Report 2018.” AVK, CCeV, Nov. 2018. [Online]. Available: https://www.avk-tv.de/files/20181115_avk_ccev_market_report_2018_final.pdf

[4] X. Su, “官宣！中国高铁突破 3.5 万公里，通达 32 个省区,” *CCTV.com*, Dec. 24, 2019. [Online]. Available: http://news.cctv.com/2019/12/24/ARTIQot1uMblzCUn8RRRgdPl191224.shtml

[5] A. Cevahir, “Glass fibers,” in *Fiber Technology for Fiber-Reinforced Composites*, Elsevier, 2017, pp. 99–121. doi: 10.1016/B978-0-08-101871-2.00005-9.

[6] J. W. S. Hearle and Textile Institute (Manchester, England), Eds., *High-performance fibres*. Boca Raton : Cambridge, England: CRC Press ; Woodhead Pub, 2001.

[7] F. T. Wallenberger, J. C. Watson, and H. Li, “Glass Fibers,” in *Composites*, D. B. Miracle and S. L. Donaldson, Eds. ASM International, 2001, pp. 27–34. doi: 10.31399/asm.hb.v21.a0003353.

[8] “Properties: E-Glass Fibre,” *AZoM.com*. https://www.azom.com/properties.aspx?ArticleID=764 (accessed Apr. 30, 2020).

[9] M. B. Volf, *Technical approach to glass*. Amsterdam ; New York : New York, N.Y: Elsevier ; Elsevier Science Pub. Co. [distributor], 1990.

[10] V. B. Gupta, Ed., *Manufactured fibre technology*, 1. ed. London: Chapman & Hall, 1997.

[11] G. Reddy, V. Krishna, and K. Shanker, “Tensile and Water Absorption Properties of FRP Composite Laminates without Voids and with Voids,” *Procedia Eng.*, vol. 173, pp. 1684–1691, 2017, doi: 10.1016/j.proeng.2016.12.195.

[12] P. K. Mallick, *Fiber-reinforced composites: Materials, manufacturing, and design, third edition*. 2007.

[13] P. K. Mallick, *Fiber-reinforced composites: materials, manufacturing, and design*, 3rd ed., [Expanded and rev. Ed.]. Boca Raton, FL: CRC Press, 2008.

[14] “Engineering Composites Mechanical Properties,” Nov. 19, 2019. http://www.matweb.com/reference/composites.aspx (accessed Nov. 20, 2019).

[15] U. Schulz, “Review of modern techniques to generate antireflective properties on thermoplastic polymers,” *Appl. Opt.*, vol. 45, no. 7, p. 1608, Mar. 2006, doi: 10.1364/AO.45.001608.

[16] H. Bal, “Thermal and mechanical properties of continuous fiber reinforced thermoplastics,” *DEÜ Fen Bilimleri Enstitüsü*, 2009, [Online]. Available: http://hdl.handle.net/20.500.12397/8283

[17] D. Ratna, *Handbook of thermoset resins*. Shawbury: iSmithers, 2009.

[18] N. C. Sekhar and L. A. Varghese, “Mechanical, thermal, and rheological studies of phenolic resin modified with intercalated graphite prepared via liquid phase intercalation,” *Polym. Test.*, vol. 79, p. 106010, Oct. 2019, doi: 10.1016/j.polymertesting.2019.106010.

[19] J. Jang and S. Shin, “Cure Studies of a Benzoxazine-Based Phenolic Resin by Isothermal Experiment,” *Polym. J.*, vol. 27, no. 6, pp. 601–606, Jun. 1995, doi: 10.1295/polymj.27.601.

[20] T. Pepper, “Polyester Resins,” in *Composites*, D. B. Miracle and S. L. Donaldson, Eds. ASM

International, 2001, pp. 90–96. doi: 10.31399/asm.hb.v21.a0003363.

[21] "A. Schulman BMC 6605A Polyester Molding Compound." https://www.matweb.com/search/datasheet.aspx?matguid=720015f12141423b99055c7d59cb8beb&ckck=1 (accessed Mar. 18, 2022).

[22] S.-J. Park and J.-R. Lee, "[No title found]," *J. Mater. Sci. Lett.*, vol. 20, no. 8, pp. 773–775, 2001, doi: 10.1023/A:1010956318415.

[23] T. Dipl.-Ing. Gietl, H. Dr.-Ing. Lengsfeld, and V. Dr.-Ing. Altstädt, "The efficiency of various toughening agents in novel phenolic type thermoset resin systems," *J. Mater. Sci.*, vol. 41, no. 24, pp. 8226–8243, Dec. 2006, doi: 10.1007/s10853-006-0879-9.

[24] "Overview of materials for Epoxy, Cast, Unreinforced," *matweb.com*, Nov. 19, 2019. http://www.matweb.com/search/DataSheet.aspx?MatGUID=1c74545c91874b13a3e44f400cedfe39&ckck=1 (accessed Nov. 20, 2019).

[25] C. Unterweger, O. Brüggemann, and C. Fürst, "Synthetic fibers and thermoplastic short-fiber-reinforced polymers: Properties and characterization," *Polym. Compos.*, vol. 35, no. 2, pp. 227–236, 2014, doi: 10.1002/pc.22654.

[26] J. L. Thomason, "The influence of fibre length and concentration on the properties of glass fibre reinforced polypropylene. 6. The properties of injection moulded long fibre PP at high fibre content," *Compos. Part Appl. Sci. Manuf.*, vol. 36, no. 7, pp. 995–1003, 2005, doi: 10.1016/j.compositesa.2004.11.004.

[27] H. Ning, N. Lu, A. A. Hassen, K. Chawla, M. Selim, and S. Pillay, "A review of long fibre thermoplastic (LFT) composites [A review of long fibre-reinforced thermoplastic of long fibre thermoplastic (LFT) composites]," *Int. Mater. Rev.*, vol. 64, no. 1, 2019.

[28] K. K. Chawla, *Composite materials science and engineering*, 3rd ed. New York ; Springer, 2012.

[29] A. D. L. Subasinghe, R. Das, and D. Bhattacharyya, "Fiber dispersion during compounding/injection molding of PP/kenaf composites: Flammability and mechanical properties," *Mater. Des.*, vol. 86, pp. 500–507, 2015, doi: 10.1016/j.matdes.2015.07.126.

[30] K. Friedrich, "Carbon fiber reinforced thermoplastic composites for future automotive applications," 2016, vol. 1736, no. 1. doi: 10.1063/1.4949575.

[31] T. Bayerl and P. Mitschang, "Rheological and mechanical behavior of long-polymer-fiber reinforced thermoplastic pellets," *J. Appl. Polym. Sci.*, vol. 131, no. 1, p. n/a, 2014, doi: 10.1002/app.39716.

[32] M. Schemme, "LFT – development status and perspectives," *Plast. Addit. Compd.*, vol. 10, no. 2, pp. 38–43, 2008, doi: 10.1016/S1464-391X(08)70060-6.

[33] K. Han, Z. Liu, and M. Yu, "Preparation and Mechanical Properties of Long Glass Fiber Reinforced PA6 Composites Prepared by a Novel Process," *Macromol. Mater. Eng.*, vol. 290, 273, no. 1, 7, pp. 688–694, 2005, doi: 10.1002/mame.200500051.

[34] P. Malnati, "Reinforced Thermoplastics: LFRT vs. GMT." https://www.compositesworld.com/articles/reinforced-thermoplastics-lfrt-vs-gmt (accessed Jan. 15, 2022).

[35] L. A. Berglund and M. L. Ericson, "Glass mat reinforced polypropylene," in *Polypropylene Structure, blends and Composites: Volume 3 Composites*, J. Karger-Kocsis, Ed. Dordrecht: Springer Netherlands, 1995, pp. 202–227. doi: 10.1007/978-94-011-0523-1_5.

[36] M. D. Wakeman, T. A. Cain, C. D. Rudd, R. Brooks, and A. C. Long, "Compression moulding of glass and polypropylene composites for optimised macro- and micro-mechanical properties II. Glass-mat-reinforced thermoplastics," *Compos. Sci. Technol.*, vol. 59, no. 5, pp. 709–726, Apr. 1999, doi:

10.1016/S0266-3538(98)00124-9.

[37] C.-T. Huang, L.-J. Chen, and T.-Y. Chien, “Investigation of the Viscoelastic Behavior Variation of Glass Mat Thermoplastics (GMT) in Compression Molding,” *Polymers*, vol. 11, no. 2, pp. 335-, 2019, doi: 10.3390/polym11020335.

[38] P. Nygard and C.-G. Gustafson, “Continuous Glass Fiber–Polypropylene Composites Made by Melt Impregnation: Influence of Processing Method,” *J. Thermoplast. Compos. Mater.*, vol. 17, no. 2, pp. 167–184, 2004, doi: 10.1177/0892705704035406.

[39] F. Ren, Y. Yu, J. Yang, C. Xin, and Y. He, “A Mathematical Model for Continuous Fiber Reinforced Thermoplastic Composite in Melt Impregnation,” *Appl. Compos. Mater.*, vol. 24, no. 3, pp. 675–690, 2016, doi: 10.1007/s10443-016-9534-z.

[40] J. Fang, L. Zhang, and C. Li, “The combined effect of impregnated rollers configuration and glass fibers surface modification on the properties of continuous glass fibers reinforced polypropylene prepreg composites,” *Compos. Sci. Technol.*, vol. 197, pp. 108259-, 2020, doi: 10.1016/j.compscitech.2020.108259.

[41] T. W. Kim, E. J. Jun, M. K. Um, and W. I. Lee, “Effect of pressure on the impregnation of thermoplastic resin into a unidirectional fiber bundle,” *Adv. Polym. Technol.*, vol. 9, no. 4, pp. 275–279, 1989, doi: 10.1002/adv.1989.060090401.

[42] R. J. Gaymans and E. Wevers, “Impregnation of a glass fibre roving with a polypropylene melt in a pin assisted process,” *Compos. Part Appl. Sci. Manuf.*, vol. 29, no. 5, pp. 663–670, 1998, doi: 10.1016/S1359-835X(97)00109-7.

[43] P. J. Bates and J. M. Charrier, “Pulling tension monitoring during the melt impregnation of glass roving,” *Polym. Compos.*, vol. 21, no. 1, pp. 104–113, 2000, doi: 10.1002/pc.10169.

[44] F. Ren, C. Zhang, Y. Yu, C. Xin, K. Tang, and Y. He, “A Modeling Approach to Fiber Fracture in Melt Impregnation,” *Appl. Compos. Mater.*, vol. 24, no. 1, pp. 193–207, Feb. 2017, doi: 10.1007/s10443-016-9521-4.

[45] S. I. Ngo, Y.-I. Lim, M.-H. Hahn, and J. Jung, “Prediction of degree of impregnation in thermoplastic unidirectional carbon fiber prepreg by multi-scale computational fluid dynamics,” *Chem. Eng. Sci.*, vol. 185, pp. 64–75, 2018, doi: 10.1016/j.ces.2018.04.010.

[46] “Composites Market Size | Industry Report, 2021-2028.” https://www.grandviewresearch.com/industry-analysis/composites-market (accessed Mar. 20, 2022).

[47] “2021 年中国连续纤维增强热塑性塑料（CFRT）行业分析报告-市场深度研究与运营商机前瞻_观研报告网,” Chinabaogao, Industrial Research 551253, 2021. Accessed: Mar. 20, 2022. [Online]. Available: https://baogao.chinabaogao.com/suliao/551253551253.html#r_data

[48] P. Nygård, K. Redford, and C.-G. Gustafson, “Interfacial strength in glass fibre-polypropylene composites: influence of chemical bonding and physical entanglement,” *Compos. Interfaces*, vol. 9, no. 4, pp. 365–388, 2002, doi: 10.1163/156855402760194719.

[49] F.-H. Su and Z.-Z. Zhang, “Friction and wear behavior of glass fabric/phenolic resin composites with surface-modified glass fabric,” *J. Appl. Polym. Sci.*, vol. 112, no. 2, pp. 594–601, 2009, doi: 10.1002/app.29444.

[50] P. Nygård and C.-G. Gustafson, “Interface and impregnation relevant tests for continuous glass fibre-polypropylene composites,” *Compos. Part Appl. Sci. Manuf.*, vol. 34, no. 10, pp. 995–1006, 2003, doi: 10.1016/S1359-835X(03)00124-6.

[51] P. Peltonen and P. Törmälä, “Melt impregnation parameters,” *Compos. Struct.*, vol. 27, no. 1, pp. 149–155, 1994, doi: 10.1016/0263-8223(94)90076-0.

[52] *ASTM D 3039. Test method for tensile properties of fiber-resin composite*. 1982.

[53] "ASTM D 3518. Practice for in-plane shear stress-strain response of unidirectional reinforced plastics".

[54] F. V. Composite Materials Testing and Design, *A Theoretical Study Of The Tensile Test For Highly Anisotropic Composite Materials*. West Conshohocken, Pa: ASTM International, 2003. doi: 10.1520/STP38419S.

[55] D. J. Wheeler, *Understanding industrial experimentation*, 2. ed., 3. pr. Knoxville, Ten: SPC Press, 1990.

Appendix A: Testing data for 160 longitudinal tensile tests.

1							
#	**THK(mm)**	WDTH(mm)	Lo(mm)	MXLD(KN)	**MXSTRS(Pa)**	**MXSTRN**	**E(Pa)**
1	0.38	48.6	366.4421053	11.77146875	6.37E+08	3.79E-02	1.68E+10
2	0.4	48.18	367.46	13.89869629	7.21E+08	3.63E-02	1.99E+10
3	0.41	47.29	366.1456311	14.24836816	7.35E+08	3.84E-02	1.91E+10
4	0.41	46.04	325.7263158	12.17307324	6.45E+08	4.14E-02	1.56E+10
5	0.38	46.17	336.3478261	9.826594727	5.60E+08	3.89E-02	1.44E+10
6	0.39	45.3	314.8372093	7.507674805	4.25E+08	3.53E-02	1.20E+10
7	0.44	44.9	357.3695652	10.55768066	5.34E+08	3.38E-02	1.58E+10
8	0.43	47.95	437.6947368	13.64133887	6.62E+08	3.49E-02	1.90E+10
9	0.4	47.89	396.47	13.62081445	7.11E+08	3.94E-02	1.80E+10
10	0.4	43.7	395.1182796	10.87018457	6.22E+08	3.94E-02	1.58E+10
AVE					6.25E+08	3.76E-02	1.66E+10
2							
#	**THK(mm)**	WDTH(mm)	Lo(mm)	MXLD(KN)	**MXSTRS(Pa)**	**MXSTRN**	**E(Pa)**
1	0.3	44.56	310.1698113	11.61409473	8.69E+08	4.53E-02	1.92E+10
2	0.34	45.66	281.6504854	12.22721875	7.88E+08	4.69E-02	1.68E+10
3	0.34	37.69	280.1588785	10.59933594	8.27E+08	4.93E-02	1.68E+10
4	0.33	49.47	319.3761468	14.26567969	8.74E+08	4.61E-02	1.90E+10
5	0.3	45.66	328.78	11.0345918	8.06E+08	4.18E-02	1.93E+10
6	0.33	48.56	358.8865979	11.9637666	7.47E+08	4.36E-02	1.71E+10
7	0.35	49.41	322.3333333	14.05158301	8.13E+08	4.69E-02	1.73E+10
8	0.35	48.97	358.8865979	14.03715234	8.19E+08	4.45E-02	1.84E+10
9	0.33	47.69	301.0471698	14.62723535	9.29E+08	5.13E-02	1.81E+10
10	0.31	45.75	335.9052632	11.13427344	7.85E+08	4.48E-02	1.75E+10
AVE					8.26E+08	4.60E-02	1.79E+10
3							
#	**THK(mm)**	WDTH(mm)	Lo(mm)	MXLD(KN)	**MXSTRS(Pa)**	**MXSTRN**	**E(Pa)**
1	0.33	48.21	285.0393972	10.96601563	6.89E+08	4.45E-02	1.55E+10
2	0.35	44.57	338.0148191	13.13235254	8.42E+08	4.18E-02	2.01E+10
3	0.37	47.57	290.1293864	13.85255469	7.87E+08	4.70E-02	1.68E+10
4	0.38	47.39	322.3659849	12.71119336	7.06E+08	4.19E-02	1.68E+10
5	0.34	44.96	323.0306571	11.29422363	7.39E+08	4.35E-02	1.70E+10
6	0.33	46.15	317.1665335	9.821774414	6.45E+08	4.22E-02	1.53E+10

7	0.34	46.13	293.9219274	13.07466016	8.34E+08	4.85E-02	1.72E+10
8	0.38	41.3	329.0127063	11.61888477	7.40E+08	4.49E-02	1.65E+10
9	0.4	41.06	341.0292788	11.94678906	7.27E+08	3.99E-02	1.82E+10
10	0.35	38.95	309.4713455	10.79454492	7.92E+08	4.30E-02	1.84E+10
AVE					7.50E+08	4.37E-02	1.72E+10
4							
#	**THK(mm)**	WDTH(mm)	Lo(mm)	MXLD(KN)	**MXSTRS(Pa)**	**MXSTRN**	**E(Pa)**
1	0.36	46.49	285.0716	10.579	6.32E+08	3.93E-02	1.61E+10
2	0.4	48.76	290.1	13.124	6.73E+08	4.35E-02	1.55E+10
3	0.42	48.95	281.9772	13.127	6.39E+08	3.96E-02	1.61E+10
4	0.41	49.65	292.034	12.903	6.34E+08	4.01E-02	1.58E+10
5	0.38	47.35	318.9166	12.258	6.81E+08	3.87E-02	1.76E+10
6	0.35	49.53	315.8222	12.247	7.06E+08	4.06E-02	1.74E+10
7	0.37	46.84	312.9212	12.946	7.47E+08	4.32E-02	1.73E+10
8	0.38	45.15	356.823	13.033	7.60E+08	4.17E-02	1.82E+10
9	0.39	47.29	332.4546	12.563	6.81E+08	3.79E-02	1.80E+10
10	0.34	42.76	325.6856	10.024	6.89E+08	3.69E-02	1.87E+10
AVE					6.84E+08	4.01E-02	1.71E+10
5							
#	**THK(mm)**	WDTH(mm)	Lo(mm)	MXLD(KN)	**MXSTRS(Pa)**	**MXSTRN**	**E(Pa)**
1	0.28	41.92	345.9926	7.932350098	6.76E+08	3.83E-02	1.77E+10
2	0.32	44.35	346.5728	13.45958984	9.48E+08	4.97E-02	1.91E+10
3	0.35	47.17	415.81	13.96442285	8.46E+08	3.81E-02	2.22E+10
4	0.36	46.55	391.635	13.11376855	7.83E+08	4.07E-02	1.92E+10
5	0.35	49.97	420.4516	11.46760449	6.56E+08	3.84E-02	1.71E+10
6	0.32	45.45	328.78	11.96986035	8.23E+08	4.08E-02	2.02E+10
7	0.32	45.26	303.4446	12.34260352	8.52E+08	4.07E-02	2.09E+10
8	0.35	44.46	328.9734	12.06729785	7.75E+08	3.85E-02	2.02E+10
9	0.36	46.66	372.6818	12.28779102	7.32E+08	3.69E-02	1.98E+10
10	0.34	45.26	332.648	9.955107422	6.47E+08	3.90E-02	1.66E+10
AVE					7.74E+08	4.01E-02	1.93E+10
6							
#	**THK(mm)**	WDTH(mm)	Lo(mm)	MXLD(KN)	**MXSTRS(Pa)**	**MXSTRN**	**E(Pa)**
1	0.3	42.93	269.793	8.861858398	6.88E+08	4.13E-02	1.66E+10
2	0.36	37.85	241.75	9.639086914	7.07E+08	4.11E-02	1.72E+10
3	0.37	43.38	285.0716	12.57082715	7.83E+08	4.01E-02	1.95E+10

4	0.36	48.93	281.5904	13.48717871	7.66E+08	3.98E-02	1.92E+10
5	0.33	45.95	264.5712	8.799012695	5.80E+08	3.99E-02	1.46E+10
6	0.37	42.98	257.222	8.575639648	5.39E+08	3.78E-02	1.43E+10
7	0.4	33.76	281.9772	8.907666992	6.60E+08	4.01E-02	1.64E+10
8	0.4	37.44	289.133	9.612499023	6.42E+08	3.53E-02	1.82E+10
9	0.37	38.15	311.9542	11.40575879	8.08E+08	3.76E-02	2.15E+10
10	0.34	47.67	291.067	9.088445313	5.61E+08	3.60E-02	1.56E+10
AVE					6.73E+08	3.89E-02	1.73E+10
7							
#	**THK(mm)**	WDTH(mm)	Lo(mm)	MXLD(KN)	**MXSTRS(Pa)**	**MXSTRN**	**E(Pa)**
1	0.36	46.62	277.7224	7.932683594	4.73E+08	3.71E-02	1.27E+10
2	0.4	48.7	302.2842	11.34742969	5.83E+08	3.49E-02	1.67E+10
3	0.42	45.75	285.265	11.91153125	6.20E+08	3.95E-02	1.57E+10
4	0.39	43.5	279.0762	12.1749834	7.18E+08	4.01E-02	1.79E+10
5	0.38	49.77	295.1284	10.70126074	5.66E+08	4.04E-02	1.40E+10
6	0.35	45.36	282.9442	9.39421875	5.92E+08	3.88E-02	1.53E+10
7	0.39	47.77	285.0716	11.99805469	6.44E+08	4.03E-02	1.60E+10
8	0.4	44.51	279.0762	12.43076465	6.98E+08	4.45E-02	1.57E+10
9	0.38	41.53	281.9772	12.95190723	8.21E+08	4.69E-02	1.75E+10
10	0.33	47.3	241.75	9.277863281	5.94E+08	4.20E-02	1.41E+10
AVE					6.31E+08	4.05E-02	1.56E+10
8							
#	**THK(mm)**	WDTH(mm)	Lo(mm)	MXLD(KN)	**MXSTRS(Pa)**	**MXSTRN**	**E(Pa)**
1	0.36	43.4	329.1668	9.783	6.26E+08	3.91E-02	1.60E+10
2	0.38	45.05	297.0624	11.48491504	6.71E+08	4.06E-02	1.65E+10
3	0.4	48.43	290.1	12.56345996	6.49E+08	4.08E-02	1.59E+10
4	0.4	44.09	309.0532	11.72402246	6.65E+08	3.76E-02	1.77E+10
5	0.36	45.22	305.3786	9.533008789	5.86E+08	4.04E-02	1.45E+10
6	0.37	49.99	335.549	11.76249512	6.36E+08	3.99E-02	1.59E+10
7	0.4	45.56	305.3786	11.61858105	6.38E+08	4.32E-02	1.48E+10
8	0.39	47.98	299.77	12.31216602	6.58E+08	4.14E-02	1.59E+10
9	0.36	47.72	342.5114	13.0448584	7.59E+08	3.94E-02	1.93E+10
10	0.34	41.37	322.3978	8.051918945	5.72E+08	4.04E-02	1.42E+10
AVE					6.46E+08	4.03E-02	1.61E+10
9							
#	**THK(mm)**	WDTH(mm)	Lo(mm)	MXLD(KN)	**MXSTRS(Pa)**	**MXSTRN**	**E(Pa)**

1	0.23	41.94	315.6288	8.635242188	8.95E+08	4.16E-02	2.15E+10
2	0.24	47.77	261.8636	8.574032227	7.48E+08	4.38E-02	1.71E+10
3	0.26	45.69	322.3978	8.651582031	7.28E+08	3.95E-02	1.84E+10
4	0.26	49.29	321.6242	10.5624707	8.24E+08	3.88E-02	2.13E+10
5	0.23	39.81	291.067	7.730441406	8.44E+08	3.97E-02	2.13E+10
6	0.25	47.9	252.5804	7.645827637	6.38E+08	4.33E-02	1.47E+10
7	0.23	39.05	295.1284	8.111187988	9.03E+08	4.23E-02	2.14E+10
8	0.27	46.64	274.628	9.624989258	7.64E+08	4.78E-02	1.60E+10
9	0.25	44.59	297.0624	9.543588867	8.56E+08	4.32E-02	1.98E+10
10	0.24	47.6	332.4546	10.44390234	9.14E+08	4.15E-02	2.20E+10
AVE					8.12E+08	4.22E-02	1.93E+10
10							
#	**THK(mm)**	WDTH(mm)	Lo(mm)	MXLD(KN)	**MXSTRS(Pa)**	**MXSTRN**	**E(Pa)**
1	0.25	47.29	275.0148	8.923371094	7.55E+08	4.10E-02	1.84E+10
2	0.25	44.18	304.2182	9.290384766	8.41E+08	3.65E-02	2.31E+10
3	0.27	49.06	281.9772	9.022749023	6.81E+08	3.74E-02	1.82E+10
4	0.27	43.98	271.9204	9.051580078	7.62E+08	3.93E-02	1.94E+10
5	0.23	47.59	270.3732	7.811841797	7.14E+08	3.40E-02	2.10E+10
6	0.24	45.89	296.0954	9.285867188	8.43E+08	4.76E-02	1.77E+10
7	0.3	46.3	285.0716	9.650636719	6.95E+08	4.01E-02	1.73E+10
8	0.26	49.94	341.351	9.909601563	7.63E+08	3.69E-02	2.07E+10
9	0.26	45.26	322.3978	8.704151367	7.40E+08	3.50E-02	2.11E+10
10	0.23	43.56	318.3364	9.129160156	9.11E+08	3.95E-02	2.31E+10
AVE					7.71E+08	3.87E-02	2.00E+10
11							
#	**THK(mm)**	WDTH(mm)	Lo(mm)	MXLD(KN)	**MXSTRS(Pa)**	**MXSTRN**	**E(Pa)**
1	0.23	47.77	299.9634	8.24324707	7.50E+08	3.53E-02	2.12E+10
2	0.24	42.83	315.242	7.426577637	7.22E+08	3.55E-02	2.04E+10
3	0.26	42.85	302.2842	9.22177832	8.28E+08	3.99E-02	2.07E+10
4	0.26	44.06	303.638	9.281380859	8.10E+08	3.75E-02	2.16E+10
5	0.25	46.59	315.0486	8.295179688	7.12E+08	3.50E-02	2.04E+10
6	0.27	48.62	315.8222	9.947103516	7.58E+08	4.08E-02	1.85E+10
7	0.26	47.63	330.9074	8.368910156	6.76E+08	3.45E-02	1.96E+10
8	0.25	43.2	386.8	8.272745117	7.66E+08	3.04E-02	2.52E+10
9	0.25	45.63	359.724	9.574330078	8.39E+08	3.83E-02	2.19E+10
10	0.22	44.53	302.2842	8.362482422	8.54E+08	3.90E-02	2.19E+10

AVE					7.72E+08	3.66E-02	2.11E+10
12							
#	**THK(mm)**	WDTH(mm)	Lo(mm)	MXLD(KN)	**MXSTRS(Pa)**	**MXSTRN**	**E(Pa)**
1	0.22	49.57	246.9718	7.993256348	7.33E+08	3.85E-02	1.90E+10
2	0.23	49.13	246.9718	8.007990234	7.09E+08	4.00E-02	1.77E+10
3	0.22	45.95	221.6364	6.847408691	6.77E+08	4.19E-02	1.62E+10
4	0.22	48.97	274.4346	8.339714844	7.74E+08	3.64E-02	2.12E+10
5	0.21	47.22	260.7032	7.190684082	7.25E+08	3.81E-02	1.90E+10
6	0.23	46.35	222.2166	7.131384277	6.69E+08	3.84E-02	1.74E+10
7	0.26	46.07	244.2642	8.016660645	6.69E+08	3.95E-02	1.69E+10
8	0.27	48.7	295.7086	9.459612305	7.19E+08	3.57E-02	2.02E+10
9	0.27	49.93	276.562	9.048396484	6.71E+08	3.83E-02	1.75E+10
10	0.26	48.06	232.2734	8.090057617	6.47E+08	4.73E-02	1.37E+10
AVE					6.99E+08	3.94E-02	1.79E+10
13							
#	**THK(mm)**	WDTH(mm)	Lo(mm)	MXLD(KN)	**MXSTRS(Pa)**	**MXSTRN**	**E(Pa)**
1	0.24	48.3	276.9488	9.661217773	8.33E+08	4.19E-02	1.99E+10
2	0.24	49.38	256.6418	10.03781055	8.47E+08	4.29E-02	1.98E+10
3	0.26	45.72	274.8214	9.225294922	7.76E+08	4.10E-02	1.89E+10
4	0.24	47.46	269.5996	9.909268555	8.70E+08	4.31E-02	2.02E+10
5	0.24	47.65	286.232	10.34870801	9.05E+08	4.10E-02	2.21E+10
6	0.25	46.82	253.7408	9.846786133	8.41E+08	4.46E-02	1.89E+10
7	0.25	45.73	264.5712	9.012168945	7.88E+08	4.12E-02	1.91E+10
8	0.25	47.72	248.9058	9.475316406	7.94E+08	4.20E-02	1.89E+10
9	0.25	47.39	303.638	10.69228711	9.02E+08	3.83E-02	2.36E+10
10	0.28	47.38	249.8728	7.91567627	5.97E+08	3.87E-02	1.54E+10
AVE					8.15E+08	4.15E-02	1.97E+10
14							
#	**THK(mm)**	WDTH(mm)	Lo(mm)	MXLD(KN)	**MXSTRS(Pa)**	**MXSTRN**	**E(Pa)**
1	0.26	38.82	276.3686	7.27851123	7.21E+08	3.98E-02	1.81E+10
2	0.27	46.92	225.311	6.421792969	5.07E+08	4.51E-02	1.12E+10
3	0.28	48.49	260.7032	8.809925781	6.49E+08	4.66E-02	1.39E+10
4	0.28	48.61	279.0762	8.18779834	6.02E+08	4.25E-02	1.42E+10
5	0.23	43.1	320.6572	8.507032227	8.58E+08	4.01E-02	2.14E+10
6	0.27	48	246.9718	8.228816406	6.35E+08	4.16E-02	1.53E+10
7	0.28	47.06	252.7738	7.43427832	5.64E+08	3.85E-02	1.47E+10

8	0.28	47.72	274.4346	9.16087207	6.86E+08	3.77E-02	1.82E+10
9	0.24	45.75	247.1652	8.703181641	7.93E+08	3.90E-02	2.03E+10
10	0.26	38.53	243.2972	7.499337891	7.49E+08	4.22E-02	1.77E+10
AVE					6.76E+08	4.13E-02	1.65E+10
15							
#	**THK(mm)**	WDTH(mm)	Lo(mm)	MXLD(KN)	**MXSTRS(Pa)**	**MXSTRN**	**E(Pa)**
1	0.26	47.79	236.7216	7.38813623	5.95E+08	4.37E-02	1.36E+10
2	0.28	46.57	264.5712	9.606405273	7.37E+08	4.21E-02	1.75E+10
3	0.3	49.8	239.2358	7.814418457	5.23E+08	3.99E-02	1.31E+10
4	0.26	49.51	271.9204	8.768241211	6.81E+08	4.68E-02	1.46E+10
5	0.23	47	267.4722	8.581702148	7.94E+08	4.08E-02	1.95E+10
6	0.28	47.03	235.948	7.397413086	5.62E+08	4.72E-02	1.19E+10
7	0.28	49.12	289.133	9.595491211	6.98E+08	3.99E-02	1.75E+10
8	0.29	48.96	269.2128	8.315037109	5.86E+08	4.50E-02	1.30E+10
9	0.28	47.24	229.3724	7.283634766	5.51E+08	5.28E-02	1.04E+10
10	0.24	47.56	270.1798	8.902543945	7.80E+08	5.87E-02	1.33E+10
AVE					6.51E+08	4.57E-02	1.44E+10
16							
#	**THK(mm)**	WDTH(mm)	Lo(mm)	MXLD(KN)	**MXSTRS(Pa)**	**MXSTRN**	**E(Pa)**
1	0.2	41.56	282.1706	7.764	9.34E+08	4.31E-02	2.17E+10
2	0.21	49.06	282.1706	8.485	8.24E+08	3.92E-02	2.10E+10
3	0.22	48.19	239.2358	8.754	8.26E+08	4.91E-02	1.68E+10
4	0.24	46.18	307.6994	8.152	7.36E+08	3.68E-02	2.00E+10
5	0.23	47.62	268.0524	8.917	8.14E+08	4.64E-02	1.75E+10
6	0.23	46.24	256.255	8.335	7.84E+08	4.57E-02	1.72E+10
7	0.25	48.25	278.496	8.611	7.14E+08	4.51E-02	1.58E+10
8	0.25	45.64	267.0854	8.412	7.37E+08	4.45E-02	1.66E+10
9	0.25	48.93	294.3548	9.629	7.87E+08	4.14E-02	1.90E+10
10	0.25	48.95	227.4384	7.198	5.88E+08	4.89E-02	1.20E+10
AVE					7.74E+08	4.40E-02	1.78E+10

Appendix B: Overall contrast of the 4 selected key testing results.

Main Effects		GAP	SPREADING GUIDE	YARN#	ROLLER/MOLD DIS	HEATING CHAMBER	ZONE TEMP12	ZONE TEMP34	MOLD TEMP	ROLLER TEMP1	ROLLER TEMP2	ROLLER PRESSURE				
Contrast Labels		A	B	C	D	E	F	G	H	I	J	K	L	M	N	O
Two-Factor Interactions		BC	AC	AB	AE	AD	AG	AF	AI	AH	AK	AJ	DH	DI	DJ	DK
		DE	DF	DG	BF	BG	BD	BE	BJ	BK	BH	BI	EI	EH	EK	EJ
		FG	EG	EF	CG	CF	CE	CD	CK	CJ	CI	CH	FJ	FK	FH	FI
		HI	HJ	HK		KN							GK	GJ	GI	GH
		JK	IK	IJ												
Overall Contrast	Thickness	-9.12E-01	-4.60E-02	1.00E-02	-5.80E-02	-5.40E-02	9.20E-02	4.00E-02	2.00E-03	-1.42E-01	-9.60E-02	-1.60E-01	-5.20E-02	-9.60E-02	-1.00E-02	-5.40E-02
	Stress	3.61E+08	-2.47E+07	-2.98E+08	1.10E+08	1.98E+08	-8.94E+06	-3.65E+08	-8.13E+07	3.83E+08	8.77E+07	6.76E+08	1.22E+08	3.17E+08	1.78E+08	-7.92E+07
	Strain	2.16E-03	-2.33E-02	7.77E-03	-1.33E-02	1.02E-02	-1.02E-04	4.09E-03	6.35E-03	1.57E-02	2.08E-02	5.34E-03	7.45E-03	5.05E-03	5.96E-03	1.04E-03
	Modulus	9.68E+09	9.39E+09	-1.06E+10	8.31E+09	1.00E+09	-1.04E+09	-9.63E+09	-3.67E+09	1.54E+09	-6.50E+09	1.43E+10	-8.41E+07	5.43E+09	2.17E+09	-2.71E+09

Appendix C: F table chosen for the ANOVA analysis with the error value of 0.05

F Table for $\alpha = 0.05$														
/	**df_1=1**	**2**	**3**	**4**	**5**	**6**	**7**	**8**	**9**	**10**	**12**	**15**	**20**	**…**
df_2=1	161.448	199.5	215.707	224.583	230.162	233.986	236.768	238.883	240.543	241.882	243.906	245.95	248.013	…
2	18.5128	19	19.1643	19.2468	19.2964	19.3295	19.3532	19.371	19.3848	19.3959	19.4125	19.4291	19.4458	…
3	10.128	9.5521	9.2766	9.1172	9.0135	8.9406	8.8867	8.8452	8.8123	8.7855	8.7446	8.7029	8.6602	…
4	7.7086	6.9443	6.5914	6.3882	6.2561	6.1631	6.0942	6.041	5.9988	5.9644	5.9117	5.8578	5.8025	…
5	6.6079	5.7861	5.4095	5.1922	5.0503	4.9503	4.8759	4.8183	4.7725	4.7351	4.6777	4.6188	4.5581	…
6	5.9874	5.1433	4.7571	4.5337	4.3874	4.2839	4.2067	4.1468	4.099	4.06	3.9999	3.9381	3.8742	…
7	5.5914	4.7374	4.3468	4.1203	3.9715	3.866	3.787	3.7257	3.6767	3.6365	3.5747	3.5107	3.4445	…
8	5.3177	4.459	4.0662	3.8379	3.6875	3.5806	3.5005	3.4381	3.3881	3.3472	3.2839	3.2184	3.1503	…
9	5.1174	4.2565	3.8625	3.6331	3.4817	3.3738	3.2927	3.2296	3.1789	3.1373	3.0729	3.0061	2.9365	…
10	4.9646	4.1028	3.7083	3.478	3.3258	3.2172	3.1355	3.0717	3.0204	2.9782	2.913	2.845	2.774	…
11	4.8443	3.9823	3.5874	3.3567	3.2039	3.0946	3.0123	2.948	2.8962	2.8536	2.7876	2.7186	2.6464	…
12	4.7472	3.8853	3.4903	3.2592	3.1059	2.9961	2.9134	2.8486	2.7964	2.7534	2.6866	2.6169	2.5436	…
13	4.6672	3.8056	3.4105	3.1791	3.0254	2.9153	2.8321	2.7669	2.7144	2.671	2.6037	2.5331	2.4589	…
14	4.6001	3.7389	3.3439	3.1122	2.9582	2.8477	2.7642	2.6987	2.6458	2.6022	2.5342	2.463	2.3879	…
15	4.5431	3.6823	3.2874	3.0556	2.9013	2.7905	2.7066	2.6408	2.5876	2.5437	2.4753	2.4034	2.3275	…
16	4.494	3.6337	3.2389	3.0069	2.8524	2.7413	2.6572	2.5911	2.5377	2.4935	2.4247	2.3522	2.2756	…
…	…	…	…	…	…	…	…	…	…	…	…	…	…	…

Appendix D: Tensile curves for the product tests.

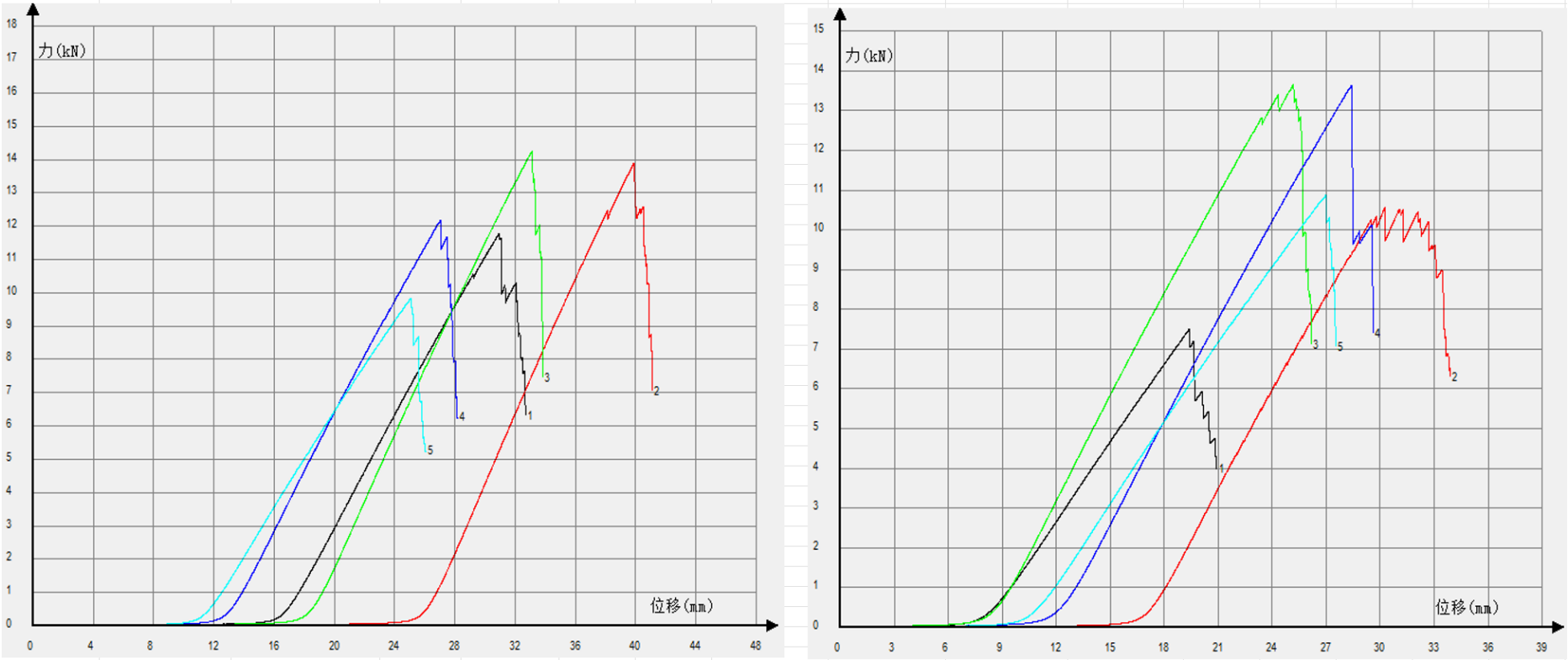

Figure 7.1 Vertical Tensile for Run #1

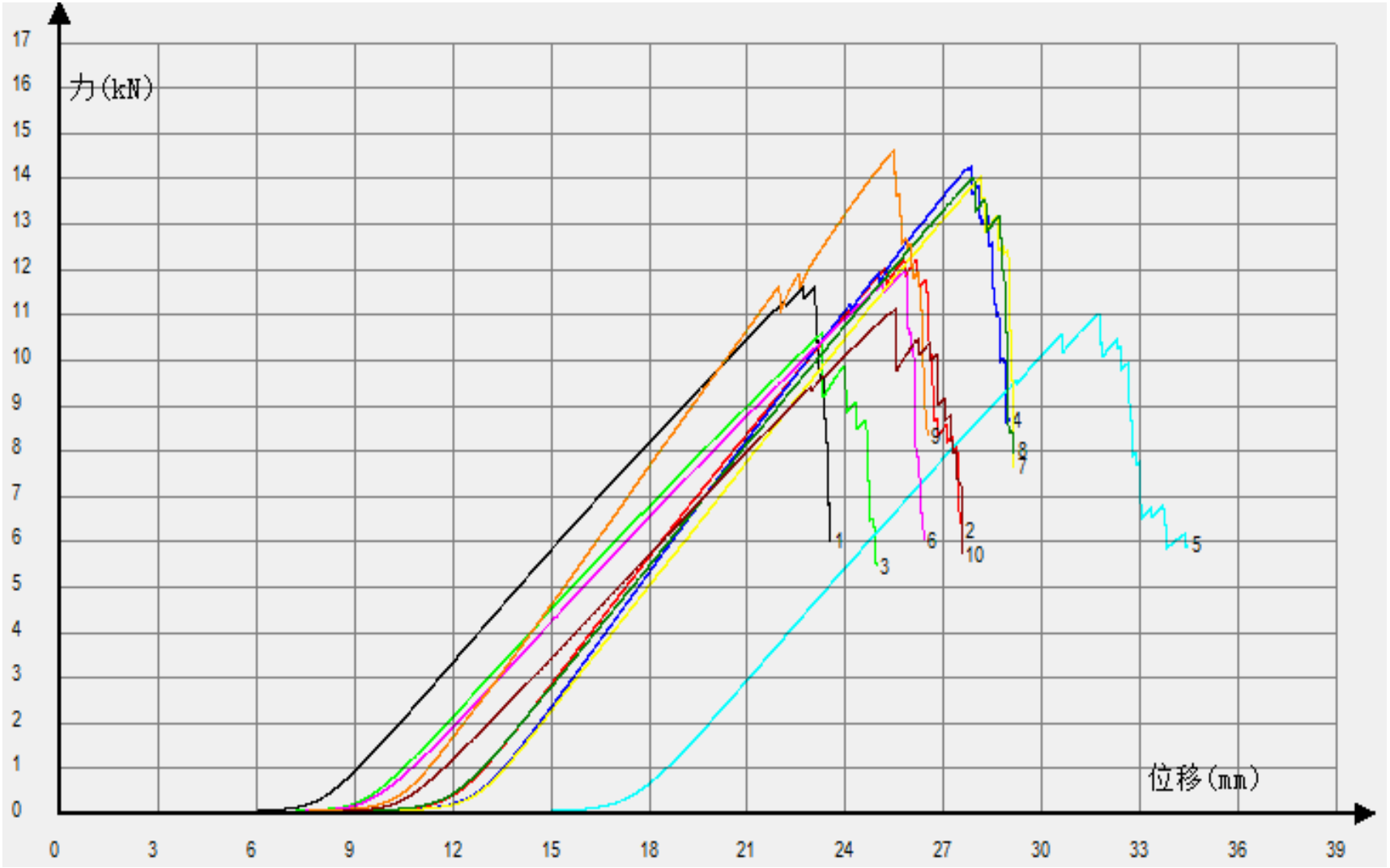

Figure 7.2 Vertical Tensile for Run #2

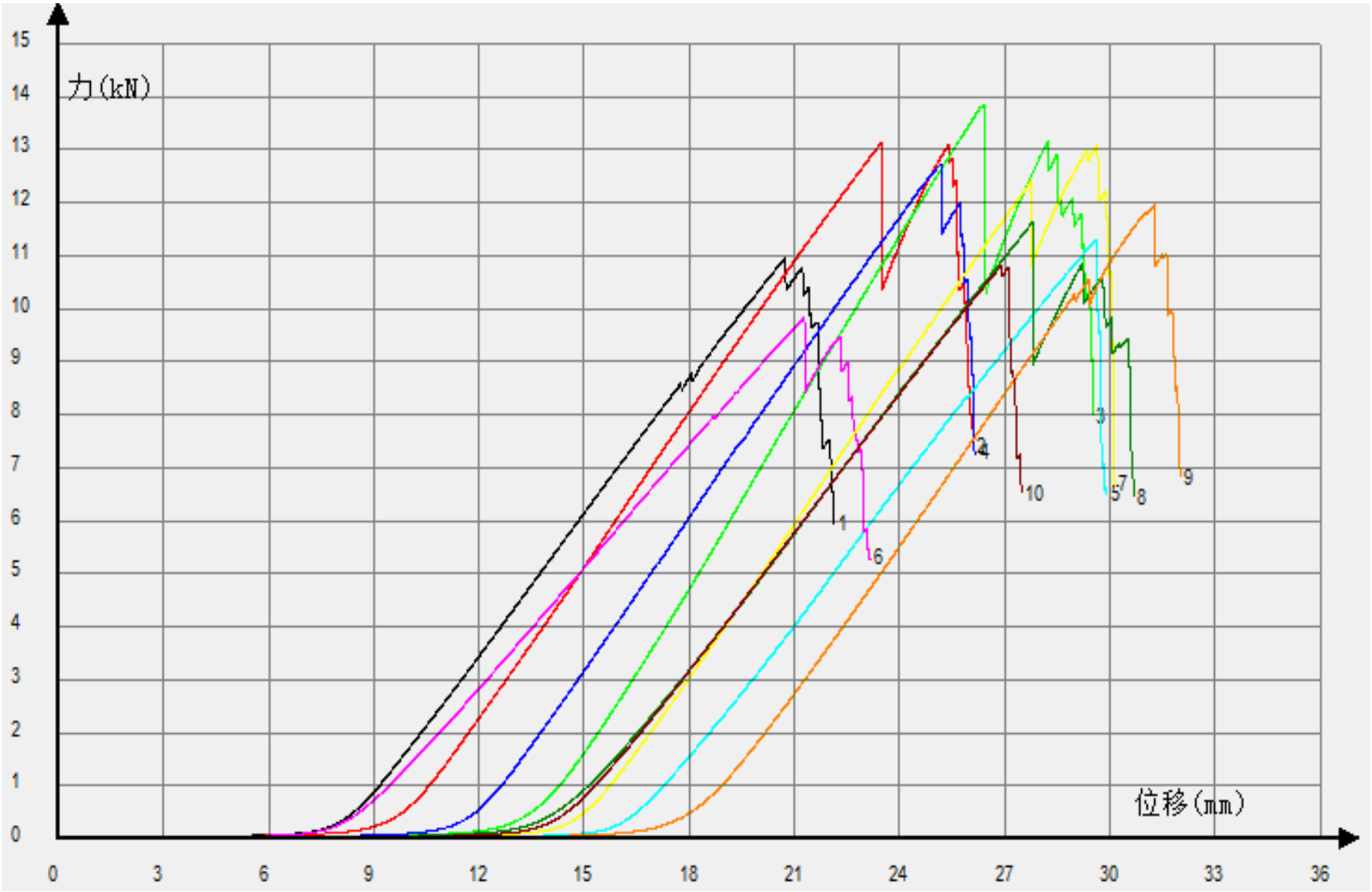

Figure 7.3 Vertical Tensile for Run #3

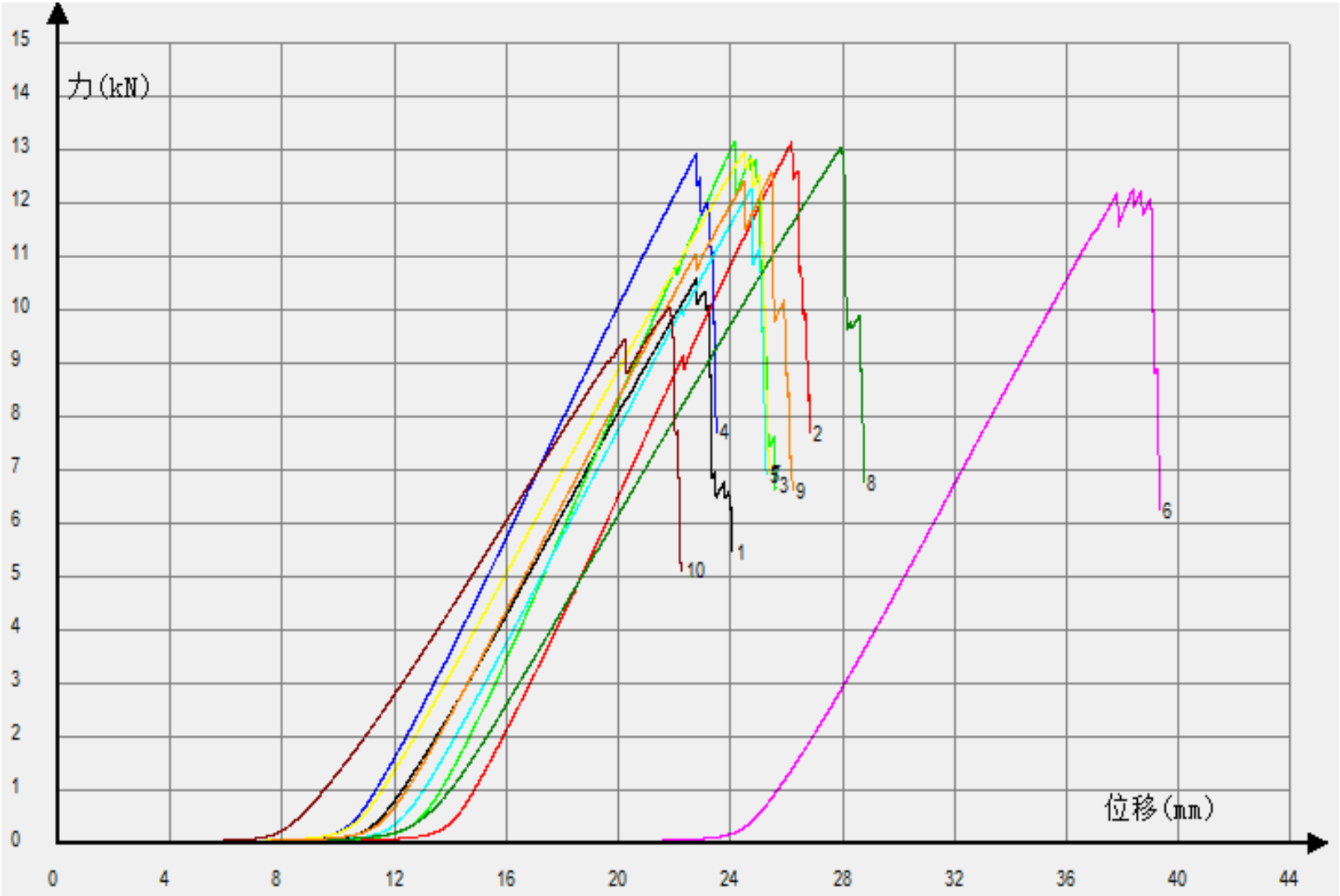

Figure 7.4 Vertical Tensile for Run #4

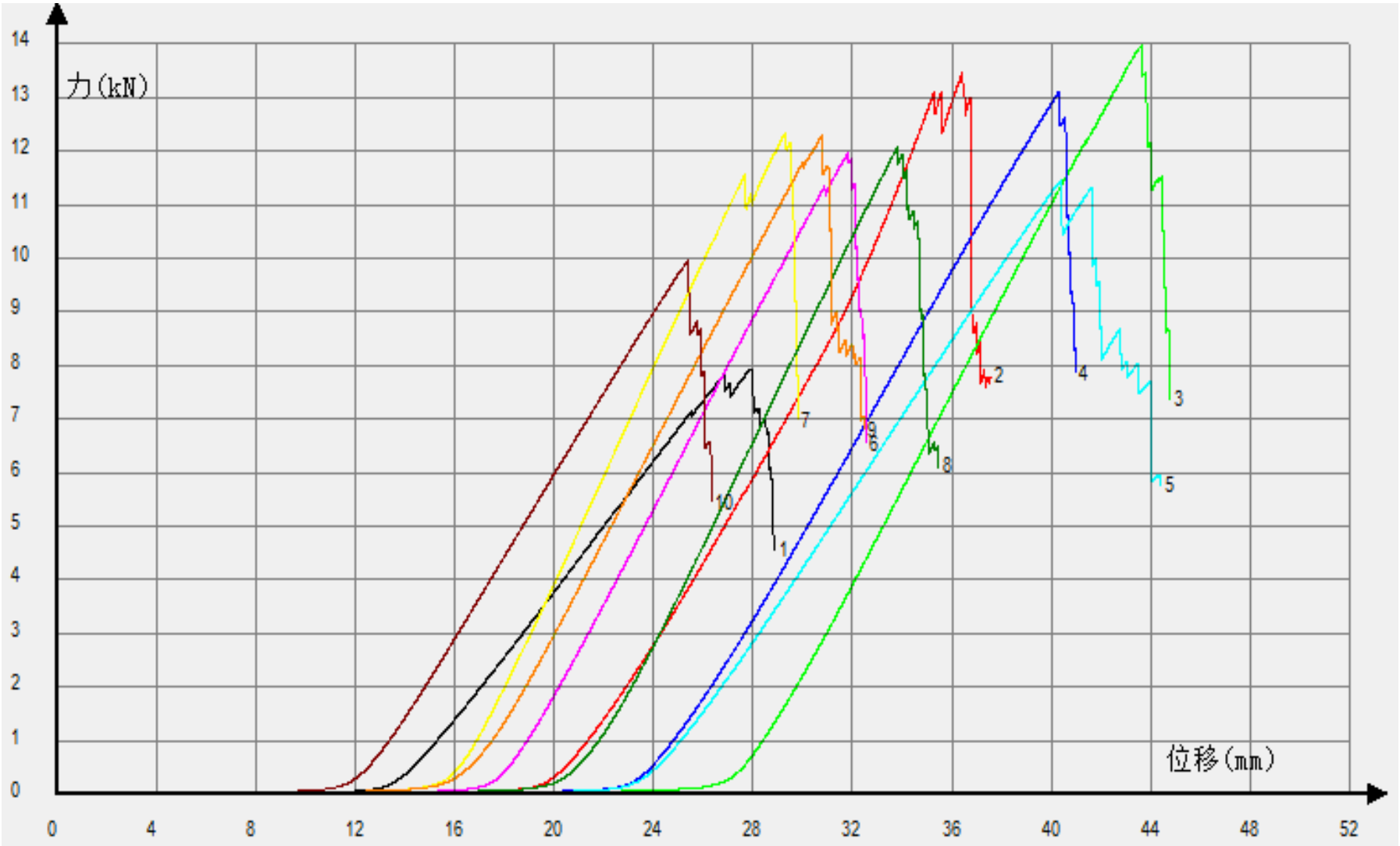

Figure 7.5 Vertical Tensile for Run #5

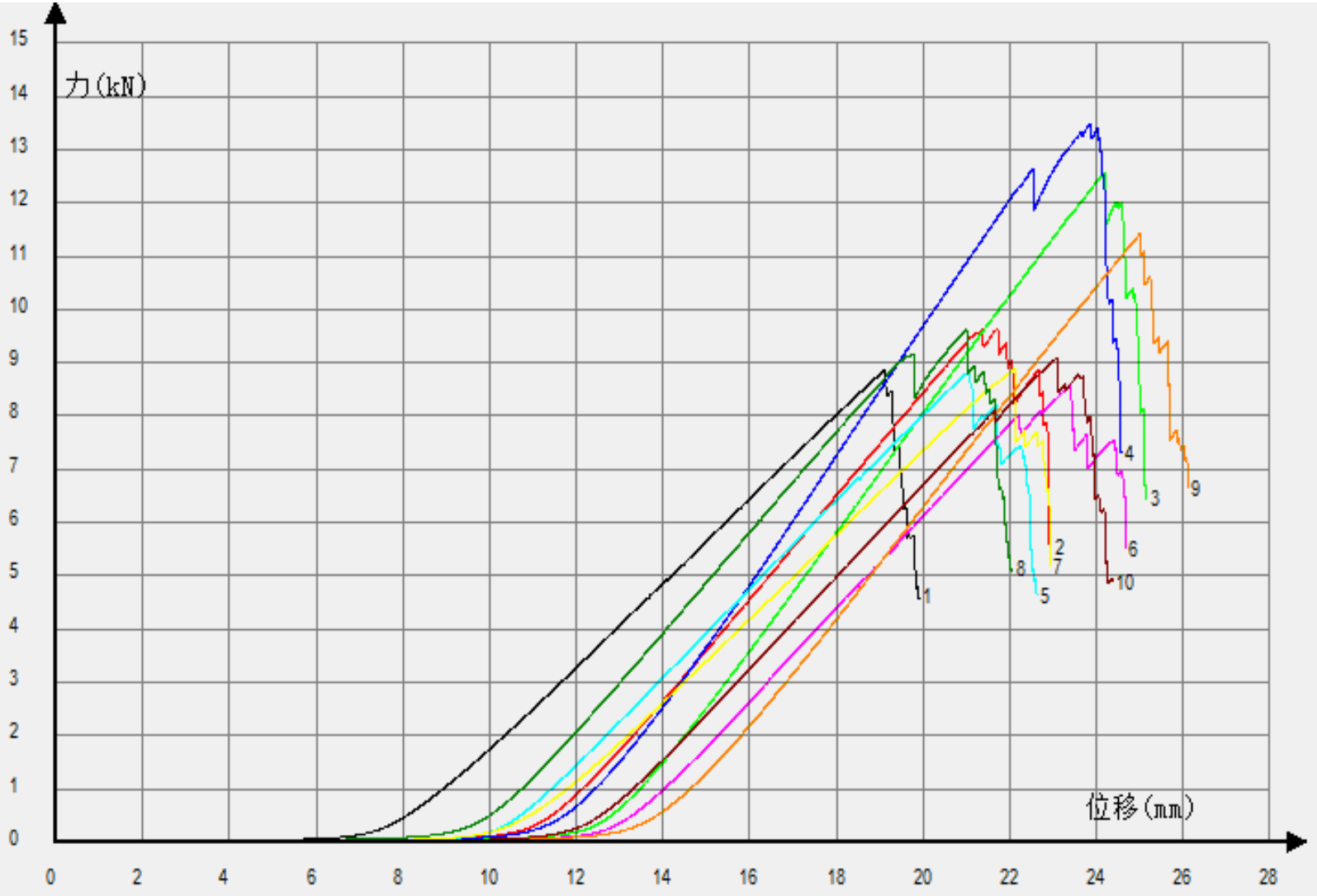

Figure 7.6 Vertical Tensile for Run #6

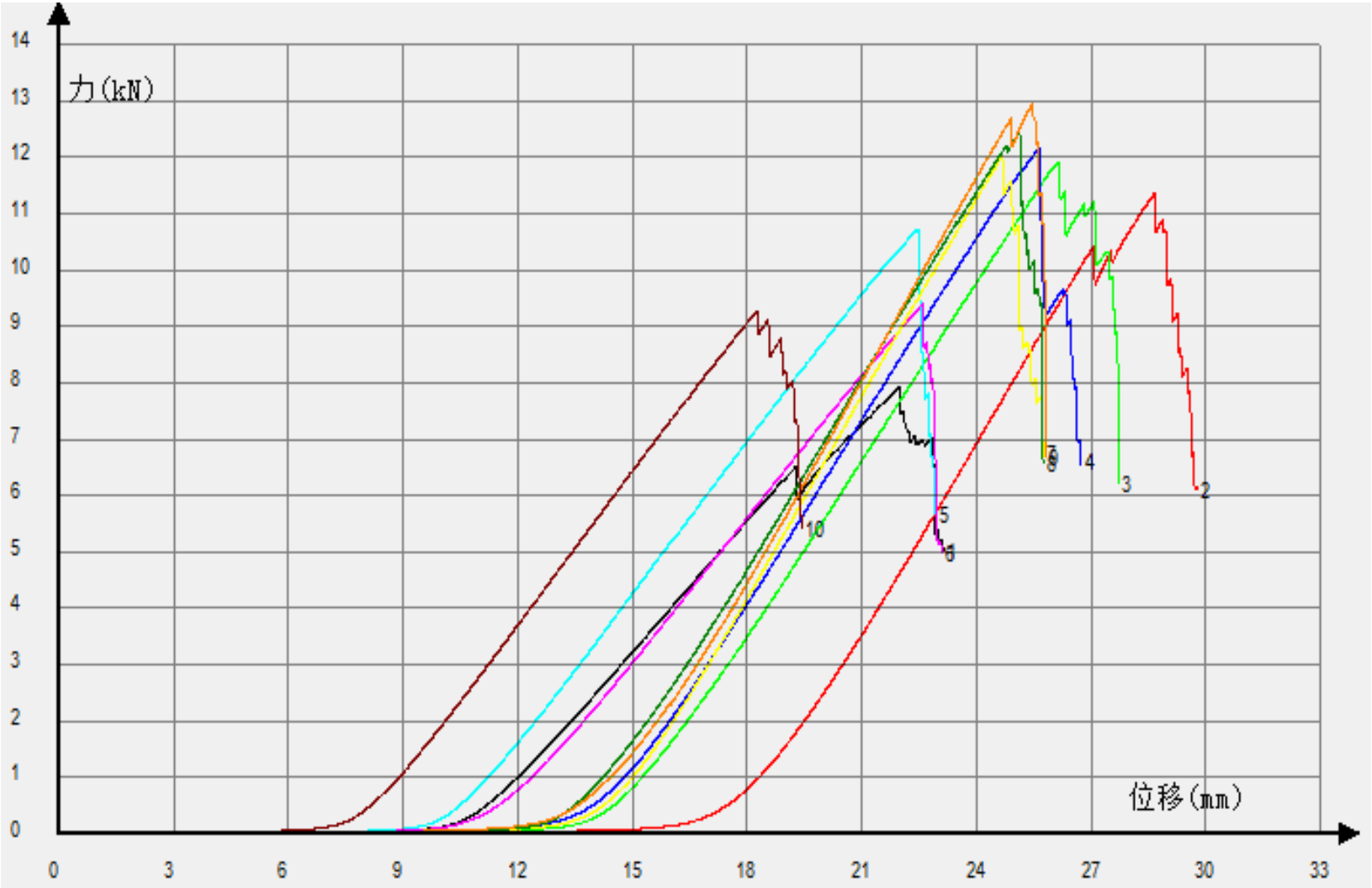

Figure 7.7 Vertical Tensile for Run #7

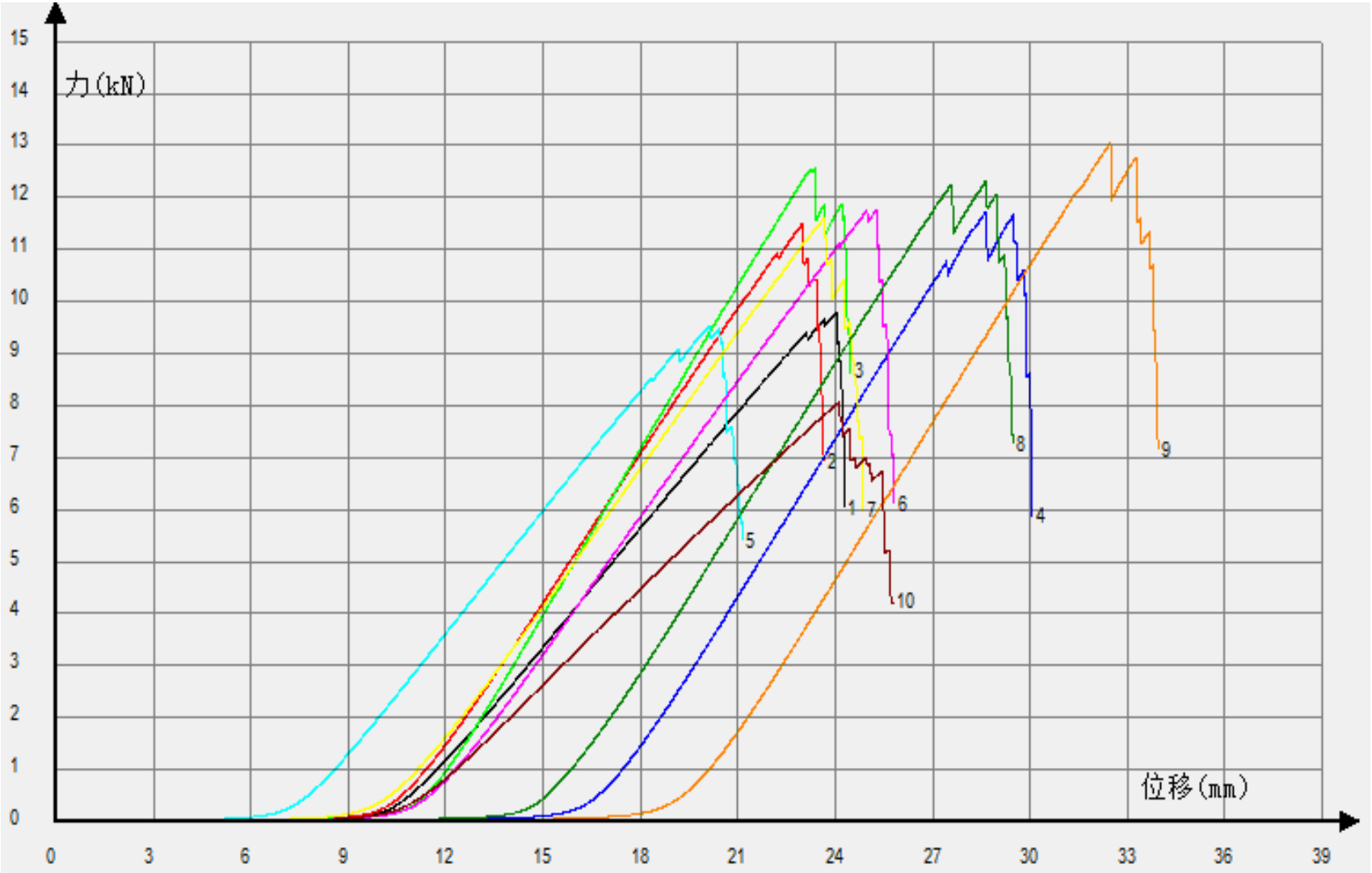

Figure 7.8 Vertical Tensile for Run #8

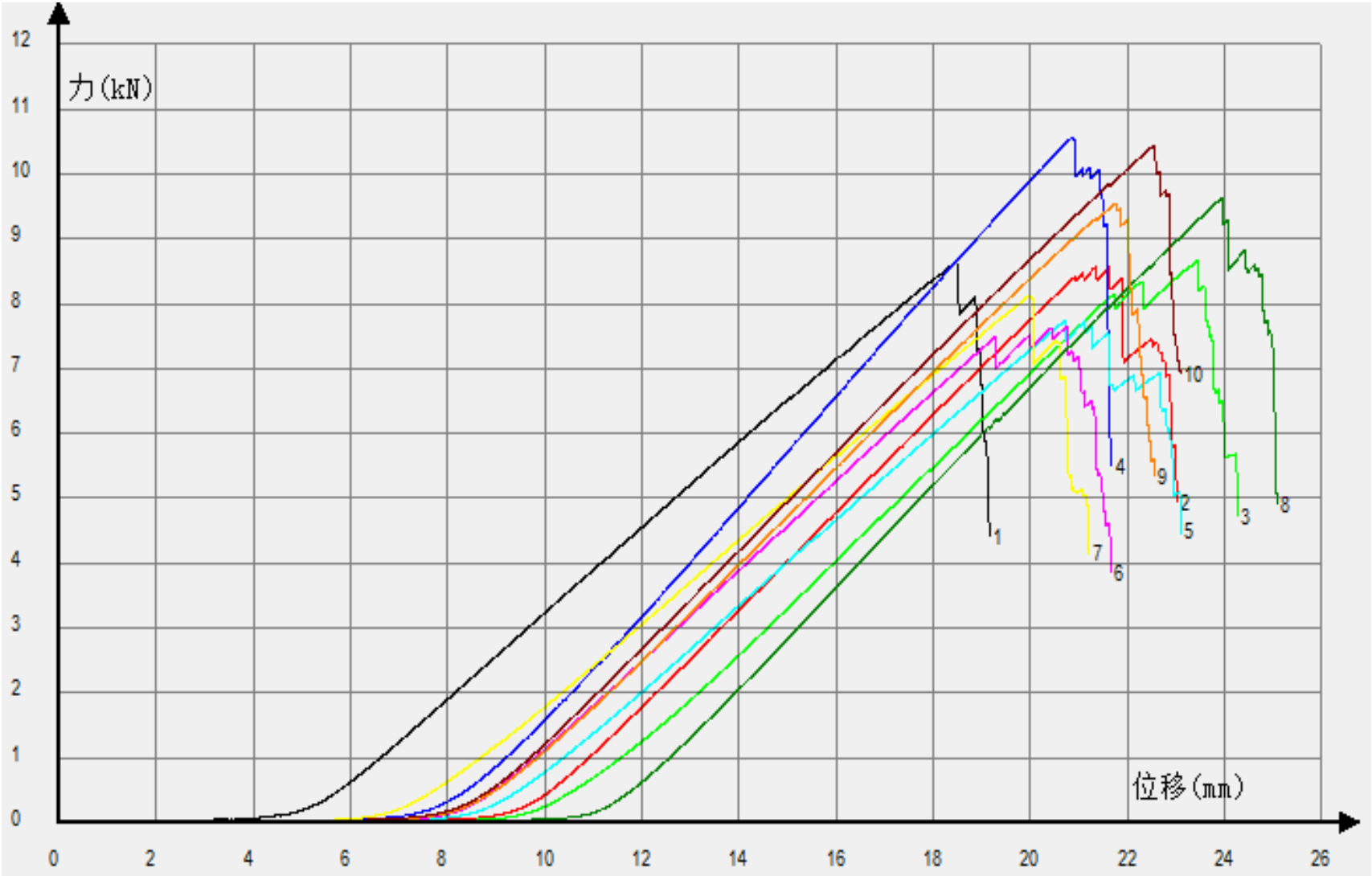

Figure 7.9 Vertical Tensile for Run #9

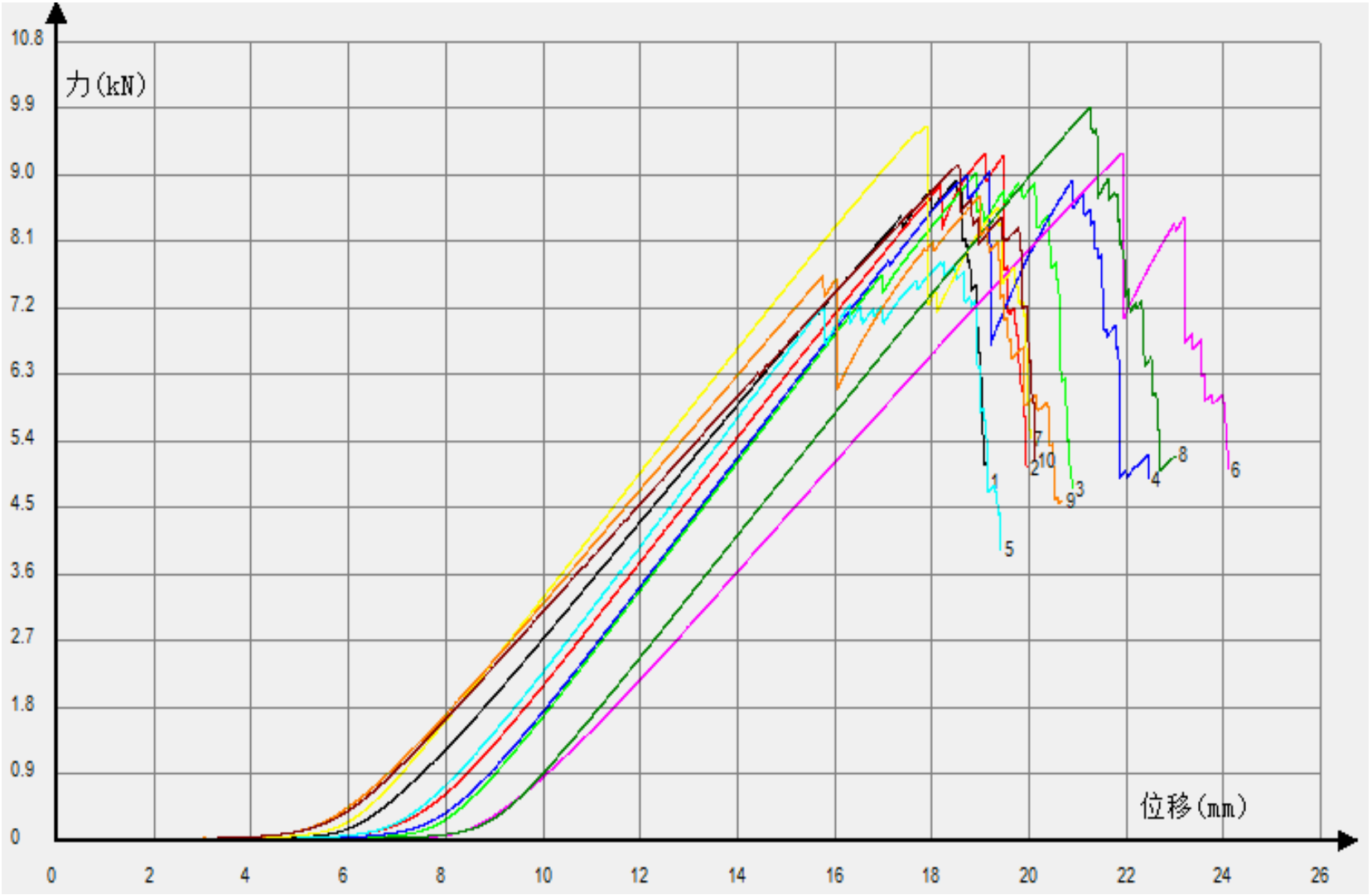

Figure 7.10 Vertical Tensile for Run #10

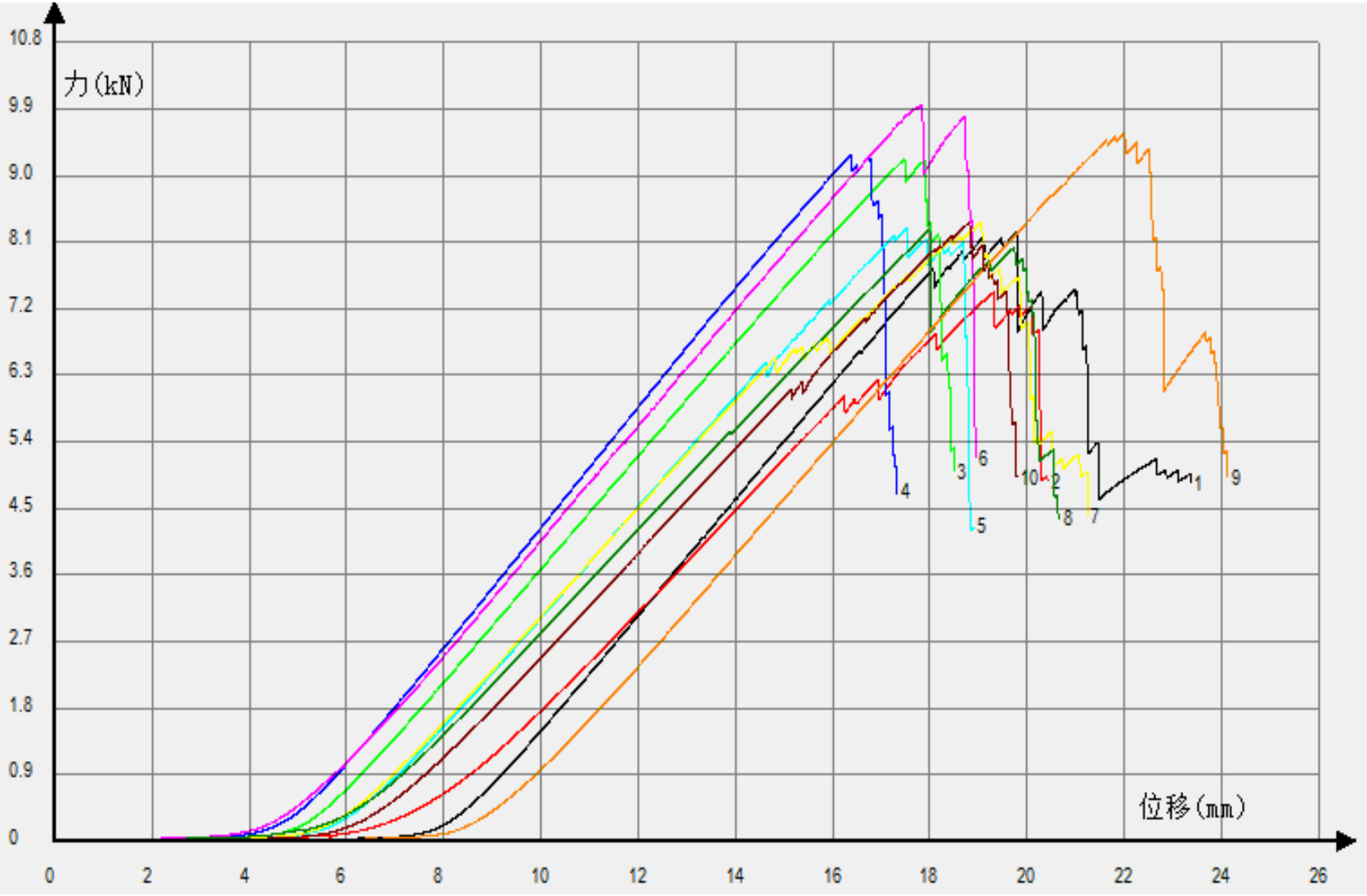

Figure 7.1 Vertical Tensile for Run #11

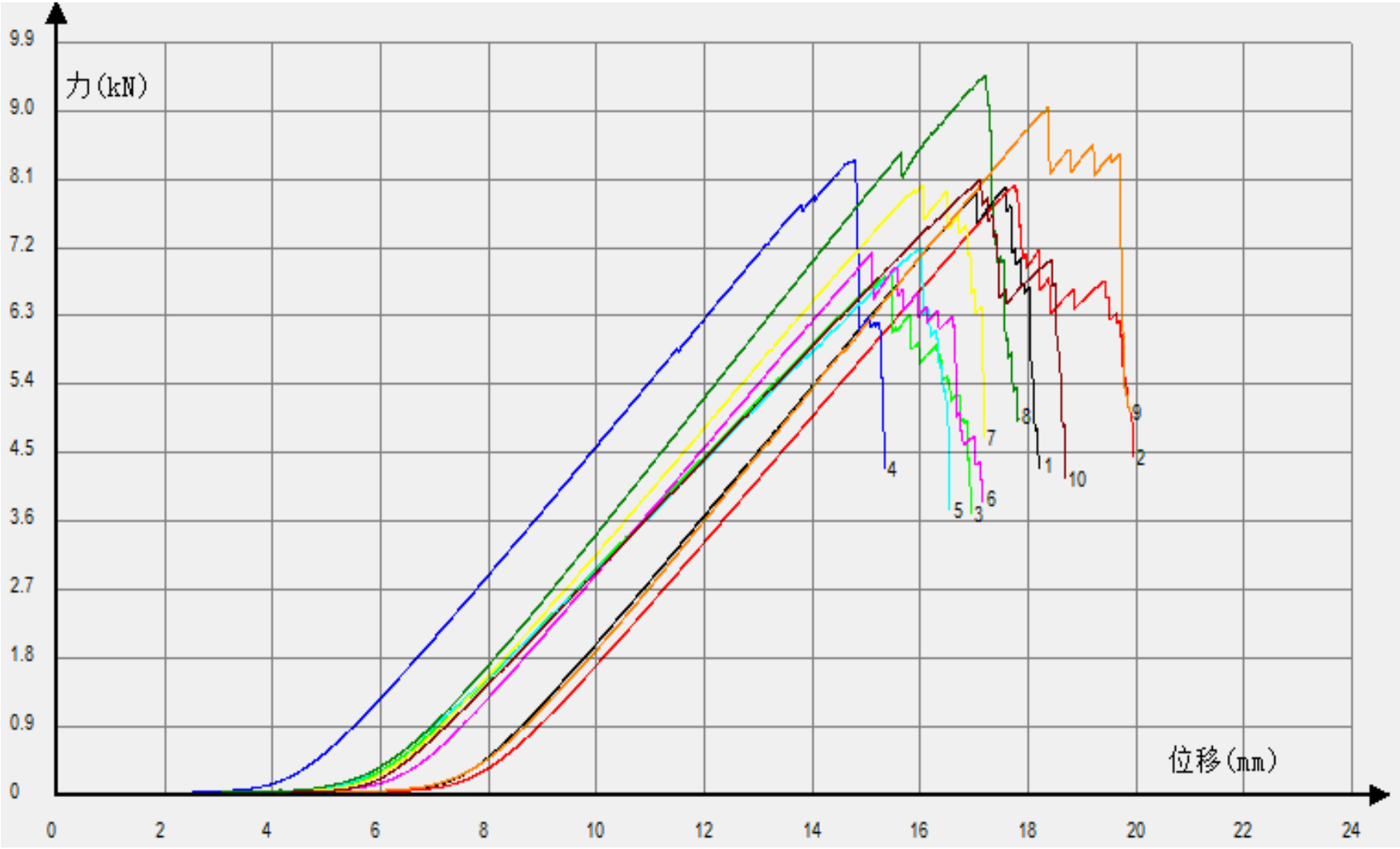

Figure 7.12 Vertical Tensile for Run #12

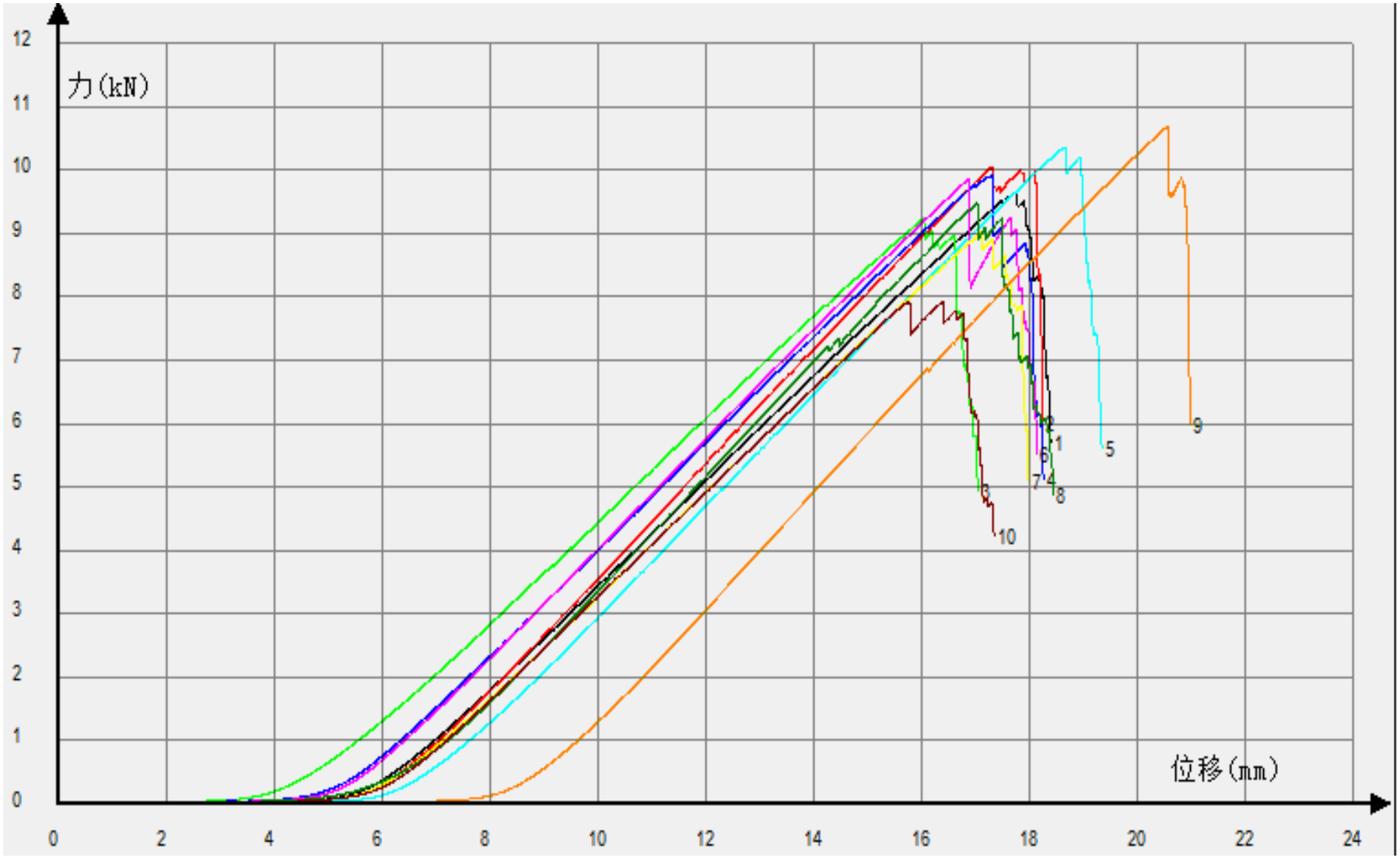

Figure 7.13 Vertical Tensile for Run #13

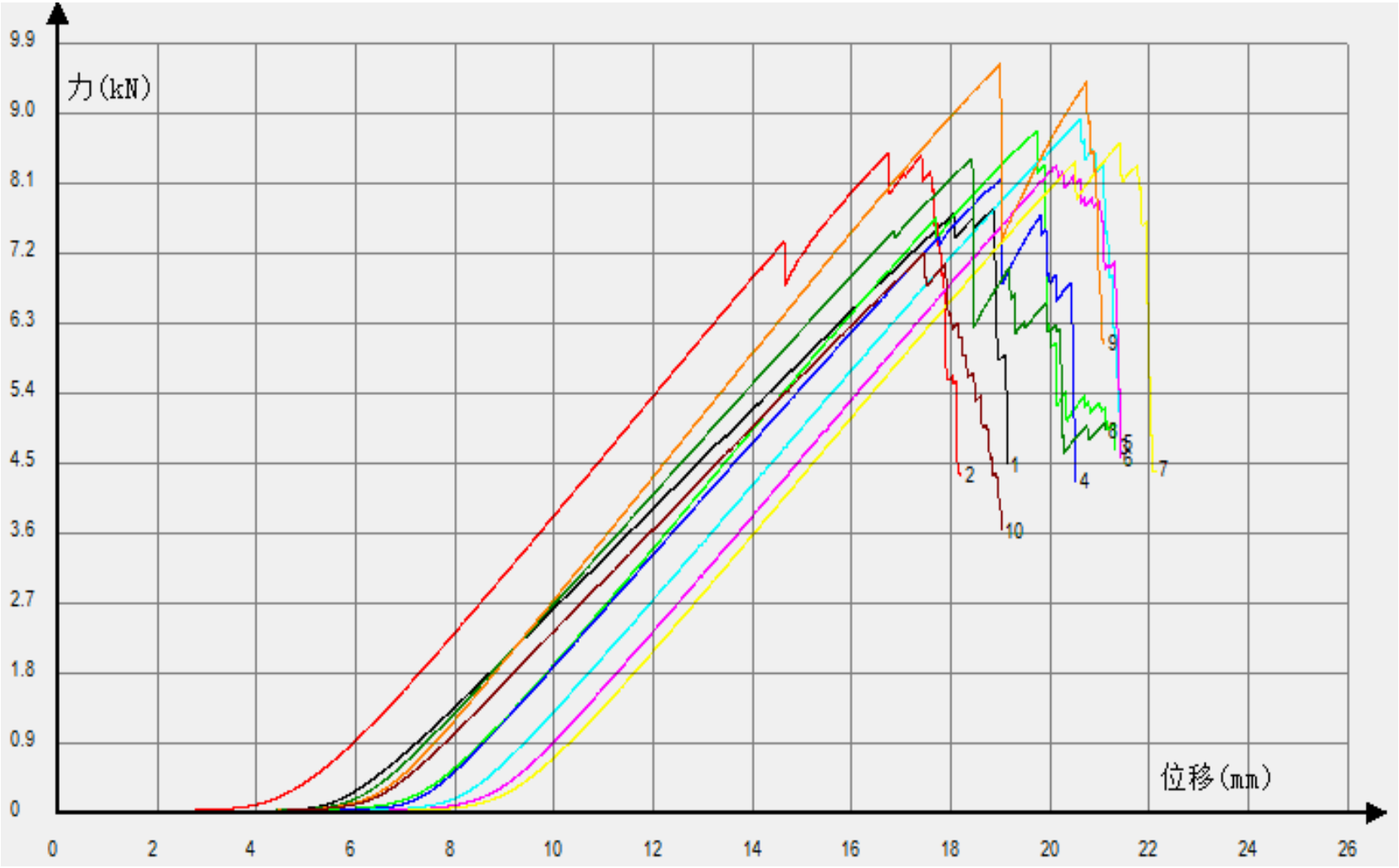

Figure 7.14 Vertical Tensile for Run #14

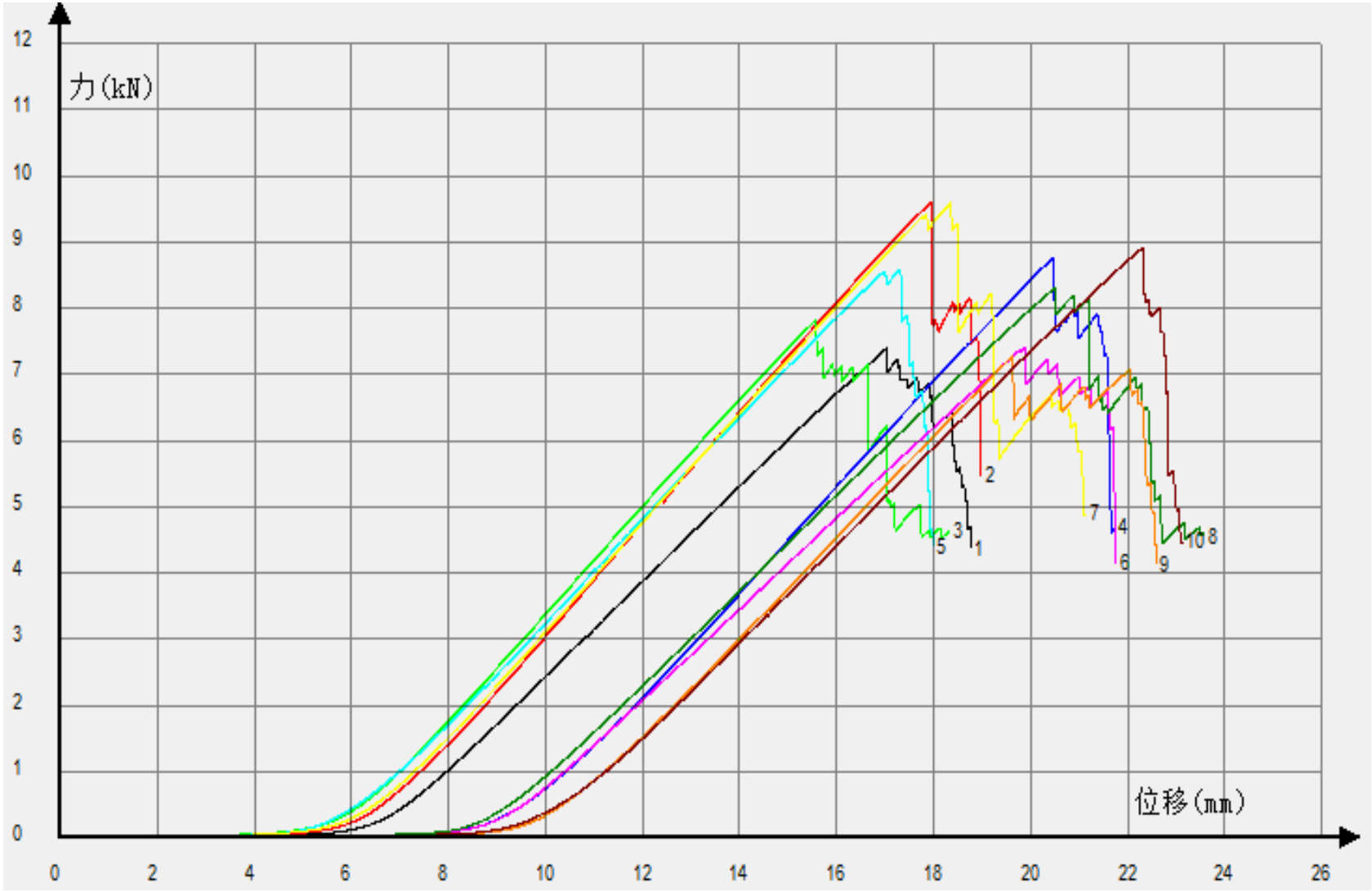

Figure 7.15 Vertical Tensile for Run #15

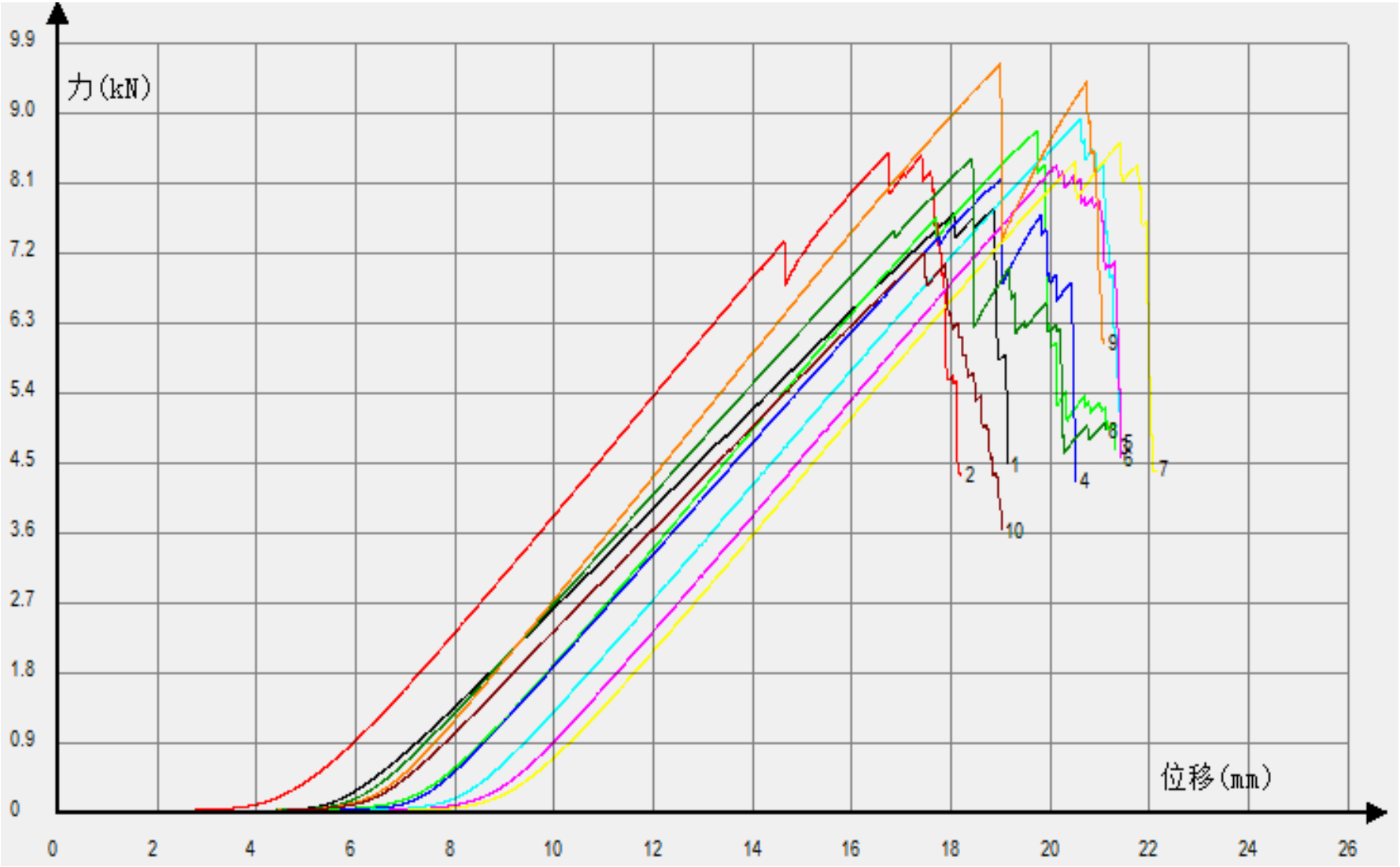

Figure 7.16 Vertical Tensile for Run #16